

Study of an onboard wired-wireless health monitoring system equipped with power save algorithm for freight railway wagons

*Original*

Study of an onboard wired-wireless health monitoring system equipped with power save algorithm for freight railway wagons / Aimar, Marco. - (2018 Apr 18). [10.6092/polito/porto/2706128]

*Availability:*

This version is available at: 11583/2706128 since: 2018-04-22T11:09:52Z

*Publisher:*

Politecnico di Torino

*Published*

DOI:10.6092/polito/porto/2706128

*Terms of use:*

Altro tipo di accesso

This article is made available under terms and conditions as specified in the corresponding bibliographic description in the repository

*Publisher copyright*

(Article begins on next page)



**ScuDo**  
Scuola di Dottorato ~ Doctoral School  
WHAT YOU ARE, TAKES YOU FAR



Doctoral Dissertation  
Doctoral Program in Mechanical Engineering (30<sup>th</sup> Cycle)

# **Study of an onboard wired-wireless health monitoring system equipped with power save algorithm for freight railway wagons**

**Marco Aimar**

**Supervisor**  
Prof. Aurelio Somà

**Doctoral Examination Committee:**

Prof. Eugenio Dragoni, Referee, Università degli Studi di Modena e Reggio Emilia  
Prof. Franco Furgiuele, Referee, Università della Calabria

Politecnico di Torino  
April 18, 2018



This thesis is licensed under a Creative Commons License, Attribution - Noncommercial - NoDerivative Works 4.0 International: see [www.creativecommons.org](http://www.creativecommons.org). The text may be reproduced for non-commercial purposes, provided that credit is given to the original author.



I hereby declare that, the contents and organisation of this dissertation constitute my own original work and does not compromise in any way the rights of third parties, including those relating to the security of personal data.

.....

Marco Aimar

Turin, April 18, 2018



# Acknowledgment

And I would like to acknowledge the company Ambrogio Trasporti S.p.a. for the wagon made available for the tests of the health monitoring system. In particular I would like to thank Ing. Andrea Zanardelli for the help and willingness show during the project and Ing. Eugenio Muzio for contributing with his experience and knowledge in the railway field.





*I would like to dedicate  
this thesis to my family  
and Lorenza.*



# Contents

1. Introduction .....	1
2. Freight railways monitoring requirements .....	9
3. Monitoring devices.....	13
3.1. Actual projects and devices .....	14
3.1.1. Devices battery powered .....	17
3.1.2. Devices with energy harvester .....	20
3.2. Proposed research solution.....	23
4. Thermal Models .....	25
4.1. Energy model .....	26
4.2. FEM model.....	29
4.2.1. FEM model characteristics.....	32
5. Design of the prototype .....	34
5.1. Wired prototype.....	34
5.1.1. Microcontroller ATmega2560 .....	35
5.1.2. Temperature sensor .....	36
5.1.2.1. Temperature uncertainty .....	36
5.1.3. Differential pressure sensors .....	43
5.1.4. GPS module .....	45
5.1.5. Accelerometer ADXL345 .....	46
5.2. Hybrid wired-wireless prototype.....	47
5.2.1. Base station .....	47
5.2.2. Axle box node .....	50
5.2.3. Monitored parameters and operating algorithm .....	52



5.2.3.1.	RMS parameter .....	53
5.2.3.2.	Operating and power save algorithm .....	56
6.	Experimental measurements .....	60
6.1.	The monitored wagon.....	60
6.2.	Brake blocks sensorization.....	61
6.3.	The monitored railway lines.....	63
6.4.	Logistical information .....	65
6.5.	Operating data .....	67
6.6.	Axle box temperature .....	72
6.7.	Braking force and longitudinal deceleration .....	74
6.8.	The RMS longitudinal acceleration.....	76
6.9.	The RMS vertical acceleration .....	84
7.	Thermal model results .....	92
7.1.	Energy model results .....	92
7.2.	FEM results .....	98
8.	S.W.A.M. rail project .....	106



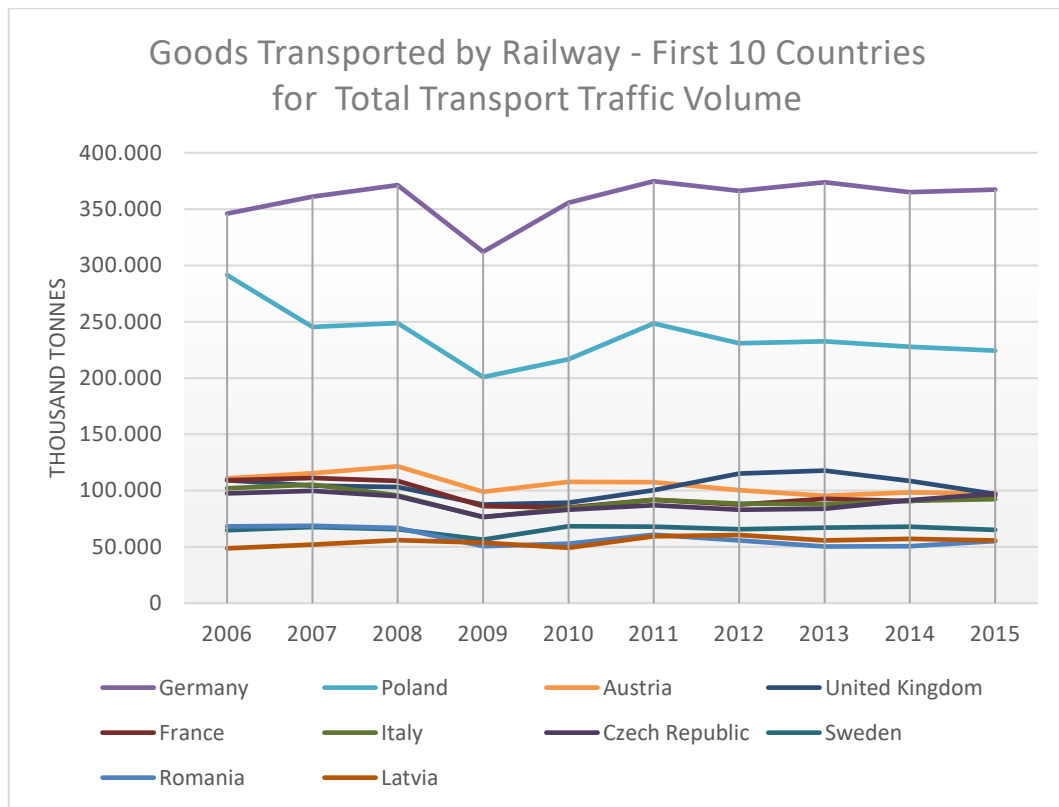
# Chapter 1

## 1. Introduction

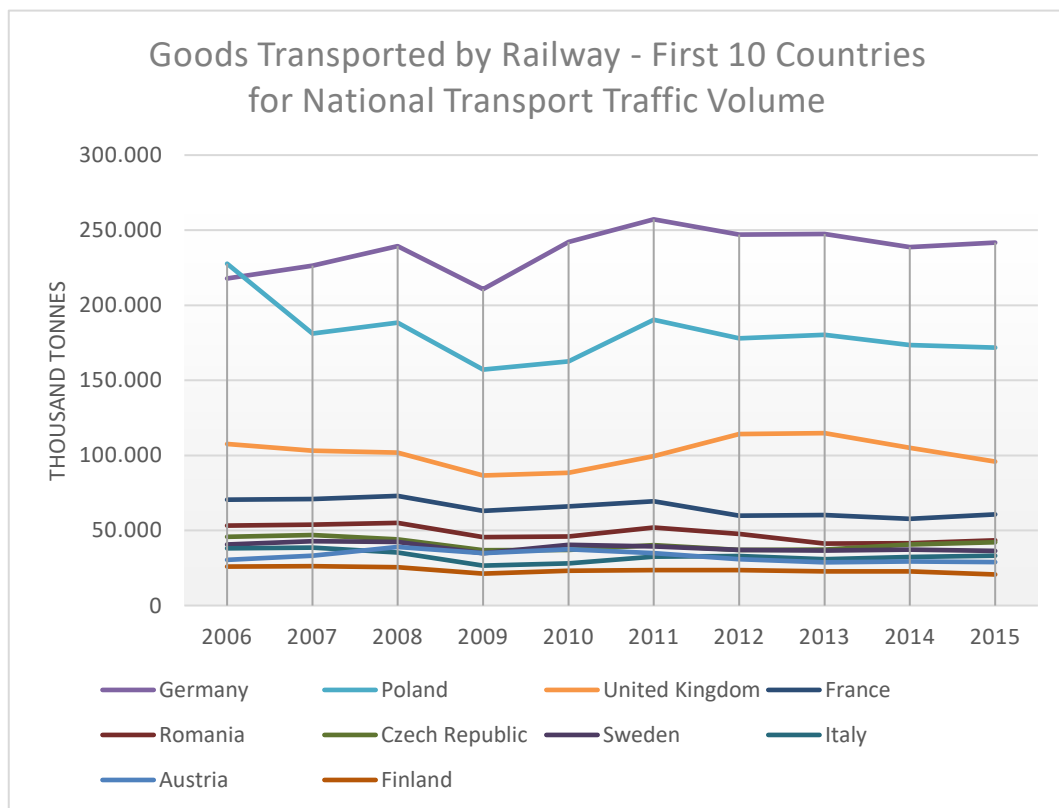
Goods transport is an essential factor for the European market for its significant contribution to economic growth and thus to the creation of new employment. Nowadays, approximately 75% of goods are transported by road within the European Union. The use of more efficient and sustainable modes of transportation, such as rail transport and inland waterways, would reduce oil imports and pollution abatement. If compared to road transport, rail transport with the same tonne per kilometer is able to emit 3.5 times less CO<sub>2</sub> [1] Freight transport is particularly competitive when the distances to be covered are medium-high, enabling to better spread the fixed costs associated with the loading and unloading of goods.

Figure 1 shows the use of rail transport in UE by the first 10 countries that make greater use of this type of transport. From the figures it is possible to observe that, excluding the 2008-2009 period, there were no sharp fall in the use of rail transport in the period shown in the graphs. However, in the last 5 years, as reported by the EUROSTAT data, it can be seen that the volume of goods transported has not increased.

The figures clearly show how Germany occupies the lead position with a traffic volume 3.5 times higher if compared with the other European countries. Furthermore, it can be observed that in Germany, the traffic of goods at national level, Figure 2, stands around 65% of its total traffic, while for Italy this value is reduced to around 36%. The data related to international transport are given by the sum of the incoming and outgoing transport.



**Figure 1. Goods Transported by Railway in EU – Total Transport Traffic Volume**



**Figure 2. Goods Transported by Railway in EU – National Transport Traffic Volume**

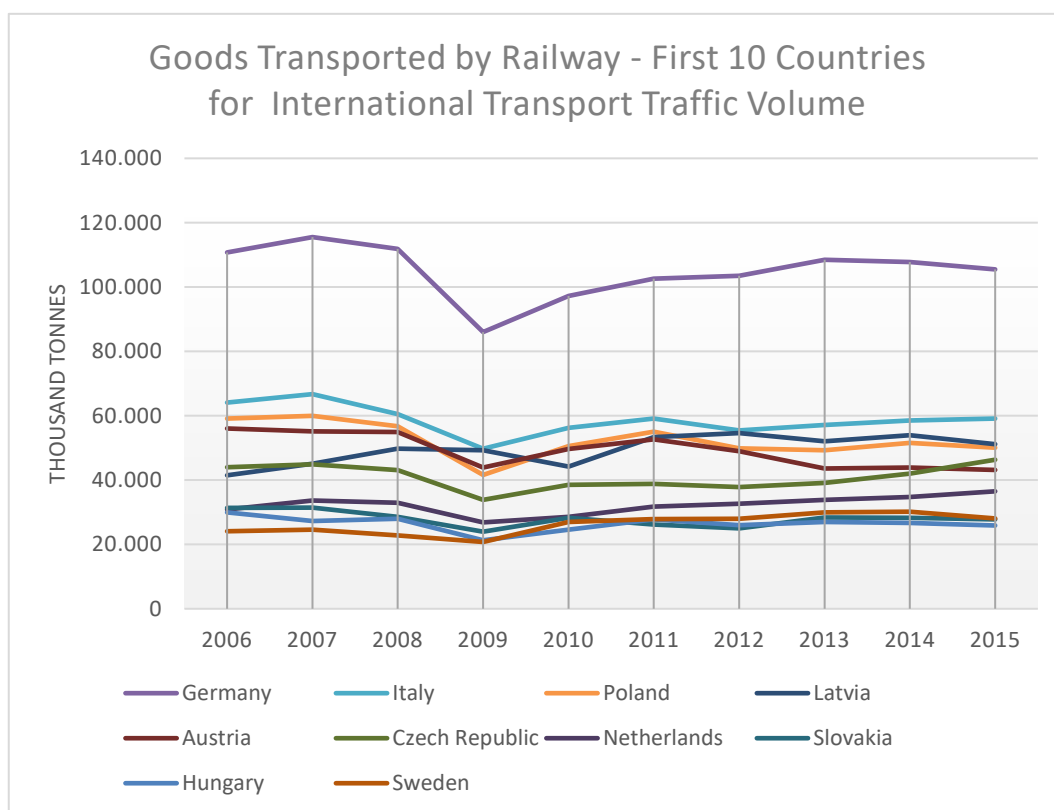


**Figure 3. Good Transported by Railway in EU – International Transport Traffic Volume**

The trend of the graphs and the daily experience of each of us clearly suggest the need to shift part of the goods traffic from the road to the rail in order to reduce the environmental impact and decongest the European roads. Implications are both economic and public health, reducing emissions and number of motorway accidents.

There are different forms of rail freight transport:

- single wagon transport (the customer need to transport his goods only in certain wagons of a train);
- complete train or block (the train is fill by only a single company);
- intermodal or combined road-rail transport (the container is loaded on a wagon).

The present thesis work, included in the Cluster ITS Italy 2020 project, is focused on this last mode of transport, the intermodal one.

In 2011, it was set by the European Commission the goal of transferring, by 2030, the 30% of road goods transport, on journeys exceeding 300 km, to other

modes of transport, such as railways or inland waterways, and to transfer more than the 50% by 2050 [1]

The growth of rail goods transport must be accompanied by an increasing introduction of tools and technologies that make possible to constantly monitor the European rolling stock. The introduction of monitoring technologies that allow to constantly know the status of the wagon would bring real and concrete benefits to the world of rail transport enabling to optimize the maintenance of rolling stock thus reducing costs but ensuring at the same time a maximization of the safety.

The increase in safety is even more important when dangerous goods are transported, whose spills could have negative and dangerous effects on public health and safety. Figure 4 shows the trend of railway accidents in which dangerous goods were involved. It can be seen that in recent years the number of accidents has decreased significantly. Over the years, however, Austria continues to hold the sad record of being the country where the greatest number of accidents involving dangerous goods occurs.

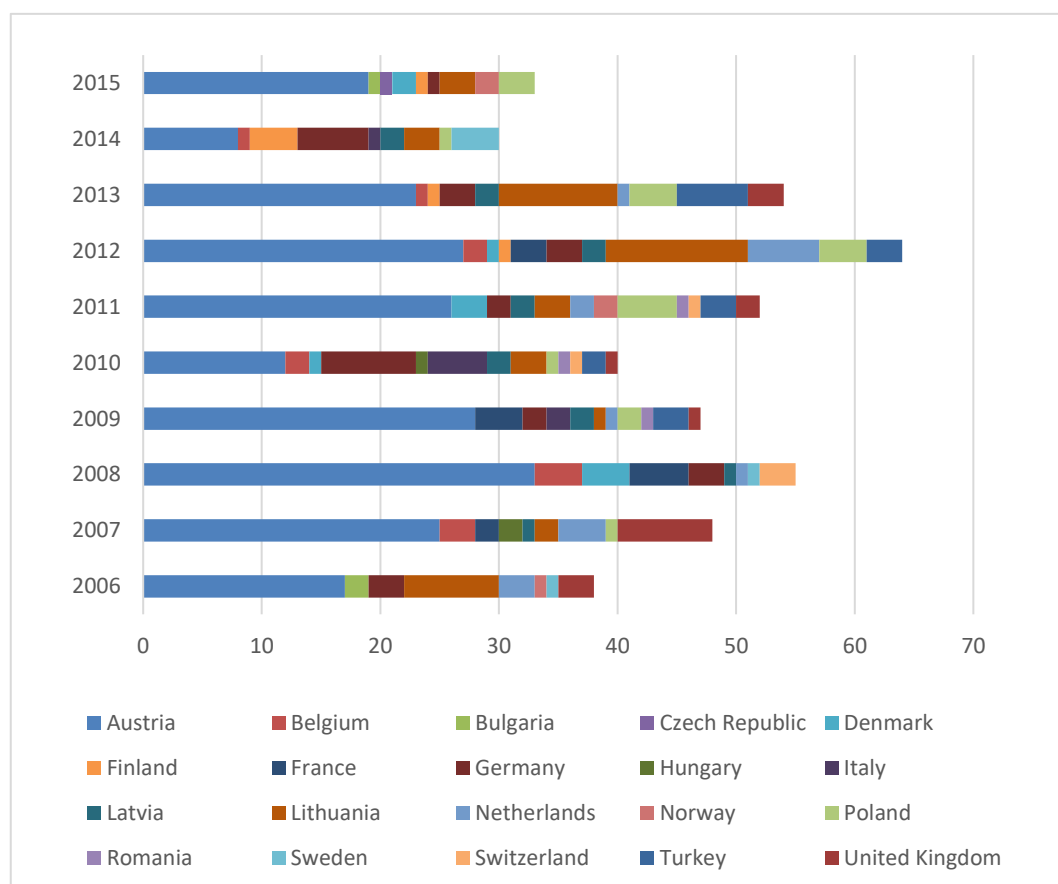


**Figure 4. Accidents involving transport of dangerous goods in UE.**

Fortunately, only a portion of the total number of accidents leads to the spillage of dangerous substances, as can be seen in Figure 5. The consequences, however, in these cases can be terrible as they can cause fires and explosions, as in the sad case of Viareggio in 2009.

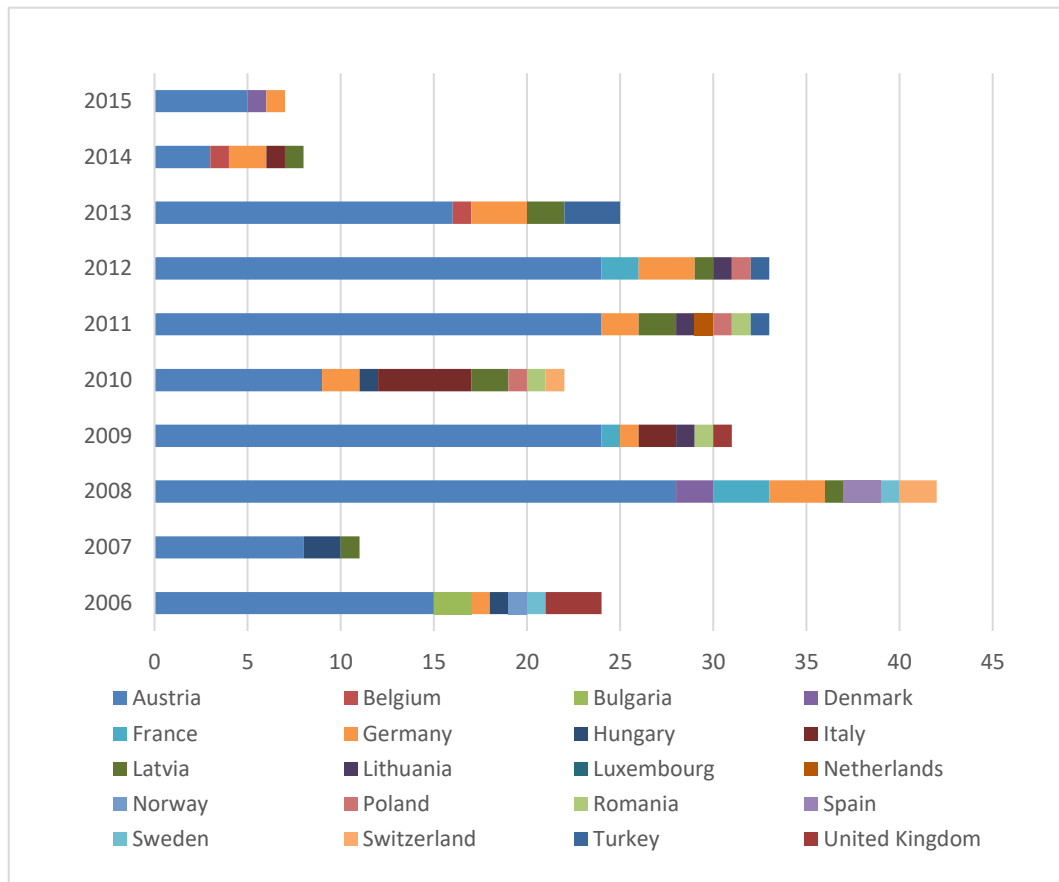


**Figure 5. Accidents in which dangerous goods are released in UE.**

Over the last few decades there has been an ever-growing development of monitoring systems dedicated to mechanical and high technology systems. This has been facilitated by the contemporary progress that involved the fields of information technology, data management and communication. In fact, the implementation of increasingly powerful hardware and software systems has facilitated the realisation of dedicated systems for the collection and management of mechanical systems operating data. Thanks to the enormous potential of modern hardware components, it is therefore possible to process a large amount of data in order to achieve the appropriate algorithms that help monitor the health of the system.

It is well known that all mechanical systems have a natural tendency to age and reduce their efficiency over time, so maintenance work is required to restore their performance. There are three possible maintenance methods:

- Corrective maintenance: only after the failure, the component should be replaced.
- Preventive maintenance: established maintenance intervals to reduce the probability of failure. The frequency of maintenance works is based on hours worked and / or on the basis of the mileage travelled by the vehicle.
- Predictive maintenance: through knowledge of the system health and the real operating conditions of the mechanical system put in place maintenance work in case of anomalous events in such a way as to avoid fault conditions.

The Health monitoring requires specific sensor, on-board data acquisition system to detect the physical operating parameters of the system, monitoring algorithms to evaluate the health status and finally diagnostic algorithms that can detect the failure, the position and seriousness.

The adoption of predictive maintenance techniques allows to maximize the operating time of the system and its components, reduce maintenance operation, resulting in cost reductions, and machine downtime.

The implementation of such health monitoring systems requires the integration and communication between different engineering environments to provide the right logistical support to fault diagnosis operations and estimate the residual useful life of the components.

Knowledge of the real operating conditions of the machine can also be used as a support during the design phase. In fact, when designing a component, loads and stresses are not known in operating conditions, and therefore both information and bibliographic data contained in regulations and safety factors are used. This way, instead, this actual operating data can be used as reference values for loads and stresses during operation of the component, with the possibility of evaluating whether the component itself has been oversized with respect to normal usage conditions.

The collected real data describing the operating condition of the machines can be used as reference values for loads and stresses, with the possibility of evaluating if the component has been oversized respect to normal operating conditions.



The foundation of the implementation of health monitoring systems is the need to perform diagnosis and prognosis of failures that occur during the components life of the mechanical systems.

It is essential to try to predict accurately the arise of a failure or estimate the residual useful life of the component as well as try to isolate the cause of the failure once the negative effects on the system are evaluated.

The benefits obtained are mainly related to increased security and reliability, as it is possible to detect and monitor incipient failure that may compromise the normal functioning of the system analysed. In this way, it is possible to carry out predictive maintenance operations on the component, reducing downtime and costs.

In order to improve the decision-making accuracy of diagnostic and prognostic systems, it is appropriate to adopt a feedback system that continuously provides useful information to optimize the level of accuracy required for the monitoring system.

In order to operate in the field of diagnostics and prognostication of mechanical systems it is essential to know the mechanisms of fault formation, the methods for evaluating the residual useful life of the components, the methodologies and the algorithms to be used for the purpose of detecting and isolating the faults on the component.

Several methodologies have been implemented and used to monitor the health of systems and for the risk analysis.

The following is a list of the main philosophies and techniques in literature:

- CBM – Condition-based Maintenance;
- FMEA – Failure Mode and Effect Analysis;
- FMECA – Failure Mode, Effect and Criticality Analysis;
- PHM – Prognostic Health Management;
- FTA – Fault Tree Analysis.

Monitoring the operating conditions it is evaluates the health status of the system and takes operational decisions, taking into account the information derived from the prognostic apparatus. Choosing the threshold value that differentiates the "faulty" situation from the "healthy" situation can heavily affect the chances of making a decision making mistake.

In recent years, interest in monitoring the operating conditions of freight wagons has grown significantly as shown in numerous publications [1] [4] [5] [10]

[12] and by first attempts of dedicated monitoring devices presented on the market. Some focus on the bogie and its components while others focus on the transported goods. The companies operating in this sector need to know the conditions of their wagons to be able to plan targeted maintenance and to reduce the costs connected with these operations. In the absence of continuous monitoring information, scheduled maintenance is carried out to prevent faults that could lead at best to discarding of wagon or, in the worst case, to derailments with serious consequences for the rail wagons and the infrastructure. In the period of time between two maintenance works, typically a multi-year period, the conditions and the mileage covered by the wagons generally are not measured.

# Chapter 2

## 2. Freight railways monitoring requirements

In the first part of this research project, the types of faults that occur typically on these kinds of wagons were evaluated by studying the literature and analysing the partner company fault database. This preliminary work allowed us to understand which subsystems are more subject to fault conditions compared to others. After analysing these subsystems, Figure 6, were chosen the necessary sensors to actively monitor the selected components.

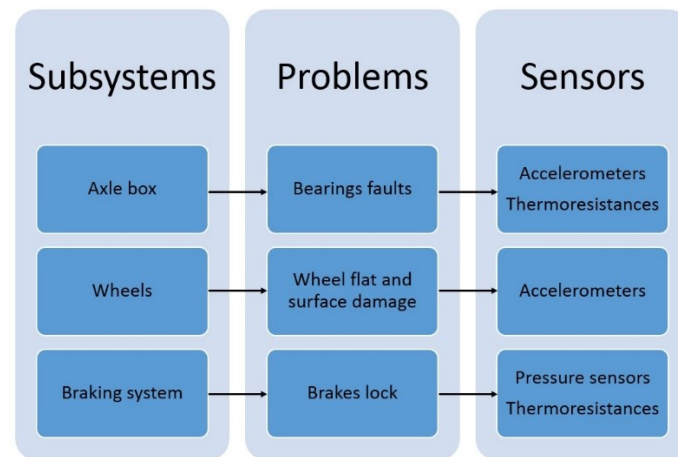


**Figure 6. Vehicle subsystems: diagram and possible failures.**

The information concerning the historical breakdowns of the wagon used in this study were collected over the last five years. Our analysis highlighted that for this type of wagon the braking system is more subject to failure than the other systems. The wheel and axlebox subsystems, due to the type of load of the wagons, have a lower failure rate. The design activity of the monitoring system, in accordance with the results obtained from the failure history, was targeted on the braking system. The problems that generally occur on this type of wagon, characterized by a uniformly distributed load, are the following:

- Irregular wear of brake blocks,
- Incorrect operating pressures of the braking system,

- Brake cylinder failures, and
- Poor performance of control valves.

These types of event in a short time can lead to the overheating of the wheelset and bearings and to wheels-flat damage. Furthermore, these problems may cause important consequences on the security and stability of the wagon.

The main goal of the project is the realization of a compact monitoring system. The first prototype realized was cabled. To meet this objective, we developed a device composed of three subsystems: the sensors for measuring the characteristic parameters of the braking system, such as temperature and pressure, an acquisition system for managing the sensors and data saving, and a power supply battery.

This chapter gives a brief overview of the braking operation in railways, in particular for the freight wagons braking systems, and the type of consequences that may occur as a result of possible braking system malfunctions.

The main requirements of a railway braking system are the following:

- automatic: the braking system must come spontaneously into action in cases of unintentional train separation or brake pipe failure;
- continuous: the braking system must connects in a single system all the vehicles of the train, and at least in emergency braking must be activated by any vehicle;
- adjustable: the braking system must be adjustable during braking and brake-release;
- inexhaustible: the braking system must never lose effectiveness, after a braking and brake-release cycle, the system must be ready again to a braking.

The braking system of a train is the set of equipment that allows to reduce the speed or to stop the train in correct and predetermined spaces. In this section is summarized the working principle of the freight wagon braking system monitored, to better understand the parameter that we collected during our research. For a more detailed description may refer to [2] .

The brake system can be divided into two major parts:

- mechanical part;
- pneumatic part.

As regards the mechanical part, it is composed by all the leverage constituting the brake rigging which transform the force applied by the brake cylinders to the braking force applied to the brake blocks.

The leverage used varies from wagon to wagon according to the number of brake cylinders and bogie.

The fundamental feature of the brake rigging structure is its isostaticity. In this way different brake blocks wear may be recovered in order to have a uniform braking on all axes, to do this is present a device for the automatic recovery of the brake rigging play (clearance) . An iperstatic brake rigging instead would cause only the braking of the axes with the minor wear of the brake blocks.

Figure 7 shows a simplified diagram of the pneumatic part of braking system. With reference to the said figure, each individual rolling stock presents a brake pipe provided at the ends of shut-off valves and semi-coupling hoses, which connect the locomotive and wagons. Connected to the brake pipe, downstream of a shut-off isolation, there is the control valve, which heads the auxiliary reservoir, the command reservoir and the brake cylinder.

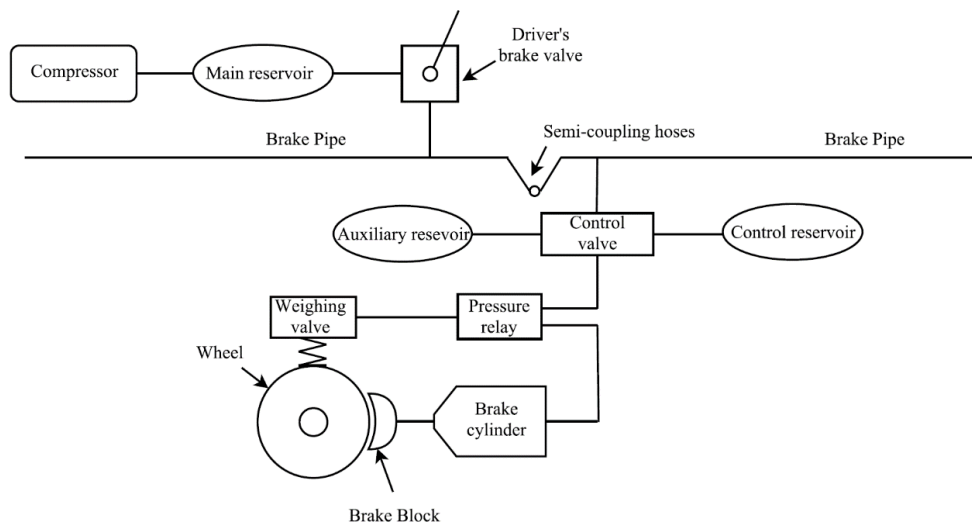


**Figure 7. Freight wagon braking system diagram.**

The locomotive also includes the compressor, which recharges the main reservoir and the driver's brake valve. The driver controls the braking acting on the faucet control valve, which determines the adjustment of the pressure of the brake pipe, placing it in connection with the atmosphere or with the main reservoir.

On the suspension of each bogie is installed a weighing valve that provides to the pressure relay a pressure value proportional to the load on the suspension in order to adjust the pressure on the brake cylinder.

The pressure created in the cylinder of the brake is almost proportional to the pressure drop in the brake pipe, with a maximum of 3.8 bar (load) for a fall of 1.5 bar (maximum service braking) and a performance characteristic dependent on the transfer curve of the control valve. The control valve is the decision-making body that compares the pressure value in the brake pipe with the one in the control reservoir.

When there is a pressure drop in the brake pipe the control valve puts in communication the auxiliary reservoir with the brake cylinder, thus determining the braking.

The fundamental element of the control valve is the “main device” whose function is to enter and discharge air from the brake cylinders on the basis of the brake pipe pressure in a predetermined time.

Regardless of the adopted constructive solution for the admission to international traffic, the control valve must guarantee the time of braking and brake release provided by the Norm UIC 540 both in the case of scheme P (passenger) and in the case of scheme G (freight).

The device for the first time is an organ inside the control valve which allows, in the first stage of braking, a fast filling of the brake cylinder, favoring the approach of the brake blocks to the wheel. In particular, it results in an “instant” peak pressure to the brake cylinder of at least 10% of the maximum pressure, which anticipates the normal filling of the brake cylinder through the orifice. The operation of such an element is independent of the braking regime, but its intervention is particularly helpful in the case of scheme G (freight) in which the filling time of the brake cylinder is longer.

Different braking regimes are prescribed according to the service that is required; for freight vehicles the G regime is adopted.

The major defect of braking systems with a single brake pipe is that the braking control is pneumatically transmitted by the pressure drop and therefore there are delays between the head and the end of the train, the braking delay can reach 45 seconds in G-mode in the case of very long train.

# Chapter 3

## 3. Monitoring devices

The potential growth of freight rail transport, due to the many benefits that this type of transport offers especially in view of a lesser environmental impact (in line with the European Horizons 2020 Sustainable Mobility Guideline), is increasing the interest of transport companies to install innovative monitoring systems for freight wagons in order to improve efficiency, reliability and safety of the service.

The current scenario, however, presents a number of issues, such as the absence of power on-board, the coexistence of new and old generation wagons, freight wagons that differ in dimensional and structural characteristics to adapt better to the goods to be transported, the use of wagons on different railway lines and in different composition depending on the transport needs.

Hence, the need to identify an onboard monitoring and diagnostic system that allows on the one hand the accurate wagon locating to improve the transport efficiency and the fleet management, and on the other hand the knowledge of the wagons operating conditions in such a way as to carry out targeted maintenance operations.

Currently, the only information available are provided by the equipment installed along the railway network, separated by tens of kilometers. However, to identify and intervene on an incipient failure, it is necessary to have continuous monitoring and a communication system that can warn the train conductor and the maintenance staff of wagon's owners.

A good monitoring system has to be:

- **Cheap:** the economic aspect is crucial because the cost of a monitoring device must be aligned with the cost of the object to be monitored. The value of a freight wagon is significantly lower if compared with a passenger car, particularly in the case of high-speed transport. Moreover, the operating life of a freight wagon can exceed three decades, so its value can then be amortized over an extremely long period. A monitoring device must be very low cost to be economically advantageous.

- **Energy autonomous:** energy autonomous or energy harvesting means technologies that seek to recover enough energy to power electronic devices to be used directly where it is generated, thus eliminating maintenance and replacement costs for batteries.
- **Wireless:** the technology that must be equipped with the system must be wireless. The many system nodes must communicate each other through wireless networks. The absence of wiring has the main advantage of allowing easy and fast installations which are reflected in a fall of installation costs. The disadvantage of this solution is the need to ensure the complete energy self-sufficiency of each node.
- **Robustness and reliability:** the monitoring system must have a level of reliability even better to the various subsystems that make up the freight wagon. It should not have any maintenance or batteries change for at least six years, namely the period of time between two complete wagon maintenance. The correct GPS location of the freight wagon must always be guaranteed in order to be able to intervene in the event of a failure.
- **Easy retrofit:** The monitoring system shall be able to be installed on both new and on existing freight wagons.

### 3.1. Actual projects and devices

Currently monitoring systems can be divided into two large groups. The former are those developed by universities or research centers within project financed by third parties, while the latter are monitoring systems developed individually by companies operating in the logistics sector.

The first ones, as is easily understood, aim to monitor many wagon parameters using numerous sensors connected to specific embedded PC that are programmed with dedicated software and algorithms. Generally these projects aim more to the development of algorithms rather than complete monitoring systems. In fact, often in these projects the development of an energy harvester able to constantly supply the installed devices is excluded. It is therefore preferable to power devices with batteries and replace them cyclically. These devices therefore have a low technology readiness level overall but a high value on the data acquisition and processing system.



The latter, on the other hand, aim to monitor substantially one quantity only, the distance covered by the wagons. This information is essential to correctly program the maintenance of a wagon. Often happens that maintenance is carried out too early if wagons have covered short distances, or too late if they have traveled more if compared with the average of wagons. To optimize company resources it is necessary to carry out maintenance when needed. These monitoring systems are therefore comparable to the hour meters of earth-moving machinery used in agriculture and construction. In the case of fleet formed by over hundreds goods wagons it is almost impossible to keep track of all the movements made by the wagon. With the GPS use this operation becomes very simple. The companies which operate in the wagons rental sector are the most mindful to this theme.

Among the research projects recently carried out in Europe, it is worth pointing out the CargoCBM project, supported by the German Federal Ministry of Economic. The partners of this project were TU Berlin, Eckelmann AG, PC-Soft GmbH, Vattenfall Europe Mining AG, WASCOSA AG, Lenord, Bauer & Co. GmbH and the HARTING Technology Group.

The system consists of a central unit called an On Board Unit (OBU), Figure 8, and a series of sensors installed inside the OBU or on the components to be monitored (e.g. wheelset bearing). The OBU contains an acceleration sensor to record the shunting impacts, a temperature sensor and a GPS receiver that provides information about the current position of the freight wagon and its mileage.



**Figure 8. CargoCBM, on the left the OBU installed on a Wascosa wagon, on the right an axle box bearing sensorized.**

In order to reduce the number of data send via GSM to the server in the OBU are embedded automatic data evaluation algorithms. These algorithms can detect wheel runouts, monitor running dynamics and an associated check of the wear

condition of the wheel profile, document heavy shunting impacts and monitor the temperature wheelset bearings. The OBU also has CAN-Bus and ZigBee interfaces, which also permit the connection of wireless sensors. During the project more than 400000 km were monitored on the railway lines of Austria and North Germany [6]

As can be seen in Figure 8, the developed system is predominantly wired and is considerably complex. Moreover, an appropriate energy harvester has not been developed.

The project was particularly focused on the development of algorithms for the identification of wheel flats which can lead to dangerous accidents if neglected [7]

Another recently presented project is the “5L” intelligent wagon. The project is supported by the Swiss Federal Office for the Environment and Transport. The partners of this project are SBB Cargo, Technical Innovation Circle for Rail Freight Services and some other partners. 5L is the acronym of the five main factors [8] that this new freight wagon aims to improve:

- Low noise: reduction of noise emission thanks to the introduction of disc brake;
- Lightweight: for a higher payload;
- Long running: thanks to a higher reliability significant reduction of downtimes;
- Logistics capable: possibility of integration into supply chains;
- LCC (Life cycle cost) oriented: integration of LCC-oriented components.

The project is being carried out in collaboration with the Swiss rail transport company SBB cargo, which has made its vehicles available to be sensorized [11] .

At the Transport Logistics 2017, a new wagon prototype was presented, Figure 9, in addition to innovations as the automatic coupler and disc brake, was installed the complete monitoring system produced by PJM.



**Figure 9. Intelligent freight wagon 5L - On the left the wagon presented and on the right the monitoring system.**

The system is equipped with a generator in the axle box for the electricity production. Also in this case the system installed is completely wired.

In this last two years, also the wagon rental companies TRANSWAGGON and ScandFibre Logistics installed the GPS tracking devices CargoTrac-R produced by SAVVY on more than 3000 wagons. In the course of 2018 they aim to monitor the remaining 3,000 wagons.

VTG is the largest European wagon rental company with a fleet of 80000 units and aims to have its fleet fully monitored with the Nexiot devices by the end of 2020 [9] .

Below are reported devices currently on the market on in advanced test phase.

### 3.1.1. Devices battery powered

# Bosch AMRA

The Bosch AMRA (Asset Monitoring for Railway Applications) is a monitoring health system battery powered, with a battery life guarantee for six years. The battery life coincides with the time between a wagon complete maintenance work and the next. This device is therefore without energy harvester.

The device, showed in Figure 10, has a very limited weight, 700 grams, and can be installed on any new or old construction wagon. The main use of this device is related to the location of the wagon and the temperature monitoring within refrigerated wagons in order to ensure the cold chain.

It is also equipped with an accelerometer for vibration monitoring recorded at the site of application of the device, particularly in the train composition. It can be connected via bluetooth or wiring to other sensors.

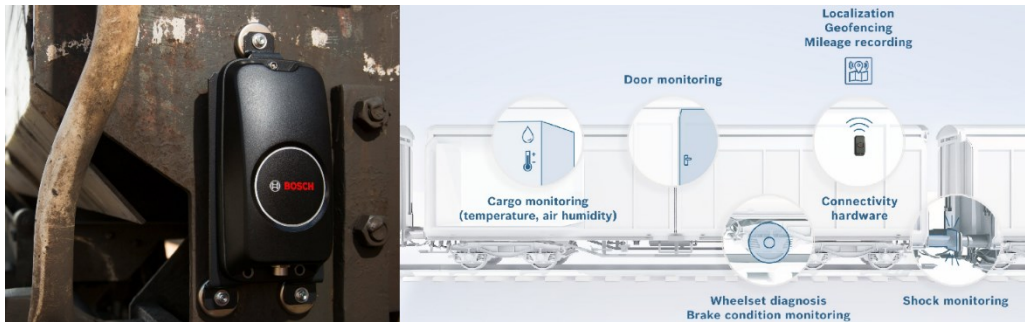


**Figure 10. On the left a Bosch AMRA installed on a wagon, on the right the operating principle of the device.**

## **Nexiot AG**

Nexiot is a spin-off company from ETH Zürich and introduced on the market a device for the geolocation and impact detection dedicated for the freight wagon sector, showed in Figure 11. Special feature of this device is the presence of energy harvesters which collect energy from the solar radiation.



**Figure 11. Nexiot AG Crossmodal.**

The presence of the energy harvester allows the complete self-sufficiency of the system. The only defect in this device may be due to the fact that as time goes by the power output of the cell may decrease due to the dirt that it may accrue on it. In any case, this device allows mainly the geolocation of the wagon.

## Savvy AG

The main product of the Savvy is the SAVVY® CargoTrac-Ex, Figure 12, a telematic device with more than 10 years of battery life, with the possibility of being used in hazardous environments (EX). It does not require maintenance throughout its life cycle and has reduced energy consumption.

A series of tests mainly focused on the problem of battery discharge in harsh weather conditions has allowed to improve the battery life of the device. The device also includes shock detection in the three directions with the possibility to set alarm threshold.



**Figure 12. SAVVY CargoTrac-Ex.**

These devices have as common denominator that they were originally designed for other fields of application and subsequently adapted to the rail world, especially to allow the geolocalization of wagons vehicles and to check and to guarantee the temperature of goods during the transportation.

This, on the one hand, allows a more efficient management of the fleet and the conditions of transport, while on the other it completely overlooked the health condition of the wagons and the improvement of their operating conditions through the planning of targeted maintenance. Knowing the position

Knowing the position can be estimate the mileage travelled by the freight wagon in a certain period of time in order to better manage the scheduled maintenance work.

These devices have been designed for other sectors, in fact in all of them there is present a battery that requires maintenance, although a long lasting. These represent additional costs maintenance for the rail operator. The choice of wire the wagon is not a viable alternative due to the high installation costs and to the fact that all wagons of the same train should be equipped with an electrical system to not interrupt the circuit.

Battery performance degrades rapidly over time, making this type of power supply not suitable for long periods if it is not intend to replace them.

An energy harvester must be absolutely present onboard the wagon in order to ensure a good battery healthy status over the years and a complete energy autonomy. Even the energy harvester must be maintenance-free and not be affected by external climatic conditions such as the absence of solar radiation. For this reason, in my opinion the choice of using solar cells is not the optimal choice.

Different technologies and solutions are available for the recovery of energy usable onboard the wagon. The choice to adopt one with respect to another is defined from the energy consumption of the monitoring device, the sampling frequency, and the type of sensors installed.

Consistent with the more recent literature, our research group, therefore, proposes to combine the development of the monitoring system with an energy harvester that can provide the necessary power to the monitoring system.

### **3.1.2. Devices with energy harvester**

#### **Kapsch Group**

The device presented by this company is the M2M monitoring system, showed in Figure 13. This solution is equipped with an energy harvester to make it energy autonomous.

The data collected are sent via mobile network to a central server, also are saved on an SD which acts as a black box. There is a GPS sensor to locate the position, mileage and speed for each wagon but can also be coupled with other sensor or devices as temperature, load and acceleration sensors.

Unlike previous devices, this replace the traditional axle box cover and allows to have information that the other devices are unable to supply. This device can also

be installed on any European freight wagon car in a very short time, around 15 minutes.



Figure 13. On the left different axle box cover for monitoring different axle box, on the right the monitoring system installed.

## PJM

PJM is on the market with the product WaggonTracker, available in many variations depending on the level of information that are available. The different models and the related functions are listed in Table 1:

	Power Supply	Mileage Counter	GPRS Modem	GPS Module	Sensor System
<b>WaggonTracker PS</b> Power Supply	✓				
<b>WaggonTracker MC</b> Mileage Counter	✓	✓	✓		
<b>WaggonTracker STD</b> Standard	✓	✓	✓	✓	
<b>WaggonTracker ADV</b> Advanced	✓	✓	✓	✓	✓

Table 1. PJM models characteristics.



The most complete version of the device, in addition to track the position and the mileage of the wagon, can handle up to 10 external sensors via analog and digital inputs.

This allows to perform a complete monitoring of the wagon including:

- Behavior in braking;
- Shock notification;
- Bearing temperature;
- Load conditions;
- Monitoring the internal pressure of the tank.

A weakness in this system is the use of a wired solution, therefore requires long installation time. In addition, as can be seen from Figure 14, the energy harvester is contained in one axle box only, so in case of failure all the system run out of energy for the power supply.



**Figure 14. The WaggonTracker ADV, the most complete monitoring system produced by the PJM.**

## **Schaeffler**

The bearing leader company Schaeffler offers an energy harvester, showed in Figure 15, to install inside the axle box with two different steps of power, 50 W and 90 W at the speed of about 100 km/h. However, a device capable of monitoring the condition of the bearings is not proposed. The power generated is more enough to power supply any type of monitoring system.



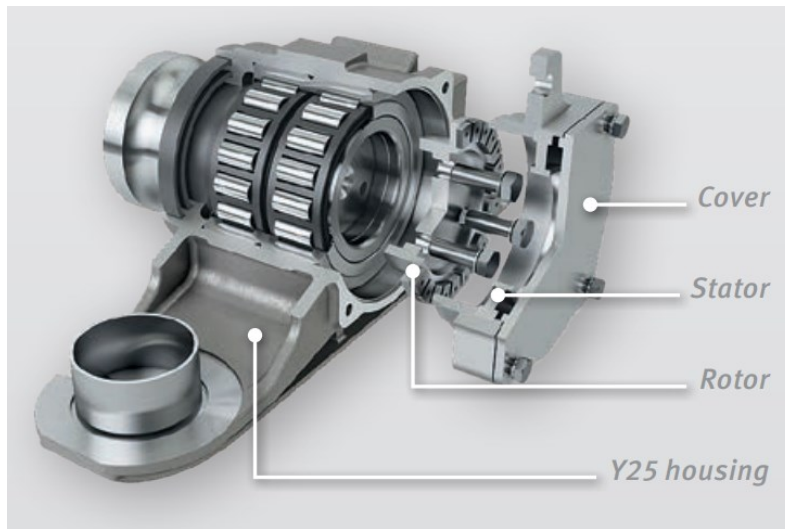


**Figure 15. Exploded view of the Schaeffler energy harvester.**

### **3.2. Proposed research solution**

In light of the existing research projects and products already available on the market, the following thesis work aims to develop a monitoring system demonstrator dedicated to freight wagons that can demonstrate the effectiveness of these devices. The two main quantities subject to monitoring in the railway field are essentially the temperature and the vibrations. Also in this project I will focus on these two aspects.

The temperatures of the cast iron brake blocks will be monitored and thermal models will be developed in order to simulate the thermal behaviour of these components. Also the external temperature of the axle boxes will be monitored as it represents an extremely important parameter to determine the state of health of the bearings and their correct operation.

The project, as is normal practice in the development of these devices, will initially focus on a wired prototype, given the shorter development times and greater reliability of this type of technology. Only afterwards the monitoring system shall be equipped with the wireless technology.

The subsystem that first will be monitored will be the brake system due to the problems related to it.

In fact, there are few articles in literature which address this topic, while this represents one of the major problems from the maintenance point of view. Often

during periodic tests on the freight wagons, incorrect operating pressures of the brake system are recorded. One of the most common problems is the locking of the brakes which can lead to wheel overheating and wheel flats.

To identify problems of overheating, the owners of freight wagons now use paints that can degrade with heat. Once applied on the inside of the wheel, it can indicate any overheating. The identification of these events, however, always takes place once the wagon has returned to the terminal and is controlled by an employee. The potential of monitoring lies in being able to identify in an accurate and timely manner the occurrence of a problem that, if not treated, could lead to much more serious consequences.

The monitoring of the braking system is also a prerequisite for the study of the operating temperatures of the brake blocks. In this historical period it is in fact proceeding with the replacement of the classic cast iron brake blocks with new synthetic type. This topic attracts particular interest not for wagons which are equipped from birth of this type of soles, but for the whole European rolling stock fleet which must be subject to a retrofit operation. In fact, there is not enough data on the behaviour of these new braking element with the old wheelset material.

The second aspect subject to monitoring in this work is vibration monitoring. Vibrations of particular interest for freight wagon monitoring are those along the vertical axis and the longitudinal axis. The accelerations along the vertical axis in fact describe the stability of the vehicle and its interaction with the rails. Vertical acceleration is a parameter that allows to determine if the car is traveling safely or not. In fact, this parameter makes it possible to identify a possible derailment, if the acceleration level recorded is anomalous. Instead, longitudinal acceleration is a parameter monitored by all railway monitoring devices present on the market. It is important to know the longitudinal accelerometric levels both in the phases of train composition and during the braking operations in order to identify possible incorrect behaviour.

To monitor these functional parameters and monitor the logistic aspects of the monitored wagon, it will be necessary to create devices that can effectively sample all the quantities involved. The devices created will be both wired and wireless and will be optimized from the energetic point of view to guarantee maximum autonomy.

# Chapter 4

## 4. Thermal Models

In this chapter is discuss the construction of the models used for the study of the thermal performances of the cast iron brake that equip the freight wagon under analysis.

The models used are based on an energetic approach to study the temperature variations of the brake blocks during the braking operation. Temperature is a key factor to determine the braking capacity of the wagons, in fact as the temperature increase the friction coefficient between the wheel and the brake blocks decrease.

Excessive temperature levels can lead to a whole series of problems as thermos cracks, wheels flat, overheating. The thermal fatigue is one of the major tread damage mechanisms and is due to the continuous thermal cycles to which the wheels is subjected during their operating life.

The most interesting and complete studies on the development of thermal models for the temperature estimation in the brake block and wheel tread were conducted by Vernersson [14] [15] . The model developed by the cited author can handle stop braking, drag braking at constant brake power, and also intermediate periods of cooling. The model has been developed taking into account the many factors involved in the real heating and cooling process, so it is possible to compare brake rig tests with in-field tests. The model developed was calibrate and validate with numerous tests.

In the case of a bearing failure, its temperature reaches in a very few seconds significantly higher values than the maximum permitted level, leading to the loss of lubricating properties of the grease contained in the axle boxes and bearings.

Cole et al [16] addressed a subject treated rarely in the literature, namely the study of the influence of the temperature of the wheel treads on the temperature level of the bearing due to the heat conduction.

The operating temperature of the wheels under braking conditions is generally between 100 and 300 ° C, but can reach 600 ° C as a result of heavy stresses due to repeated braking, as in the case of overcoming alpine passage downhill or in the

presence of brake lock. The subsequent rapid cooling of the wheels can lead to the formation of martensite introducing significant change in the hardness with the risk of abnormal wear.

## 4.1. Energy model

To study the thermal performance of the brake blocks sensorized in this research project was decided to apply an energy study. In fact, it can be stated that, during braking, the kinetic and potential energies of the wagon are transformed into thermal energy according to the principle of energy conservation.

The following type of approach has been used previously by Talati and Jalalifar [17] which has been applied in the study of the disc brakes, and Vakkalagadda et al.[18]. The nomenclature used for the thermal model is shown in Table 2.

Nomenclature			
$m$	Sum of mass wagon and mass transported [kg]	$E_{tt}$	Total thermal energy [J]
$v_2$	Speed at the start of brake [m/s]	$\Delta E_c$	Variation of kinetic energy [J]
$v_1$	Speed at the end of brake [m/s]	$\Delta E_p$	Variation of potential energy [J]
$\Delta h$	Change in elevation during the braking [m]	$E_{ar}$	Energy loss for aerodynamic resistance [J]
$\alpha$	Heat partition coefficient [-]	$E_{rr}$	Energy loss rolling resistance [J]
$\beta_r$	Thermal effusivity of the wheel [Ws <sup>1/2</sup> /k m <sup>2</sup> ]	$r_{ar}$	Aerodynamic resistance [kg/t]
$\beta_s$	Thermal effusivity of the cast iron brake blocks [Ws <sup>1/2</sup> /k m <sup>2</sup> ]	$r_{rr}$	Rolling resistance [kg/t]
$\beta$	Thermal effusivity [Ws <sup>1/2</sup> /k m <sup>2</sup> ]	$D$	Distance covered during braking [m]
$k$	Thermal conductivity [W/m K]	$E_{ts}$	Thermal energy in brake blocks [J]
$\rho$	Density [kg/m <sup>3</sup> ]	$m_s$	Brake block mass [kg]
$c$	Thermal capacity [J/kg K]	$c_s$	Brake block thermal capacity [J/kg K]
$S_r$	Relative surface of the wheel [m <sup>2</sup> ]	$C$	Drag coefficient [-]
$S_s$	Relative surface of the brake block [m <sup>2</sup> ]	$S$	Surface of the locomotive [m <sup>2</sup> ]

**Table 2. Nomenclature used in the model.**

During braking operations, the change in kinetic energy between the instants of beginning and end braking is equal to:

$$\Delta E_c = \frac{1}{2} m (v_2^2 - v_1^2) \quad (1)$$

The change in potential energy it is equal to

$$\Delta E_p = m g \Delta h \quad (2)$$

During the braking operations the heat generated at the interface between the wheels and the brake blocks, due to the friction, flow in different way in the two bodies.

The heat partition coefficient between the wheel and the cast iron brake blocks is calculated with the following equation:

$$\alpha = \frac{\beta_r S_r}{\beta_r S_r + \beta_s S_s} \quad (3)$$

The term  $\beta$  is the thermal effusivity and is calculated as:

$$\beta = \sqrt{k \rho c} \quad (4)$$

This approach for evaluate the heat partition can also be applied in the case of synthetic brake blocks as the term  $\beta$  takes into account the different physical characteristics of the materials.

The total thermal energy generated during braking was calculated by the following expression:

$$E_{tt} = \Delta E_c + \Delta E_p - E_{ar} - E_{rr} \quad (5)$$

The energy loss due to the aerodynamic resistance of the head and lateral inside of the train is evaluated [19] with the following expressions:

$$r_{ar} = 0,0005 C S V^2 \quad (6)$$

Where  $V$  is the speed. The unit of measurement of this formula is [kg/t], in order to obtain  $E_{ar}$  it is necessary to use the following formula:

$$E_{ar} = r_{ar} m g D \quad (7)$$

The rolling resistance ( $r_{rr}$ ) was assumed to be equal to 2 kg/t [19] , in this case in order to obtain  $E_{rr}$  it is necessary to use the following formula:

$$E_{rr} = r_{rr} m g D \quad (8)$$

The curve resistance, in accordance with the literature [19] [20] , was ignored.

The fraction of total heat energy flowing in blocks is equal to:

$$E_{ts} = (1 - \alpha)E_{tt} \quad (9)$$

For the analysis of the single block, it was necessary to divide by the total number of brake blocks installed on the six axes, which is equal to 48.

Using the thermal capacity of the body, the increase of temperature  $\Delta T$  recorded on the single brake blocks after braking can be calculated with the following expression:

$$\Delta T = \frac{E_{ts}/48}{m_s c_s} \quad (10)$$

From the simplified model previously described and using the vehicle data and the measured data, the energy evaluations that allow us to estimate the temperatures of brake blocks as a function of the running conditions of the vehicle can be performed. For this model, it was important to know the mass of the wagon because this parameter strongly influences the results. Table 3 reports the physical properties used for the calculation.

Physical quantity	Wheel	Cast iron brake block
Thermal conductivity k [W/m K]	49	48
Density [kg/m <sup>3</sup> ]	7850	7100
Thermal capacity [J/kg K]	460	520
Mass [kg]	—	7.5

**Table 3. Physical properties**

The model was applied for the study of single braking located along the railways line on sections that did not present too steep gradients. In fact, the potential energy plays an essential role due to the high mass of the wagons.

In this work we did not consider the effects of the braking of the locomotive and the forces generated by the other wagons. This choice was supported by the good results obtained.

## 4.2. FEM model

To be able to focus in more detail the thermal behavior of the brake blocks has been developed a FEM model. This model, unlike the one presented in the previous chapter, allows to study temperature-time histories in different point of the brake blocks and also allow to estimate the temperature at the interface between the brake blocks and the wheels.

Again, an energy-based approach based on the thermal energy generated by friction between the wheel and the brake during braking operations has been used. Key parameters for this type of analysis are friction coefficient, the brake block geometry, the pressures value reached by the brake cylinder during the braking and the geometry of the brake rigging and leverages.

The friction coefficient between brake blocks and wheels tread depends on the instantaneous speed of the wagon, the applied force to each strain and the contact pressure. During braking the temperature at the interface increases rapidly, this results in a reduction in the friction coefficient.

The friction coefficient can be evaluated by different equations obtained by experimental test or using tables or diagram indicating the trend of this physical quantity depending on the speed of the train.

The UIC formula is

$$\mu_f = 0.49 \frac{\frac{10}{3.6} V + 100}{\frac{35}{3.6} V + 100} \frac{\frac{875}{g} p_s + 100}{\frac{2860}{g} p_s + 100}$$

This formula take into account the speed of the train  $V$  and the pressure of contact on the surface  $p_s$ .

The average values of  $\mu_f$  used for the design of the model were chosen in agreement with the literature and the technical data sheets of the braking component manufacturers.

The FEM model was built reproducing the geometric characteristics of the wagon sensorized. Each wheel of the monitored wagon is equipped with four cast iron brake blocks, for a total of sixteen brake block for each bogie. Each bogie is equipped with a dedicated brake cylinder.

The angle of contact between the cast iron brake block friction surface and the wheel tread is  $29.4^\circ$ . With this value, it is possible to calculate the relative contact surface between the two bodies, which is the surface concerned the thermal exchange during braking.

The thermophysical quantities of the cast iron brake blocks are shown in Table 4. The thermal conductivity, thermal capacity and density values were taken from Vernersson [14] .

Physical quantity	Cast iron brake block
Thermal conductivity, $k$ - [W/m K]	48
Density, $\rho$ - [kg/m <sup>3</sup> ]	7100
Thermal capacity, $c$ - [J/kg K]	520

**Table 4. Thermophysical quantities of cast iron brake blocks**

The fundamental input parameter for the energy evaluation is the pressure value inside the brake cylinder during braking operations. The pressure value is discriminative of the braking condition, in order to obtain an average value for the calculation of the thermal flow, the average pressure was calculated through the mean integral as shown in formula:

$$P_{cyl\ mean} = \frac{1}{t_f - t_i} \int_{t_i}^{t_f} P(t) dt \quad (11)$$

Where  $t_i$  is the moment of activation of the brake cylinder that is the instant when the pressure inside the brake cylinder become greater than zero and  $t_f$



correspond the end of the braking when the pressure return to be null. The brake cylinder pressure profile depends on the driver's braking intensity imposed by the control valve with a pressure drop inside the brake pipe.

Once the average pressure value is obtained, it is possible to determinate the pressure force of each brake blocks on the wheels.

$$F_{br\ block} = \frac{\beta P_{cyl\ mean} A_{br\ cyl}}{16} \quad (12)$$

The term  $\beta$  is the brake rigging multiplication factor. In this case is equal to two. The value in the denominator is the number of brake blocks for each bogie, all the sixteen brake shoes are activate by the same brake cylinder so we decided to assume a uniform distribution of forces.

From the product of the of  $F_{br\ block}$  with the average friction coefficient of the braking is obtained the friction force

$$F_{mean\ frict} = F_{br\ block} \mu \quad (13)$$

The information obtained through the monitoring system allows us to know accurately the time, position and distance values that characterize the single braking.

The total thermal energy generated on the interface of the single brake blocks by the braking operation is then calculated by the following expression

$$E_{thermal\ braking} = \frac{F_{br\ block} d_f}{t_f} \quad (14)$$

$d_f$  is the distance covered with the brake activated and  $t_f$  the corresponding time duration.

The thermal flow that is generated on the contact surface between the two bodies is obtained with the expression

$$H_{thermal\ braking} = \frac{E_{thermal\ braking}}{A_{contact}} \quad (15)$$

Where  $A_{contact}$  is the surface of the brake block in contact with the wheel.

#### 4.2.1. FEM model characteristics

The FEM thermal model was developed using the software ANSYS. Figure 16 shows the model used, as can be seen the mesh has been tightened in the area where the temperature sensor was installed on the sensorized cast iron brake block. The mesh was obtained using the element SOLID 90.

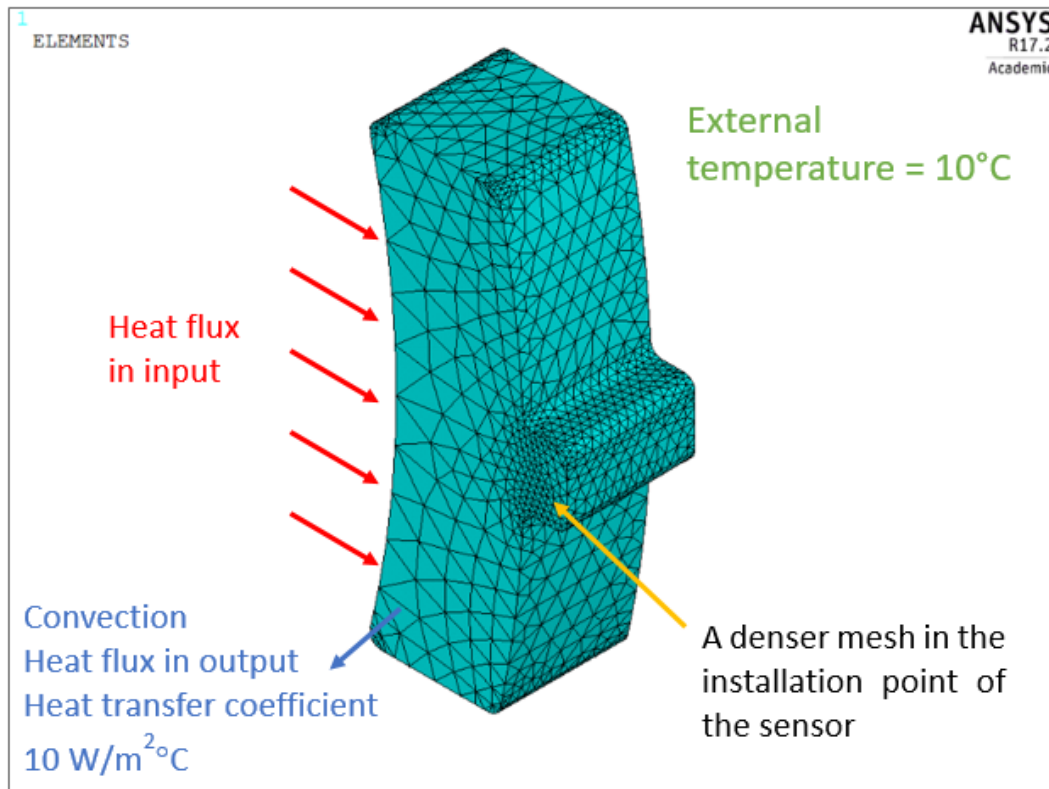


Figure 16. Brake block mesh.

SOLID90 is a higher order version of the 3-D eight node thermal element (SOLID70). The element has 20 nodes with a single degree of freedom, temperature, at each node. The 20-node elements have compatible temperature shapes and are well suited to model curved boundaries. The 20-node thermal element is applicable to a three-dimensional, steady-state or transient thermal analysis.

The model consists of a total of 21076 nodes.

The thermal flow found with the previous equations has been applied for a time duration equal to the monitored braking on the contact surface between the two bodies. At the end of the braking process the transient was simulated, giving the

heat the time to migrate inside the body until reaching the maximum measured temperature value.

On the lateral surface of the brake block, the only in direct contact with the air flow, was applied a heat transfer convective coefficient of  $10 \text{ W/m}^2\text{°C}$ . The value was chosen in accordance with the literature [15] .

The geometric model was based on the dimensioned drawings provided by the company partner. It was also verified that the mass calculated by the software was equal to the mass measured in laboratory. The correct mass value is essential to allow a simulation that gives results more realistic as possible, an incorrect mass value provide results that were too low in the case of overestimation and vice versa.

The model provides for the application of the average thermal flux previously calculated starting from the pressure of the brake cylinder collected with the monitoring system. Being a medium load, it was applied using a step function that rising from zero to the value calculated before in the exact instant of brake application and falling to be null when the pressure in the brake cylinder returns to be zero. The experimental data obtained with the monitoring system were studied and was calculated the time spent by the heat to flow to the point of application of the sensor, reaching a temperature peak in the point sensorized. This time is also simulate with the software, conducting a transient heat analysis.

This type of simulation allows to observe the temporal evolution of the temperature in the point of application of the sensor on the brake block, and to compare it with the real trend monitored during the tests conducted.

The same model was studied for a second time. In this second case the data in input were modified with the aim of obtaining data as realistic as possible. In fact a constant average thermal flow was no longer applied for the duration of the single braking, but was applied a thermal flow profile as much as possible equal to the pressure profile monitored inside the brake cylinder of the central bogie. To do this the time integration the equation (11) was reduced to a few seconds and no longer equal to the entire braking. Also in this case the braking and subsequent brake release were simulated, giving time to the heat to flow toward the sensorized point.

The results obtained in the sensorized point with the application of this thermal load were compared with the data obtained by the previous one to verify the concordance of the two models.

# Chapter 5

## 5. Design of the prototype

The design of the first device prototype was performed following the company needs about knowing the operating conditions of the wagon focusing on the subsystems most affected by breakdowns.

The analysis of the maintenance data of the company partner of the project showed that on the Turin (IT) – Modane (FR) railway line the main problems spotted affected the braking system with consequent overheating of the wheel. The partner company uses a particular paint with which it covers the inside of the wheels. In the event of overheating, this paint cracks allowing the operator to identify the wheels overheated during the journey. More rarely there have been problems with the axle boxes of the wheelset.

The devices presented in the dedicated section of this thesis allow to observe the main solutions developed over the last years by the main companies operating in the world of railway monitoring.

The task of the first prototype was to understand what were the most interesting quantities for the study of the maintenance problem and with which sampling frequency they were to be sampled.

In the first design phase, therefore, I am not concerned to determine and limit the energy consumption.

### 5.1. Wired prototype

In the first version, the developed monitoring system, whose scheme is shown in Figure 17, was composed of the following parts:

- A data acquisition system based on a microcontroller ATmega2560
- Temperature sensor
- Differential pressure sensors
- Tri-axial accelerometer
- GPS module with external antenna

- SD memory.

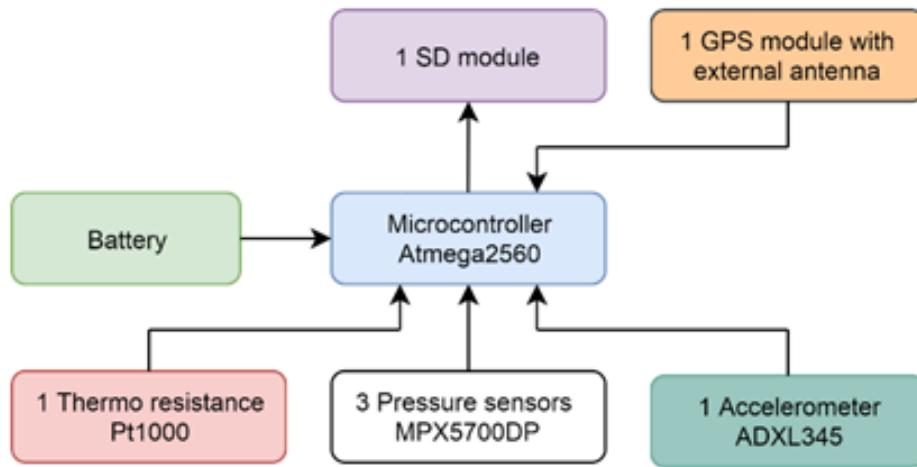


Figure 17. Wired prototype scheme.

### 5.1.1. Microcontroller ATmega2560

The data acquisition system was based on a microcontroller ATmega2560, on which were embedded a software and a firmware developed entirely by our group. The characteristics of the ATmega2560 are shown in Table 5.

Processor	Memory			I/O	
	Flash [kb]	EEPROM [kb]	SRAM [kb]	Digital I/O pins	Analogue I pins
<b>ATmega2560</b>	256	4	8	54	14

Table 5. ATmega2560 characteristics.

The decision to use the ATmega2560 microcontroller was dictated by the numerous potentialities offered by this device, particularly for its simple programming, the high number of digital and analogue ports, and the low power consumption compared to the possibility of acquiring and processing data. Furthermore it is possible to develop and install the codes on the microcontroller using free compilers.

The microcontroller ATmega2560 has the possibility of being placed into sleep mode to reduce energy consumption in the phases in which no activities or calculations are required. The characteristics of the processor enable a further significant development of the acquisition software having still available a considerable amount of memory.

### **5.1.2. Temperature sensor**

These sensors were adopted for monitoring the temperature of the brake blocks. After a number of laboratory tests, we decided to adopt a type of Pt1000 resistance thermometer with a measuring range between  $-50^{\circ}\text{C}$  and  $500^{\circ}\text{C}$ . Vernersson [15] report a thermal image generated by a thermos camera during a brake rig experiment. The image was taken after 30 min of braking at 31.5 kW, axle load 25 ton and speed 100 km/h. The highest temperature reached at the interface between the wheel tread and the brake block was  $410^{\circ}\text{C}$ . For this reason, I decided to adopt a temperature sensor with this measurement range. This extreme measuring range was adopted because in the literature there are no reports; to our knowledge, the maximum temperature values can be reached by the cast iron brake blocks in normal operating conditions on a track with a high gradient slope and so frequent braking. Some literature studies show the trend and the temperature peaks of brake blocks during tests on test benches or test circuit.

#### **5.1.2.1. Temperature uncertainty**

Temperature is a fundamental parameter in this thesis. It is therefore essential to know exactly the errors resulting from the measure of temperature.

An analog / digital converter is already present in the selected microprocessor. The number of bit used in the A/D conversion can be different, from 10 bit go to 8 bit of resolution, depending on the sampling frequency used.

In the case of this monitoring system a sampling frequency of 1 Hz is used, the available bits are therefore 10. The full range voltage (VFR) used for data sampling is 5V.

Resistance thermometers exploit the resistivity variation of particular materials due to temperature variation. In this case the material used by the sensor is platinum.

For metals there is a physical law that link the resistivity  $\rho$  and temperature  $T$ . The linear relationship is as follows:

$$\rho(T) = \rho_0 \cdot [1 + \alpha \cdot (T - T_0)] \quad (17)$$

The value  $\rho_0$  indicates the resistivity of the material at the temperature  $T_0$ , equals to  $0^\circ\text{C}$ . In the case of the Resistance thermometers PT1000 at the temperature  $T_0$  the resistance is  $1000^\circ\text{C}$ . The  $\alpha$  coefficient, called Temperature Coefficient of Resistance, indicates the average variation of the resistance value between  $0^\circ\text{C}$  and  $100^\circ\text{C}$ . In this case the value of  $\alpha$  is equal to  $3.90802 \cdot 10^{-3} (^\circ\text{C})^{-1}$ .

Once the resistivity value is known it is possible to obtain the resistance value through the relation:

$$R = \frac{\rho L}{S} \quad (18)$$

The term  $L$  is the length and  $S$  is the section area of the conductor.

In the specific case of Resistance thermometers, in the range between  $0^\circ\text{C}$  -  $850^\circ\text{C}$  the relation used is the following:

$$R(T) = R_0 \cdot [1 + \alpha \cdot T + \beta \cdot T^2] \quad (19)$$

In case of temperatures below  $0^\circ\text{C}$ , in the range  $-200^\circ\text{C} - 0^\circ\text{C}$ , the relation is:

$$R(T) = R_0 \cdot [1 + \alpha \cdot T + \beta \cdot T^2 + \gamma \cdot (T - 100) \cdot T^3] \quad (20)$$

Where

$$\alpha = 3,9083 \cdot 10^{-3} (^\circ\text{C}^{-1}), \beta = -5,7750 \cdot 10^{-7} (^\circ\text{C}^{-2}) \gamma = -4,1830 \cdot 10^{-12} (^\circ\text{C}^{-4}).$$

For the calculation of the overall uncertainty related to the temperature measurement, was used the following simplified linear relation:

$$R(T) = R_0 \cdot [1 + \alpha \cdot T] \quad (21)$$

Which does not includes the second order term.

Characteristics of the temperature sensor are as follows in Table 6:

<b>Temperature range</b>	-50°C to +500°C
<b>Resistance @ <math>T_0</math></b>	1000 $\Omega$
<b>Basic Range (from 0°C to 100°C)</b>	385 $\Omega$
<b>Auto heating</b>	<0.5°C/mW

**Table 6. Temperature sensor characteristics.**

The sensor is in class B so its tolerance is:

$$\delta T^{Sensor} = 0,3^\circ C + 0,005 |T|$$

The conditioning circuit for acquiring the temperature value chosen for the Pt1000 resistance thermometer is the voltage divider.

The voltage divider is a circuit made up of two or more passive elements, in our case a known resistance ( $R_1$ ) and the resistance thermometer ( $R_2$ ), connected in series. A voltage  $V_{in}$  is applied to the terminal and is divided on two components according to the resistance values. In Figure 18 it is possible to observe the diagram of a voltage divider:

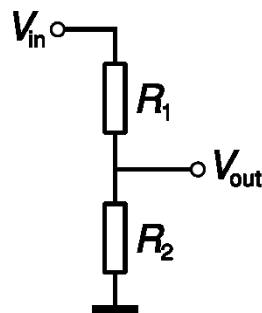


**Figure 18. Voltage divider scheme.**

The relation between  $V_{in}$  and  $V_{out}$  is:



$$V_{out} = V_{in} \frac{R_2}{R_1 + R_2} \quad (22)$$

Knowing  $V_{out}$  is determined the value of  $R_2$ .

$$R_2 = R_1 \left( \frac{V_{out}}{V_{in} - V_{out}} \right) \quad (23)$$

And from this the temperature (24) value

$$T = \left( \frac{R_2 - R_0}{R_0} \propto \right) \quad (24)$$

It is therefore necessary to correctly size the known resistance of the voltage divider.

Figure 19 shows the trend of the output voltage ( $V_{out}$ ) in the temperature range between 0 °C and 200 °C assuming a voltage  $V_{in} = 5V$ , the same provided by our microcontroller, and three different known resistances  $R_1$  respectively equal to 1200  $\Omega$ , 4700  $\Omega$  and 7000  $\Omega$ .

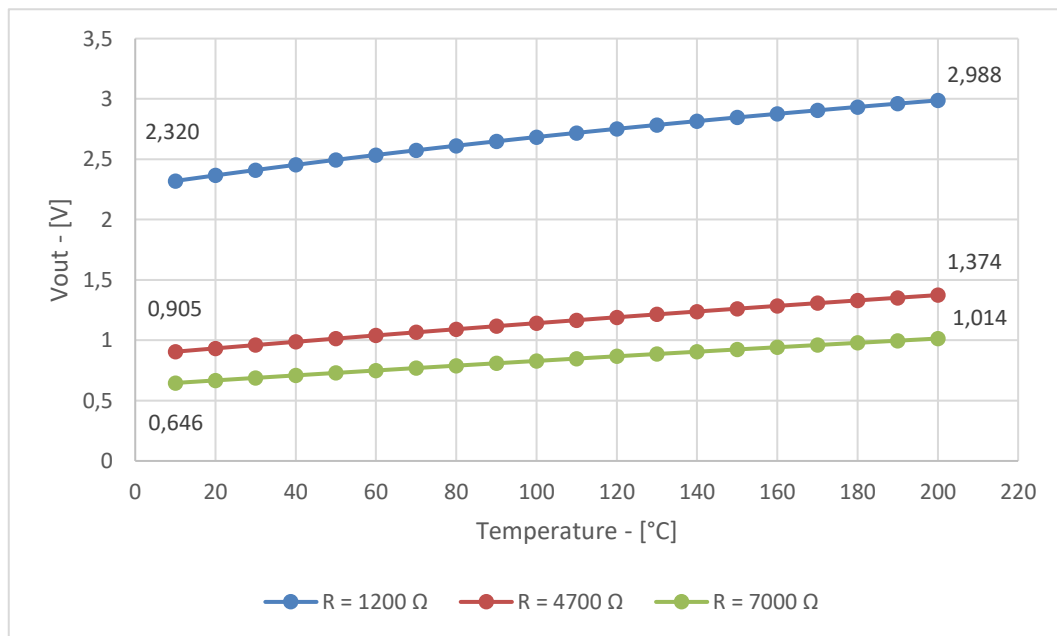


**Figure 19. Voltage range with different fix resistance value in the voltage divider circuit.**

Table 7 shows the average sensitivity of the voltage output when the known resistance R1 change. The sensitivity is calculated as:

$$S_v = \frac{\Delta V_{out}}{\Delta T} \quad (25)$$

With a  $\Delta T=190^\circ\text{C}$  is obtain:

	<b>R=1200 <math>\Omega</math></b>	<b>R=4700 <math>\Omega</math></b>	<b>R=7000 <math>\Omega</math></b>
<b>V<sub>out</sub> @ 200°C - [V]</b>	2,987698	1,374386	1,014421
<b>V<sub>out</sub> @ 0°C - [V]</b>	2,320332	0,905269	0,64627
<b>Delta V<sub>out</sub> - [V]</b>	0,667367	0,469116	0,368151
<b>Sensitivity - [V/°C]</b>	0,003512	0,002469	0,001938

**Table 7. Average sensitivity.**

The greater sensitivity is therefore obtained with the resistance equals to 1200  $\Omega$ . In the interval between 10 ° C and 200 ° C the resistance values will be included in the following range:

$$R_{min} = R_0 (1 + \alpha T_{min}) = 1039,08 \Omega$$

$$R_{max} = R_0 (1 + \alpha T_{max}) = 1781,66 \Omega$$

Setting the voltage full range  $V_{FR} = 5 \text{ V}$  and number of bit  $N_b=10$ , the quantization voltage  $V_q$ , is obtained as resolution of the analog/digital converter:

$$V_q = \frac{V_{FR}}{N_b} = 4,88 \text{ mV} \quad (26)$$

From the equation:

$$V_{out} = V_{in} \frac{R_0(1 + \alpha T)}{R + R_0(1 + \alpha T)} \quad (27)$$

At 50°C, with a  $V_T=2,495\text{V}$  ed  $R_1=1200 \Omega$  is obtained un uncertainty of:

$$\begin{aligned}
\Delta T &= \frac{\partial T}{\partial V_{out}} \Delta V_T \\
&= \frac{\frac{R + R_0}{V_{in}} R_0 A \left(1 - \frac{V_{out}}{V_{in}}\right) + \frac{R_0 A}{V_{in}} \left[\frac{V_{out}}{V_{in}} (R + R_0) - R_0\right]}{\left[R_0 A \left(1 - \frac{V_{out}}{V_{in}}\right)\right]^2} V_q \\
&= 1,19^\circ\text{C}
\end{aligned} \tag{28}$$

For the temperature value the equation is

$$T = \frac{\frac{V_T}{V_R} (R + R_0) - R_0}{R_0 A \left(1 - \frac{V_T}{V_R}\right)} \tag{29}$$

The temperature is therefore a function of:

$$T = f(V_{in}; V_{out}; R_1; R_0; A)$$

The absolute value  $\delta T$  of the temperature uncertainty is obtained starting from the absolute uncertainties  $\delta x_i$  of the quantities  $x_i$  through the relation:

$$\begin{aligned}
\delta T &= \left| \frac{\partial T}{\partial V_{out}} \right| \cdot \delta V_{out} + \left| \frac{\partial T}{\partial V_{in}} \right| \cdot \delta V_{in} + \left| \frac{\partial T}{\partial R_1} \right| \cdot \delta R_1 \\
&\quad + \left| \frac{\partial T}{\partial R_0} \right| \cdot \delta R_0 + \delta T^{sensor}
\end{aligned} \tag{30}$$

With a temperature of  $50^\circ\text{C}$  is obtained

$$\begin{aligned}
\left| \frac{\partial T}{\partial V_{in}} \right| &= \left| \frac{-R_0 [R_0 A V_{in} - R_0 A V_{out}] - [V_{in} (R_1 + R_0) - R_0 V_{in}] R_0 A}{[R_0 A V_{in} - R_0 A V_{out}]^2} \right| \\
&= 122,08^\circ\text{C}/V
\end{aligned}$$

$$\left| \frac{\partial T}{\partial R_0} \right| = \left| \frac{\left( \frac{V_{out}}{V_{in}} - 1 \right) \left( R_0 A \left( 1 - \frac{V_{out}}{V_{in}} \right) \right) - \left( \frac{V_{out}}{V_{in}} (R + R_0) - R_0 \right) A \left( 1 - \frac{V_{out}}{V_{in}} \right)}{\left[ R_0 A \left( 1 - \frac{V_{out}}{V_{in}} \right) \right]^2} \right|$$

$$= 0,31^\circ C / \Omega$$

$$\left| \frac{\partial T}{\partial R_1} \right| = \left| \frac{\left( \frac{V_{out}}{V_{in}} \right) \left( R_0 A \left( 1 - \frac{V_{out}}{V_{in}} \right) \right)}{\left[ R_0 A \left( 1 - \frac{V_{out}}{V_{in}} \right) \right]^2} \right| = 0,26^\circ C / \Omega$$

For the absolute uncertainties of the different quantities can be assumed

$$\delta V_{out} = \delta V_{in} = V_q = 4,88 \text{ mV}$$

For the measurement of the various resistances was used a digital multi-meter with the following features:

#### ■ DC Characteristics

Accuracy Specifications $\pm$ ( % of reading + % of range ) [ 1 ]						
Function	Range [ 3 ]	Test Current or Burden Voltage	24 Hour [ 2 ] 23°C $\pm$ 1°C	90 Day 23°C $\pm$ 5°C	1 Year 23°C $\pm$ 5°C	Temperature Coefficient /°C 0°C – 18°C 28°C – 55°C
DC Voltage	100.0000 mV		0.0030 + 0.0030	0.0040 + 0.0035	0.0050 + 0.0035	0.0005 + 0.0005
	1.000000 V		0.0020 + 0.0006	0.0030 + 0.0007	0.0040 + 0.0007	0.0005 + 0.0001
	10.00000 V		0.0015 + 0.0004	0.0020 + 0.0005	0.0035 + 0.0005	0.0005 + 0.0001
	100.0000 V		0.0020 + 0.0006	0.0035 + 0.0006	0.0045 + 0.0006	0.0005 + 0.0001
	1000.000 V		0.0020 + 0.0006	0.0035 + 0.0010	0.0045 + 0.0010	0.0005 + 0.0001
Resistance [ 4 ]	100.0000 $\Omega$	1 mA	0.0030 + 0.0030	0.008 + 0.004	0.010 + 0.004	0.0006 + 0.0005
	1.000000 k $\Omega$	1 mA	0.0020 + 0.0005	0.008 + 0.001	0.010 + 0.001	0.0006 + 0.0001
	10.00000 k $\Omega$	100 $\mu$ A	0.0020 + 0.0005	0.008 + 0.001	0.010 + 0.001	0.0006 + 0.0001
	100.0000 k $\Omega$	10 $\mu$ A	0.0020 + 0.0005	0.008 + 0.001	0.010 + 0.001	0.0006 + 0.0001
	1.000000 M $\Omega$	5 $\mu$ A	0.002 + 0.001	0.008 + 0.001	0.010 + 0.001	0.0010 + 0.0002
	10.00000 M $\Omega$	500 nA	0.015 + 0.001	0.020 + 0.001	0.040 + 0.001	0.0030 + 0.0004
	100.0000 M $\Omega$	500 nA    10 M $\Omega$	0.300 + 0.010	0.800 + 0.010	0.800 + 0.010	0.1500 + 0.0002

Figure 20. Multi-meter accuracy.

So were calculated the following quantities:

$$\delta R_0 = 0,31 \left[ 1000 \frac{0,010}{100} + 1000 \frac{0,001}{1000} \right] = 0,03131 \Omega$$

$$\delta R_1 = 0,26 \left[ 1200 \frac{0,010}{100} + 10000 \frac{0,001}{1000} \right] = 0,0338 \Omega$$

$$\delta T^{Sensor} = 0,55\text{ }^{\circ}\text{C}$$

In conclusion, we can state that the global uncertainty of the measurement system used is equal to:

$$\delta T = 1,19 + 0,5958 + 0,03131 + 0,0338 + 0,55 = 2,40^{\circ}\text{C}$$

The value found meets the temperature monitoring needs for the cast iron brake blocks.

With a temperature of 200°C, instead of 50°C, the global uncertainty is lower than the 3% of the reading.

### **5.1.3. Differential pressure sensors**

In the initial phase of this project in order to describe and define the operating phases of a freight wagon was decided to monitor the braking system. Moreover, as evidenced from the study of the company's historical failures and as reported in the literature, the main problems of freight wagons concern the pressures of the braking system. Often the pressure values at which the braking system operates do not correspond to those established during the revision due to the deterioration of components inside the devices inside the pneumatic brake system such as gaskets, springs and calibrated holes.

The monitoring of the pressures of the braking system is important both during the run and during stops at the train station.

In fact, while in the first case, during the run it should be check the correct level of pressure, in the second it is possible to determine the presence of pressure losses if the brake pipe pressure falls beyond a specific value in a given period of time established by the regulations.

Moreover, during the train run it is also possible to verify that the train engineer has taken a full brake release before proceeding with a new traction phase.

Due to the operating pressure of the braking system, was decided to install three differential pressure sensors with a measuring range from 0 to 7 bar. The resolution

of the pressure sensor obtained by our monitoring system was 7mbar. The specific model chosen for the realization of the system was the NPX MPX5700DP, a sensor specifically designed to work with acquisition systems employing a microcontroller or microprocessor with A/D inputs.

Figure 21 shows the operating characteristics of the sensors obtained from the datasheet.

Characteristic	Symbol	Min	Typ	Max	Unit
Pressure Range <sup>(1)</sup> Gauge, Differential: MPX5700D Absolute: MPX5700A	P <sub>OP</sub>	0 15	— —	700 700	kPa
Supply Voltage <sup>(2)</sup>	V <sub>S</sub>	4.75	5.0	5.25	Vdc
Supply Current	I <sub>O</sub>	—	7.0	10	mAdc
Zero Pressure Offset <sup>(3)</sup> Gauge, Differential (0 to 85°C) Absolute (0 to 85°C)	V <sub>off</sub>	0.088 0.184	0.2 —	0.313 0.409	Vdc
Full Scale Output <sup>(4)</sup> (0 to 85°C)	V <sub>FSD</sub>	4.587	4.7	4.813	Vdc
Full Scale Span <sup>(5)</sup> (0 to 85°C)	V <sub>FSS</sub>	—	4.5	—	Vdc
Accuracy <sup>(6)</sup> (0 to 85°C)	—	—	—	±2.5	%V <sub>FSS</sub>
Sensitivity	V/P	—	6.4	—	mV/kPa
Response Time <sup>(7)</sup>	t <sub>R</sub>	—	1.0	—	ms
Output Source Current at Full Scale Output	I <sub>O+</sub>	—	0.1	—	mAdc
Warm-Up Time <sup>(8)</sup>	—	—	20	—	ms

**Figure 21. Differential pressure sensor characteristics.**

The pressure monitoring was obtained by connecting the sensors at the same attachment points used during the periodical brake tests performed at the maintenance workshop.

It was possible to monitor the pressure of the brake pipe, the brake cylinder, and the weighing valve of the central bogie, one of the three bogies of the intermodal freight wagon sensorized. The pressure values of the weighing valve were essential to correctly estimate the mass of the load transported. In fact, to establish the load of a freight wagon it is necessary to monitor the weighing valve or to install load cells on the bogie.

The pressure sensors, after having been calibrated in the laboratory, were tested in the maintenance workshop by connecting them to the braking system. To make this link, we used the diagnostic connection on the braking system. With the brake tester equipment, we supplied a known value of pressure to the braking system. Then these data were compared with those provided by the monitoring system. The mean of the relative errors of the various measurements was 3.2%.

#### 5.1.4. GPS module

The information related to the position of the train, collected using GPS, was extremely important because it allows to know the position and speed of the train and to correlate the parameters measured with the track of the train. Without the knowledge of the position, in fact, there is no space reference and it is impossible to carry out any further analysis by correlating the monitored data with the behavior of the freight wagon along the railway track.

The GPS information also allows us to calculate the distance traveled by the train during the entire monitoring period. This information represents an important data for the maintenance of the train and an essential data for the reliability related to the monitoring system. All the devices presented in the paragraph concerning the solutions available on the market have a GPS device.

The simple information on the kilometers traveled by a wagon makes it easier to program its ordinary scheduled maintenance, bringing it forward if the wagon travels many kilometers, delaying it if it is not used for long periods of time.

The GPS signal was sampled with a frequency of 1 Hz, the maximum sampling frequency allowed by the device. The GPS signal, as mentioned above, also allows synchronization of measured data with time.

In case of no GPS signal (e.g. inside the railway galleries), the monitoring system is able to continue sample the physical parameters with the same sample frequency, equals of 1 Hz. In these cases the reconstruction of the behavior of the wagon on the section of track without GPS information is more complicated.

Table 8 reports the essential characteristics of the GPS module selected for this first installation. Higher performance for a GPS are not necessary in a device like this, whose purpose can also be to make only geolocation.

<b>GPS characteristics</b>	
Horizontal position accuracy	2.5 m
Maximum navigation update rate	1 Hz
Speed accuracy	0.1 m/s

**Table 8. GPS characteristics.**

The railway environment is hostile to the reception of the GPS signal due to the high amount of iron present and the position in which the monitoring system is

installed. It is therefore necessary to use a high performance GPS module or to adopt an antenna that allows signal reception. The GPS signal can also be used to temporally synchronize the different nodes of the wireless monitoring system, ensuring a time reference for communications.

### **5.1.5. Accelerometer ADXL345**

A digital accelerometer was used to monitor the dynamics of the body frame. The accelerometric sensor is produced by the Analog Device and is the ADXL345 model. This product is widely used in consumer electronics due to its characteristics.

The main advantages of this device are:

- low cost;
- low energy consumption;
- the possibility of recognizing different phases, detect the presence or lack of motion and if the acceleration on any axis exceeds a user-set level. This feature was used to develop a power saving algorithm to extend the life of the power supply batteries;
- high reliability;
- the possibility of being programmed by offering four different measurement range, with the related scale factor.

In the configuration adopted, with the measuring range equal to  $\pm 2g$ , the sensitivity is 3.9 mg. This sensitivity made it possible to measure the on board accelerations due to the phases of deceleration and interaction with the railway line.

In particular, we studied the longitudinal acceleration, key determinant of the braking operations, and the vertical acceleration. The vertical acceleration values, in addition to providing an important information on the interaction of the wagon with the railway track, represent an excellent basis for the correct design of an energy harvester device [21] [22] that is able to satisfy the energy consumption of the system.



## 5.2. Hybrid wired-wireless prototype

The second prototype developed adopts, if compared with the first one, two main novelties:

- The integration of a wireless device for the communication of the central node with a monitoring system installed outside the axle box cover.
- The implementation of a power saving algorithm to allow a strong reduction in energy consumption. This algorithm has to be developed due to the greater amount of energy introduced by the wireless communication.

Also in this second device developed no energy harvester has been installed, as it is not the purpose of this thesis.

### 5.2.1. Base station

The arrangement and connections of the components of the central node have been modified in order to ensure the reduction of energy consumption thanks to the total shutdown of the various sensors. The developed software must therefore correspond to a dedicated hardware part. In addition, some hardware connections have been revised to ensure greater system reliability. The Figure 22 below shows a block diagram of the central node.

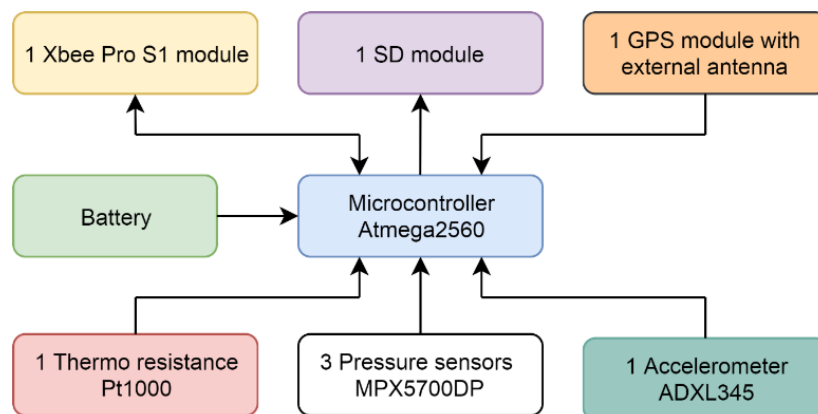


Figure 22. Base station diagram.

As can be seen, an Xbee Pro S1 radio module was introduced to allow radio communication between the two nodes. The Xbee radio modules adopt the

communication standard IEEE 802.15.4, this device was the base for the wired-wireless monitoring system presented. This radio technology is widely used, in fact it offers a good radio range and easy management of data to be sent and received thanks to the serial communication with which it is equipped.

The Xbee/Zigbee and RF modules are widely present in the literature for the implementation of monitoring systems dedicated to rail transport [27].

The need to monitor the axle box temperature trend for our study, led us to develop a new monitoring system equipped with a small WSN (Wireless Sensor Network). Grudén [23] developed and tested on a train wagon a device for monitoring the temperature of the bearing using WSN, highlighting which are the key aspects that have to be taken into account when a WSN is applied on a wagon. They also investigated which energy scavenging technique might be used for the power supply of the WSN. Franceschinis [24] introduced some network architectures adopting low-power wireless communication technologies. Their research suggests that the combined use of WSN and Wi-Fi in a hierarchical architecture is adequate for long trains with a large number of sensing nodes. Chiocchio [25] proposed a plug-and-play solution for continuous monitoring of both wagon units and trains in order to improve freight trains safety and enable a more efficient overall management. The prototype developed was tested in lab facility. Hodge [26] analyzed the wireless sensors network technology for monitoring in the railway industry. They focused on practical engineering solutions highlighting advantages and disadvantages of each solution in a comparative review. Mahasukhon [27] studied the existing wireless technologies such as the IEEE 802.15.4 communication protocol and the fact that they are unable to provide reliable service. They propose a multi-tier multi-hop network to overcome the typical issues of performance and reliability of this protocol in a railroad environment.

In this project it was decided to adopt a 2.4 GHz Xbee XBP24-AWI-001 module for monitoring the temperature of the axle box. For this project and prototype stage, the objective was not to create a wireless monitoring system but to investigate if the high temperatures reached both by the cast iron brake blocks and the wheels, during the descent of the alpine railways, can influence the temperature inside the axle boxes.

In any ways a good wireless monitoring system developed for freight wagons must be focused on the single wagons and not on the whole train. In fact the wagons that make up the train are not always the same and are not owned by the same company. They must communicate with the train driver and the company owners of the wagon in case of fault or derailments.

The Figure 23 below shows the central node before the installation on the wagon.

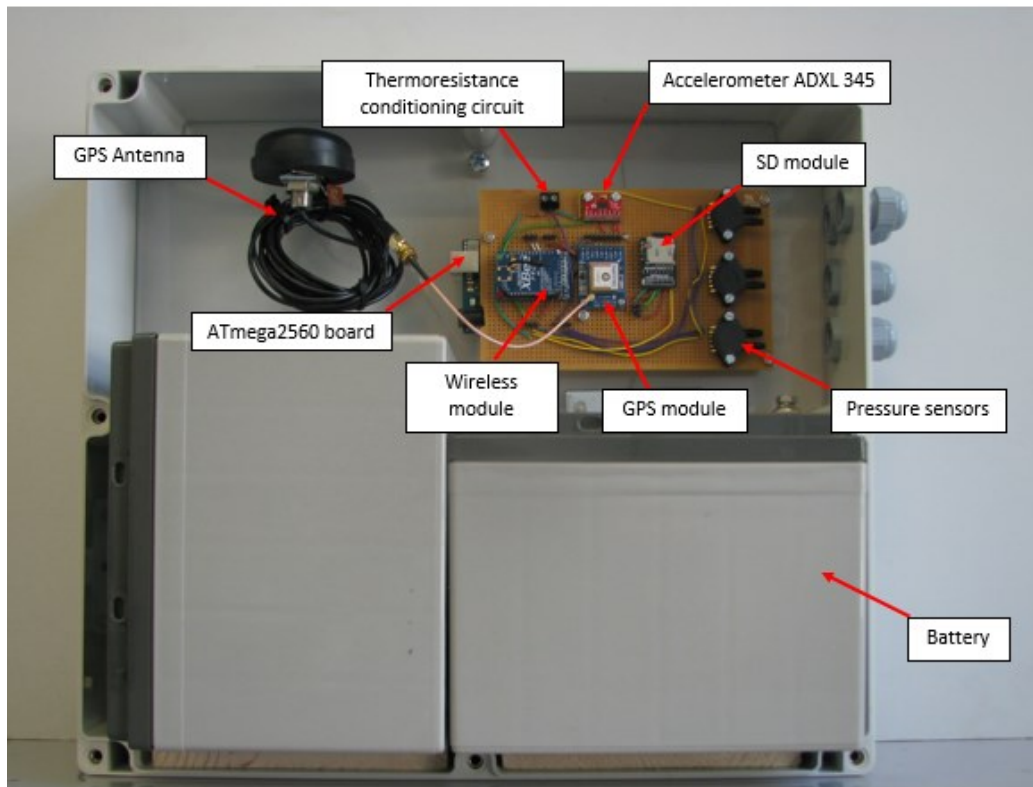


**Figure 23. Base station with battery pack.**

As can be seen the battery pack is composed by two 12V 35Ah gel lead acid battery connect in parallel. The installation of a battery pack with a so high energy content is due to ensure a sufficient autonomy to monitor with safety a few round trips without having to go to the company terminal to replace the batteries with new ones.

### 5.2.2. Axle box node

The axle box node was designed following the experience gained with the base station. The two devices in fact share many hardware parts and much of the software. The power save software presented in paragraph 5.2.3.2 is in fact the same for both devices.

The Figure 24 below shows a block diagram of the axle box node.

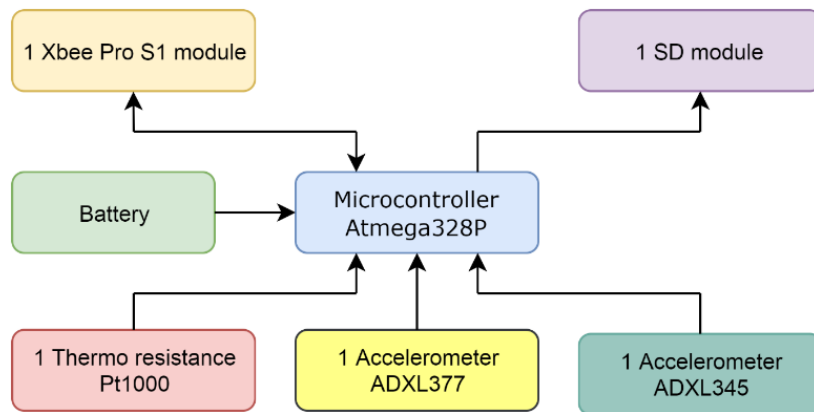


**Figure 24. Axle box node diagram.**

Due to the limited availability of space, for housing the battery, inside the box and the need to minimize the energy consumption of this node the design and realization of the axle box node was completely new. The axle box node owns, as is already the case for the base station, a wired part for monitoring the axle box temperature and a wireless part for communicate with the base station.

The axle box node consist of the following hardware components:

- 1 microcontroller Atmega328P,
- 1 accelerometer ADXL345
- 1 accelerometer ADXL377
- 1 thermos resistance Pt1000
- 1 Xbee Pro S1 module
- SD module

The performance of the microcontroller Atmega328P, shown in Table 9, are lower than those used for the base station, but in this application less computational efforts are required. Here the microcontroller has to manage only the two

accelerometers and the temperature sensor, as well as send, receive and save the wireless communication data.

Processor	Memory			I/O	
	Flash [kb]	EEPROM [kb]	SRAM [kb]	Digital I/O pins	Analogue I pins
<b>ATmega328P</b>	32	1	2,5	14	6

**Table 9. ATmega328P characteristics**

The ADXL345 accelerometer is the same used in the base station. In this application the accelerometer was used at first to manage the power save algorithm, leaving the other accelerometer to monitor the dynamics of the wagon.

The ADXL377 is an analogue accelerometer and allows to monitoring the accelerations in the  $\pm 200g$  range. The resolution of the monitoring system, equipped with an 8-bit microcontroller, on a range between 0 - 3.3 V is therefore about 0.5g. Such a resolution value makes it suitable for detecting shock events in which acceleration levels easily exceed 10g, but not for monitoring the axle box dynamics during normal operating conditions.

For the monitoring it was therefore necessary to use the digital accelerometer, thus programming it both for the management of the device and for the dynamics of the axle box.

The Figure 25 below shows the axle box node before the installation on the wagon.

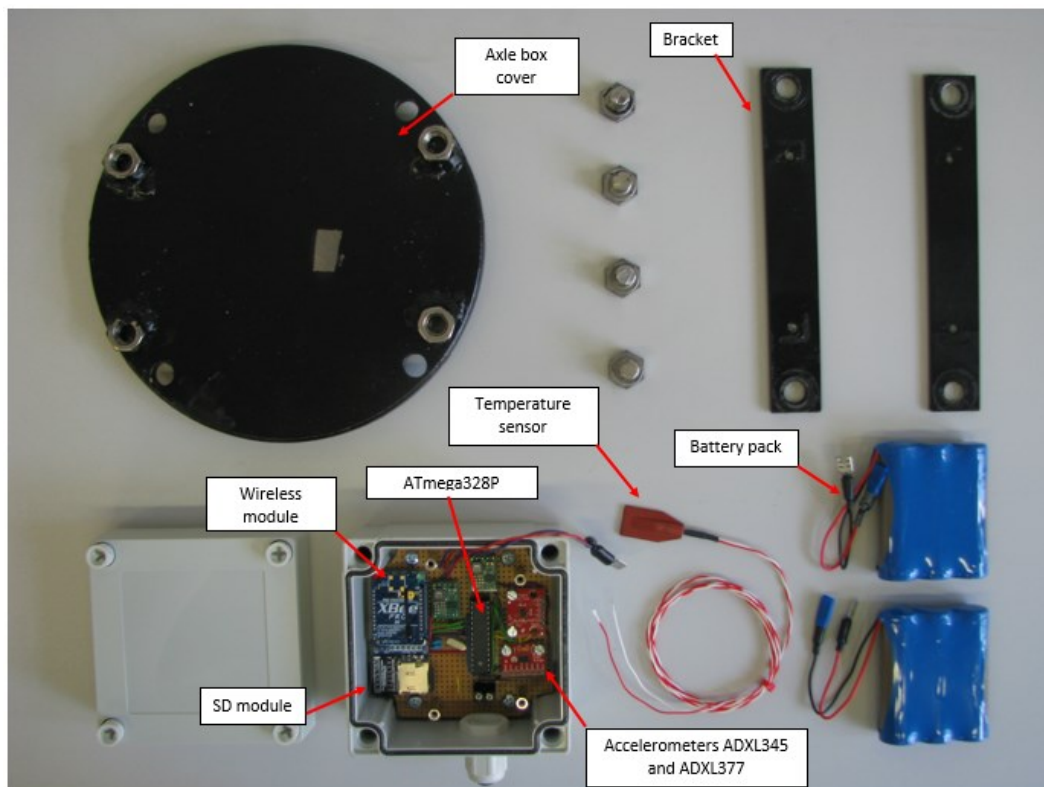


Figure 25. Axle box node.

### 5.2.3. Monitored parameters and operating algorithm

Summarizing what has been presented so far, the parameters monitored are respectively:

- Wired prototype and base station
  - Temperature of a brake block of the central bogie of the intermodal freight wagon monitored
  - Pressure of the brake pipe
  - Pressure of the brake cylinder of the central bogie
  - Pressure of the weighing valve of the central bogie
  - Accelerations on the three axes, expressed using the RMS (Root mean square), the maximum and the minimum.
  - GPS position
  - Speed of the wagon
  - Altitude
- Axle box node

- Accelerations on the three axes, expressed using the RMS (Root mean square), the maximum and the minimum, monitored using the two accelerometers present.
- External temperature of the axle box cover

### 5.2.3.1. RMS parameter

The accelerometric signal in its classic vibration wave contain a lot of information not simple to extrapolate. It is clear that the technique for the acquisition and analysis of data is very importance, in this sense: the study method, the sampling frequency, as well as the synthesis parameters to consider are not always the same, depending on the study that you want to play and the information that you want to find.

Against this background, it is necessary to consider appropriate parameters that are able to summarize the data sample by the accelerometer.

Often the analysis of a vibration signal expressed in terms of acceleration in the time domain is carried out by calculating different synthesis parameters, which allow the quantification of the level to be compared with the reference levels where these are potentially normed. Among these, one of the most widely used is the RMS value.

The RMS or Root Mean Square, in equation is the most significant measure of amplitude because it takes into account the history of the wave in time and gives an amplitude value directly related to the energy content of the vibration:

$$RMS = \sqrt{\frac{1}{T} \int_0^T x^2(t) dt} \quad (31)$$

where  $x(t)$  represent the trend of the signal in function of time and  $T$  is the duration of the signal.

In the case of digital signals consisting of  $N$  samples, the RMS value is evaluated by the following expression:

$$RMS = \sqrt{\frac{1}{N} \sum_{i=1}^N x_i^2} \quad (32)$$

The vibrations are closely linked to the forces that are exchanged between the bogie and rail during the driving. The RMS is a kind of average of the accelerations that are recorded, so it is also connected to the loads on the axle, but in mediated form.

This aspect, if on the one hand can be positive avoiding to create false alarms due to rare and isolated stress, on the other hand makes the system less reactive and less specific in detecting the cause of vibration of the bogie.

As can be seen from the formulas, the parameter RMS is much easier to calculate and, being a numerical value, is also very simple to be transmitted. However its calculation is influenced by the sampling frequency of the data, and especially from the time interval on which it is reported.

During the drive very often the railway vehicle is subject to sudden accelerations, maybe also of strong intensity, but insistent for a very short time lower than the second.

These sudden shock can be caused by several factors: a railroad switch, a stone, a weld joint between two rails. Therefore the RMS calculated in a span of more seconds has the advantage of reducing the importance of these events, highlighting instead excitations and phenomena which continue in time. On the other hand if the time interval used for the calculation becomes too long you may miss important information or worse would generate an alarm when it is too late and the event has already occurred.

A further parameter of analysis of the accelerometric signal is the CR or Crest Factor. This factor indicates how many times the RMS value is contained in the peak value.

$$CF = \frac{\text{Peak value}}{RMS} \quad (33)$$

The crest factor is a number fast and easy to calculate able to provide to engineers and technicians, some useful information in different situations. Its use is usually done with two different purposes:

- Obtaining information "hidden" on systems that produce the observed waveforms;



- Obtain information and estimates regarding the impact that an assigned waveform would have on systems designed to treat it, measure it or absorb it.

The effective value (RMS) of a variable over time is an index of the energy associated with it. There are many situations in which, in addition, it is necessary to know the highest value, maximum or minimum, assumed by the physical quantities. In this way it is possible to evaluate the stress excursion and to dimension the monitoring systems associated with it.

All the advantages of the crest factor are its definition. The simple relationship between the effective value and peak value of a waveform is very sensitive to short spikes present since it is independent of their duration, and then by their energy content. All the advantages of the crest factor are inside its definition. The simple relationship between the effective value and peak value of a waveform is very sensitive to short spikes since it is independent of their duration, and then by their energy content.

In the light of the above, it was decided to use the RMS parameter for the vibration monitoring. This parameter was calculated both from the base station device and from the axle box node.

With references to the literature and the experience gained over the years by the research group, it was decided to use a sampling frequency of 200 Hz for calculating the RMS, the maximum and the minimum of the signal once a second.

The absence of electricity on board also influences the hardware and software choices to take during the development of a monitoring device dedicated to the freight transport. The amount of energy that can be generated on board the wagon without developing excessively invasive and expensive systems is of the order of Watt. The adoption of a microcontroller with the above characteristics allows to have low energy consumption but, on the other hand, to perform a limited processing of the sampled data.

During this project it was decided to focus on this simple parameter thanks to the considerable amount of information contained in it and the low computational effort required.

### 5.2.3.2. Operating and power save algorithm

The aim of the thesis is the development of a demonstrator of a monitoring system dedicated to freight wagons, so we did not focus on the development of an energy harvester system able to recharge the batteries of the system.

In the absence of this algorithm, it was only possible to monitor a single round trip if the duration of the journey had not exceeded 12 days. Twelve days is in fact the energy autonomy of the system given by the battery packs. In the case of long stops of the wagon in the various European terminals of the partner company only the outward journey can be monitored.

The development of this algorithm [30] was therefore an obligatory choice to ensure a continuous and reliable monitoring of the outward and return trips on the lines.

For the development of this algorithm was exploited the use of two interrupt pins, one on the two microcontrollers and one on the accelerometer for the motion detection, as shown in Figure 26.

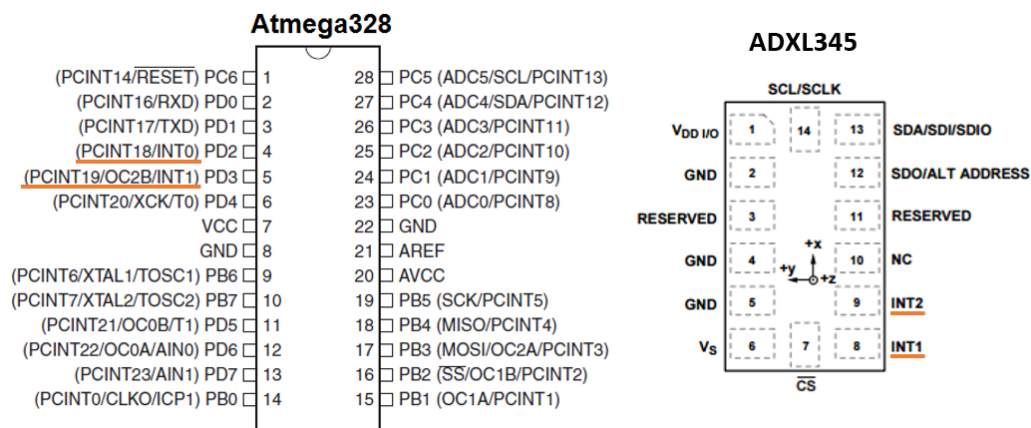


Figure 26. Interrupt used for the power save algorithms.

The sleep mode algorithm was the same for the two devices. The accelerometers ADXL345, installed on both devices, were used to detect the status of the wagon in order to distinguish the phase of motion from the phase of stop. This distinction was obtained by fixing a threshold value along the vertical axis.

The threshold value set on the vertical axis of the accelerometer is equal to the acceleration of gravity plus the sensitivity of the accelerometer, in order to ensure the starting of the device at every movement of the wagon.

When the threshold is exceeded, the devices exit from the sleep mode, turn on the sensors and the radio modules, start sampling the sensors and communicate with each other.

In Figure 27 can be observe a diagram that shows the sleep mode algorithm.

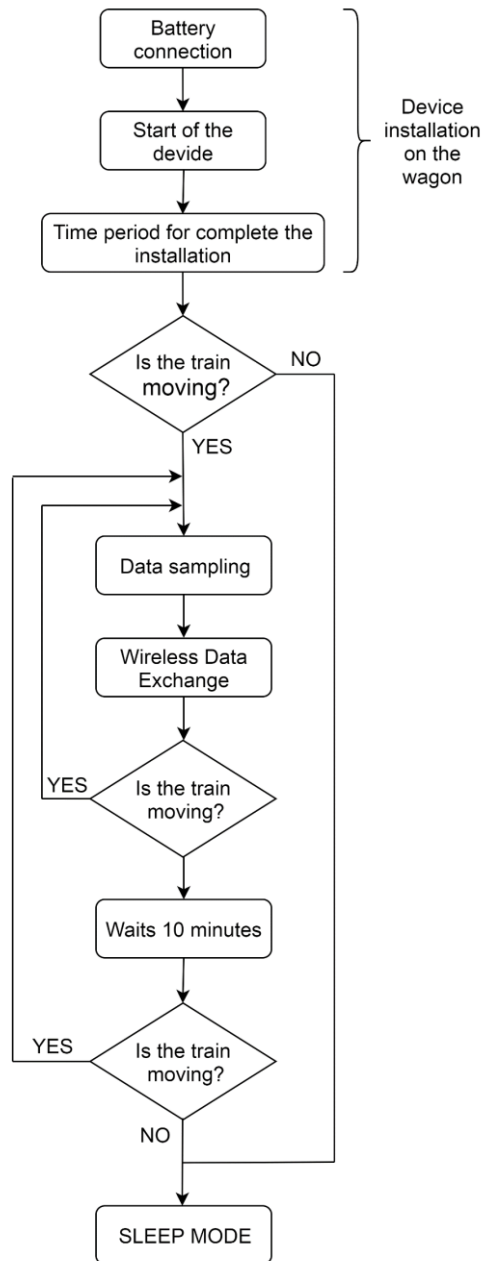


**Figure 27. Diagram of the power save algorithm.**

The first part of the algorithm was necessary to allow us to install the devices on the freight wagon. We have decided to do not install any switch for the start-up and shutdown of the monitoring system in order to obtain the maximum level of reliability.

Once the installation time has expired, if no activity is detected, the device goes into sleep mode. When the train leaves the terminal or the station and the acceleration along the vertical axis exceed a certain level, established through the previous on board measurements [29] and verified in laboratory using a shaker equipment, the devices turn on.

Every sampling cycle the devices control that the acceleration level is respected. Following sampling activity, there is the part of transmission of the data. The transmission of the data is different for the two installed devices.

Due to the high impact on the energetic consumption of the wireless transmission, it was necessary to adopt different solutions for the management of the Xbee modules.

The wireless module of the axle box node was only activated for the transmission of the data twice a minute in order to minimize the energetic consumption. Instead, the wireless module of the base station was always on in order to receive the data send by the axle box node. This choice was also dictated by the fact that the axle box node, despite having lithium batteries, has at its disposal a much lower amount of energy.

The Base Station sent to the axle box node the GPS position and the brake block temperature, while the axle box node sent his temperature. This data exchange was necessary for the subsequent analysis of the data collected along the track.

The parameters received by both devices are saved on the SD memories present in the two devices. The two monitoring systems and their Xbee modules were not synchronized with each other, but the sampling software, embedded in both, provide a certain time slot for the completion of the data transmission. In case of no communication in the available time slot the sampling software continues its work, trying again to contact the module at the next communication cycle.

When the train stops, the algorithm begins the phase to put the device into sleep mode. All the sensors and modules, except the accelerometer ADXL345, are switched off. If in the consecutive ten minutes, the train resumes to travel (e.g. short stops in station or along the track for red light) the devices come back completely active. Otherwise, if the train stops for a longer period, the microcontroller enter into sleep mode in order to reduce the energy consumption.

This algorithm, together with a correct sizing of the battery pack, will allow us to monitor multiple trips without the need to stop the wagon to replace the batteries.

The absence of an electrical system that can adequately power the necessary electronic devices is the major obstacle that is essential to overcome. Despite the great progress made by electronics to reduce the power consumption, in absence of a suitable on board energy source, the operation of the monitoring systems is limited by the capacity of the power supply batteries.

In Table 10 are reported the energy consumption of the two devices.

	<b>Sleep Mode</b>	<b>Start Sleep Mode Phase</b>	<b>Max Operating Consumption</b>
<b>Base Station powered @ 12.5 V</b>	54 mA (0.675 W)	100 mA (1.25 W)	200 mA (2.50 W)
<b>Axle box Node powered @ 7.9 V</b>	5 mA (0.039 W)	15 mA (0.119 W)	54 mA (0.426 W)

**Table 10. Energy consumption in different phases**

With the battery packs used and the energy consumption shown in the table, it was possible to monitor a total of about one month of monitored wagon activity.

As concern the line 1 presented in the previous section the average time to complete a round trip is equal to ten days, this time duration may further extend due to strike or breakdowns along the railway line.

The consumption data presented in the table can still be significantly improved by using the most modern miniaturization and electronics manufacturing techniques, reaching the levels of companies already present on the market with their devices. The values shown in the table, however, represent a valid energy reference point for the design and realization of energy harvesters capable of powering the monitoring systems and at the same time charging the battery packs.

# Chapter 6

## 6. Experimental measurements

### 6.1. The monitored wagon

The prototypes were installed on an intermodal wagon, type “Sggmrs”, which is a special type of wagon used for container transport. This is a two-unit articulate wagon with 3 bogies Y25 for a total of 6 axles. Each axle is equipped with 8 cast iron brake blocks. This type of wagon is equipped with folding fastening devices having the cone of the fixing devices in line with the UIC 571-4 regulation. The loading of the wagon is normally achieved directly on the platform with specific lifting installations, with containers being placed on the cones of the devices. Figure 28 shows an example of the monitored wagon.

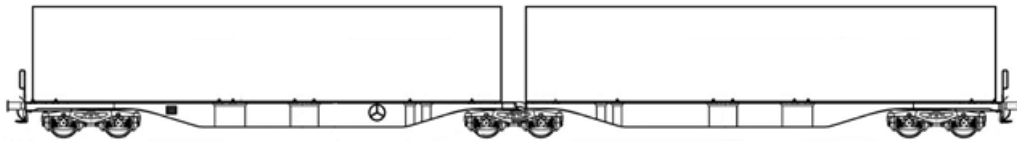


**Figure 28. Intermodal freight wagon Sggmrs 90.**

During this research activity only the central bogie was sensorized because, being the most heavily loaded, it is the most stressed during braking operations. The installation of the devices was made following a complete inspection of the wagon so that the data recorded during the monitored installations were not influenced in any way by faults or malfunctioning.

The central monitoring systems [31] , Figure 29, were fixed to a steel plate of the freight wagon, on the inner side of the frame.



**Figure 29. Central monitoring systems installed on steel plate.**

For the axle box node [30] , Figure 30, was modified an axle box cover, levelling the surface to allow the welding of nuts for fixing the box in which the device was housed.

The temperature sensor was glued and siliconised on the outer surface of the cover, so the recorded temperature values are slightly lower than the real values inside the axle box.

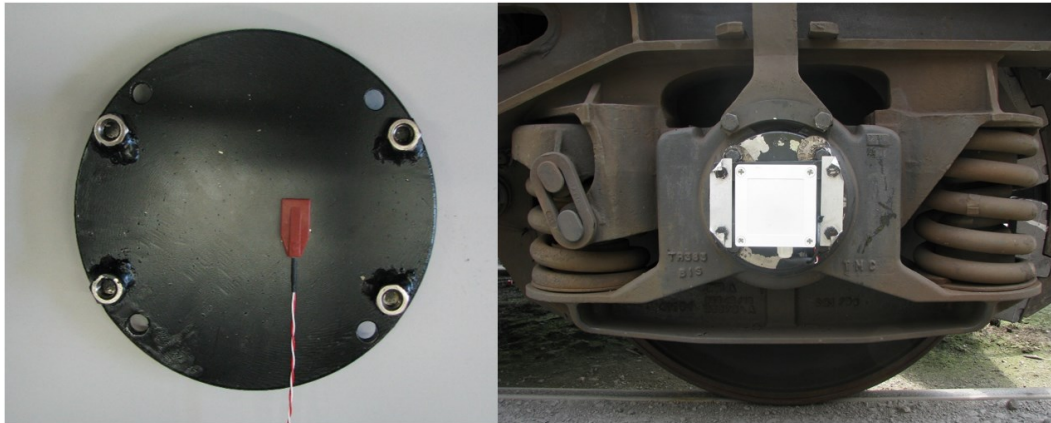


**Figure 30. Axle box node monitoring system.**

## **6.2. Brake blocks sensorization**

Particular attention was given to the sensorization of the brake blocks. Before proceeding with the installation on the wagon, several bench tests were conducted comparing the value of the temperature detected by the monitoring system to the

one measured with an infrared thermometer in order to verify its calibration and its accuracy. The infrared thermometer had an accuracy of 1% of reading. Our monitoring system instead had an accuracy lower than the 3% of reading at 200°C.

Numerous adhesives were tested to find the one that offered the best performance at high temperatures. After a series of preliminary laboratory tests, a silicone glue produced by Loctite was chosen and a further protective layer was applied above this first layer using a refractory glue resistant up to 1000°C.

During the first installation the temperature sensors were simply glued to the brake blocks near to the attack point for the brake hanger. This solution, however, was abandoned because it did not guarantee an exhaustive sensors lifetime due to the mechanical and thermal stresses.

Subsequently, it was decided to perform a seating, Figure 31, in which the temperature sensor was drowned, thereby making it more resistant to stress. The seating used had a depth of about 2 mm, a length of 20 mm, and a width of about 4 mm. The wiring of the sensor was also adequately fixed to the brake hanger so that the weight of the connecting cables did not burden on the sensor.



**Figure 31. Brake block sensorization.**



The sensorization of the brake block was carried out in our laboratories. It was necessary to make the seating for the sensor, install it, and apply the necessary glue. Furthermore, at each step, it was necessary to verify the correct functionality of the sensor to ensure the subsequent operation.

Every time the brake block and the relative sensor were replaced, to guarantee a uniform braking, it was necessary to replace all the brake blocks of the same wheelset.

### **6.3. The monitored railway lines**

Generally measurements presented in literature not exceed 200 km on railway lines [32] [33] or are conducted on European railway test circuits (e.g. Velim (CZ)) [15]. This work shows the monitoring of a freight wagon, under normal operating conditions, for distances over 500 km for each individual journey.

The railway lines monitored were two and connect the terminals of the company partner of the project. The first line, Figure 32, connects the terminal of Candiolo (TO-Italy) to the one in Mouguerre (FR), the distance between these two points is about 1400 km. Instead the second line, Figure 33, connects the terminal of Gallarate (VA-Italy) to the one in Mechelen (B), in this case the distance is about 900 km.

The two lines are distinguished by the different altitude profile of the route. The Line 1 (Candiolo - Mouguerre) is characterized by the crossing of the Frejus alpine Railway and the tunnel of the same. On the route connecting the Italian terminal with the French one, the railway wagons must cover the railway between Bardonecchia (IT) and Modane (FR). For the braking system, this stretch is considered one of the hardest alpine railways, due to the altitude profile of the route that reaches gradients of 30‰ on the French and Italian sides (the Gotthard railway reaches 26 ‰, the Brenner railway 25 ‰ and Simplon railway 9.5 ‰). The altitude profile of the route monitored is thus the main cause of the high consumption of the brake blocks. Along the same lines, it was also possible to monitor the long sector of the track in plains. This was the ideal situation for the study of the braking operation.



**Figure 32. The railway line Candiolo (IT) - Mouguerre (FR).**

The altitude profile of the line 2 (Gallarate - Mechelen) is characterized by a reduced maximum altitude thanks to the Swiss railway infrastructure built in the last twenty years, especially when the Lötschberg base tunnel is crossed instead of the historical Lötschberg tunnel, dating back to 1913.



**Figure 33. The railway line Gallarate (IT) - Mechelen (B).**

Between November 2015 and June 2016, the developed monitoring system covered various outward and return journeys on the lines presented. On the first line were monitored approximately 25,000 km of railway track, on the second line instead less than 2,000 km. The hybrid wired-wireless prototype was only tested on the second line.

Thanks to its modularity, between two consecutive installations it was possible to make changes in both software and hardware, allowing us to find the best configuration for the installed sensors. In particular, it was necessary to try different solutions for the fixing of the temperature sensors to obtain a continuous signal on the outward and return journeys.

The processing of the collected data has allowed to obtain two different types of information: logistical and general operation of the wagon.

## **6.4. Logistical information**

Logistical information are low-level information and devices currently on the market made this data available. Very few wagons in Europe right now adopt this device, but they are essential to maximize the fleet potential. In Europe and in the entire world are present railway operators that own and rent thousands of wagons every year without the possibility of knowing the position of the cars. Knowing the position it is possible to reconstruct with a high precision the mileage covered by wagons. This information allows to anticipate or delay scheduled maintenance operations, thus maximizing the economy and safety of rolling stock.

Logistical information, obtained using the GPS module, includes the kilometers covered, the travel time, the commercial speed, and the average speed calculated on the whole track. The kilometers traveled were identical in all the monitored trips, whereas the remaining logistical parameters are changed depending on the line status.

Table 11 and Table 12 summarize some logistical and overall behavior information for the outward and return journeys of two different cases. The two cases had the same type of on-board unit hardware and operate in the same season but in different months. These parameters are strongly influenced by the state of the line. They are also influenced by specific days of the week in which the wagon was travelling. It can be observed that there is a significant difference between the

average speed and the commercial speed, which is the distance between the origin and destination of a train divided by the total journey time, including intermediate stops, due to the change of locomotive made once exceeded the national borders. The number of braking and the kilometers covered with the brake activated are other parameters strongly influenced by the train driver.

		Outward journey	Return journey
<b>Case A</b>	Length [km]	1394	1394
	Kilometers monitored	1394	1394
	Time for terminal to terminal [h]	28.3	87.4
	Effective time of travel [h]	18.6	20.7
	Commercial speed [km/h]	48.3	15.6
	Average speed [km/h]	73	64.9
	Average pressure weighing valve [bar]	3.9	3.6
	Number of brake activation	136	121
	Distance covered with brake active [km]	87.3	113.5

**Table 11. Logistical information: Line 1 - Case A.**

		Outward journey	Return journey
<b>Case B</b>	Length [km]	1394	1394
	Kilometers monitored	1394	1394
	Time for terminal to terminal [h]	29	42.6
	Effective time of travel [h]	19.5	19.4
	Commercial speed [km/h]	47.3	32.3
	Average speed [km/h]	70.4	70
	Average pressure weighing valve [bar]	3.5	3.8
	Number of brake activation	176	98
	Distance covered with brake active [km]	91.3	64.4

**Table 12. Logistical information: Line 1 - Case B.**

Comparing Table 11 and Table 12, it can be seen that the values of travel time, average and commercial speed are very similar, particularly for the outward journeys. The number of brake activations, and consequently the distance covered with the brake working, is a parameter strongly influenced by the status of the railway line and connected with the presence or absence of passenger trains on the line. This fact highlights the extreme repeatability of the measurements performed.

Table 13 and Table 14 report a comparison between the outward and return journeys of the previous two installations in the limited part of the track inside Frejus Tunnel.

		<b>Outward journey</b>	<b>Return journey</b>
<b>Case A:</b>  <b>Frejus Tunnel</b>	Length [km]	13.636	13.636
	Kilometers monitored	13.636	13.636
	Travel time [s]	862	846
	Average pressure brake cylinder [bar]	1.1	0.9
	Number of brake activation	7	1
	Time with brake active [s]	311	35
	$\Delta$ Temperature between enter and exit [°C]	147	22

**Table 13. Frejus Tunnel Line 1 - Case A.**

		<b>Outward journey</b>	<b>Return journey</b>
<b>Case B:</b>  <b>Frejus Tunnel</b>	Length [km]	13.636	13.636
	Kilometers monitored	13.636	13.636
	Travel time [s]	684	765
	Average pressure brake cylinder [bar]	0.8	0.5
	Number of brake activation	6	1
	Time with brake active [s]	255	52
	$\Delta$ Temperature between enter and exit [°C]	96	25

**Table 14. Frejus Tunnel Line 1 - Case B.**

## 6.5. Operating data

The following four figures (Figure 34–Figure 37) summarize the parameters of altitude, speed, brake cylinder pressure, and temperature of brake block of two trips including outward and return journeys. The graphs in the figures show the data of about 5600 km of the 25,000 km monitored on the line 1 between Candiolo (IT) and Mouguerre (FR). To monitor a such extent distance and period of time, it was necessary to accurately size the battery pack to be sure to monitor the whole journey, take advantage of the rare opportunity offered by this research project and the willingness of the company to make available his wagon and his skills.

As can be seen, the monitored temperature trends were almost specular in both outward and return journeys for both installations. The maximum temperature levels reached on the mountain section were almost identical and demonstrate that the temperatures reached by cast iron brake blocks on this section of the railway track are higher than 200°C. The temperature values recorded are related to the point application of the sensor. At the interface wheel-brake blocks, the achieved

values are much higher as emphasized the measurements value obtained by Vernersson and Lundén [15] .

It should be pointed out that these data were measured on a wagon just inspected and with excellent operating conditions. In case of failure, the brake temperature may exceed  $250^{\circ}\text{C}$  in the measurement point.

It can be observed that in flatland driving conditions, especially in the section between 600 and 800 km, the temperature never exceeds  $100^{\circ}\text{C}$  but rather stands at  $70^{\circ}\text{C}$ .

The figures also show that, in some plain parts of the route, the brake were not activated for tens kilometers, allowing the brake blocks to dissipate the heat accumulated in the previous braking.

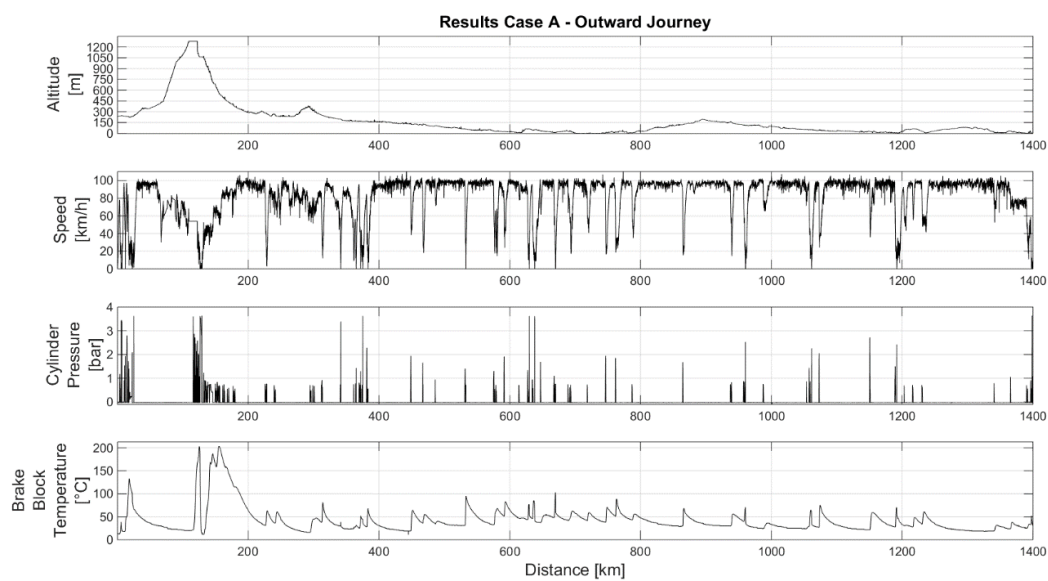


**Figure 34. Line 1 - Case A: Outward journey.**

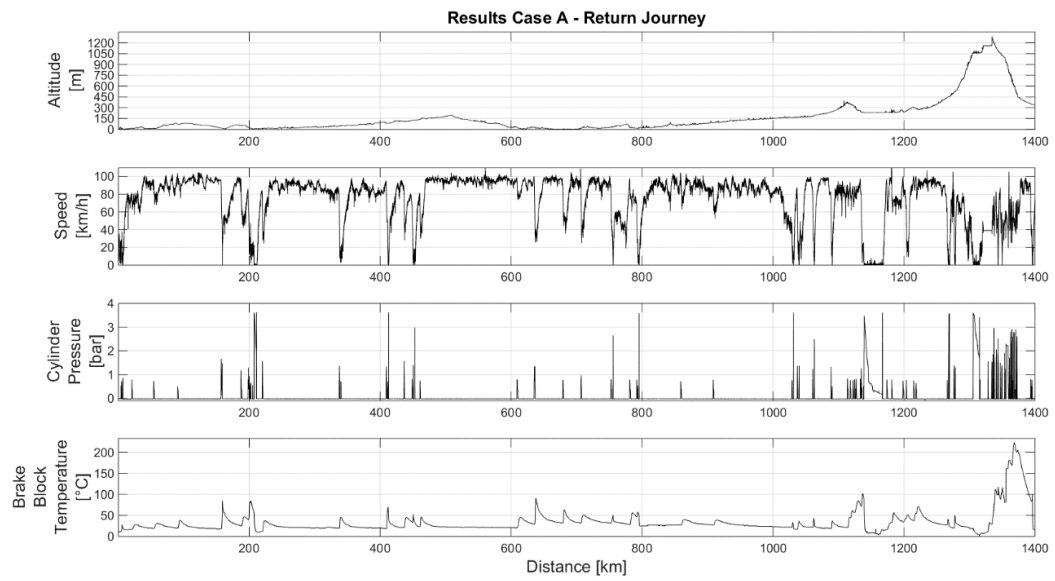


**Figure 35. Line 1 - Case A: Return journey.**

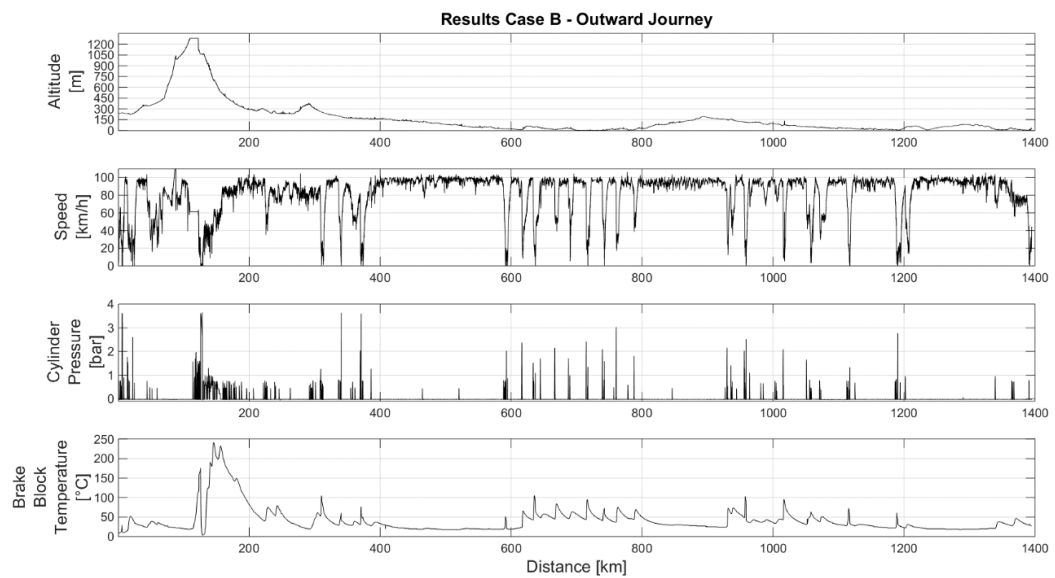


**Figure 36. Line 1 - Case B: Outward journey.**

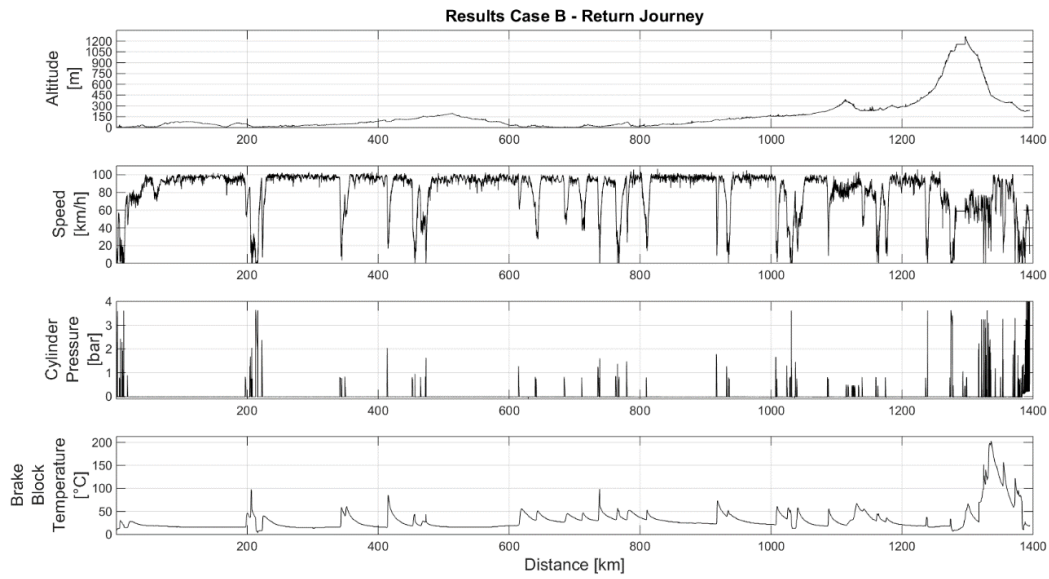


**Figure 37. Line 1 - Case B: Return journey.**

Figure 38 and Figure 39 show the data relating to the outward and return journey on the line 2, which connects the terminal of Gallarate (IT) to the one Mechelen (B). As can be seen from the figures, the line covered for the outward journey is different to the one for the return. The newest infrastructure allows to considerably reduce the altitude variation if compared with the historical line. All this results in less components wear.

The average temperatures on the line 2 are on average lower but reach peaks completely comparable with those of line 1. The temperature peaks are also strongly influenced by the driving behavior adopted by the train driver.



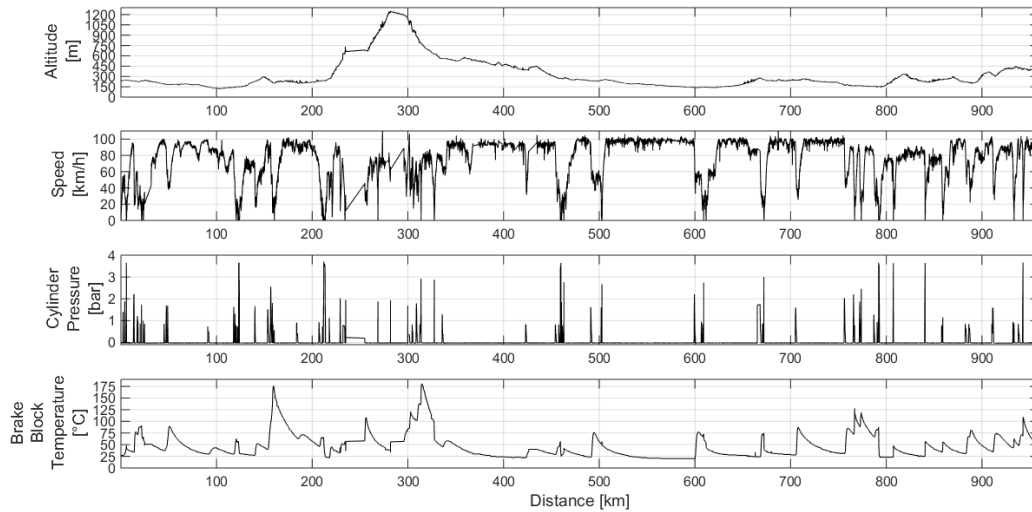


**Figure 38. Line 2 - Case A: Outward journey.**

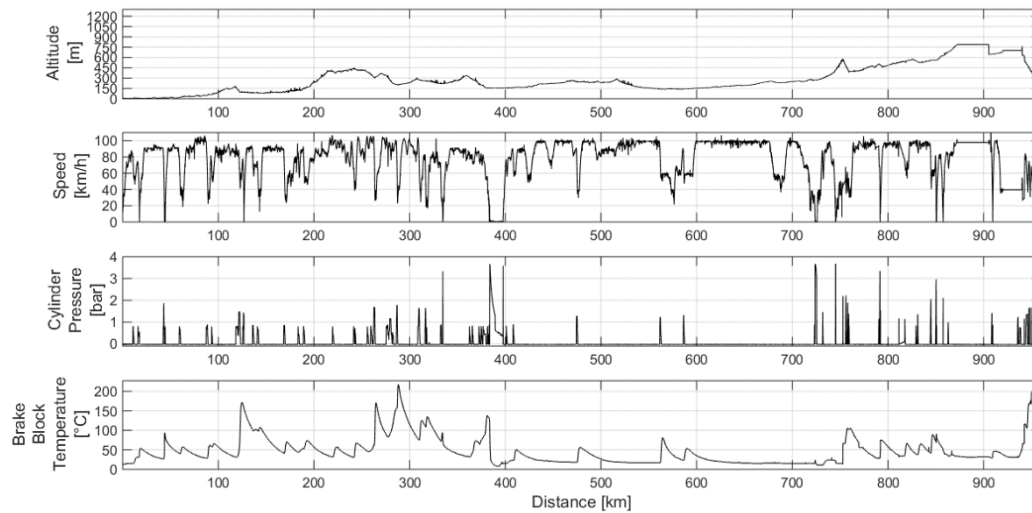


**Figure 39. Line 2 - Case A: Return journey.**

Observing the graphs, which show the distance parameter on the abscissa axis, can be seen that the train can travel distances close to one hundred kilometers without the need to activate the brakes. Every single braking, however, presents a net and significant increase in the temperature increase at the point of application of the sensor, which is one of the most distant points from the interface wheel tread brake block.

A parameter not analysed in this study, but present in literature, is represented by the different temperature variation depending on the position of the wagon inside the train composition. Due to the braking delay generated by the propagation of the

depression wave, it is clear how the brakes of the first wagons remain activated for a longer period of time and must initially also brake for the cars in which the brakes have not yet operated. This event is amplified as the length of the train increases.

## 6.6. Axle box temperature

Currently the temperature of the axle boxes are measured with devices positioned along the railway line known as RTB. This system is currently in use on most existing lines and a regulation currently in force regulates the operation and layout along the track. The RTB system is a temperature detection technique for moving organ based on infrared sensors. It is well known that everybody emits electromagnetic waves, or radiation, depending on its temperature level. During radiation dispersion, energy is transported: this means that radiation can be used to measure the body temperature without contact, as the irradiated energy and its typical wavelengths depend mainly on the temperature of the irradiating body.

This property is extremely useful for measuring the temperature on moving parts such as the axle box of railway bogie. Measurement techniques are based on infrared systems, which allow the capture of temperature during fast and dynamic processes, thanks to the support of dedicated sensors and systems.

The system is able to provide two types of alarms:

- ABSOLUTE, the temperature exceeds a predetermined temperature ( $T_{\text{ass}}$ );
- RELATIVE, an axle box exceeds the mean temperature measured on other bushings by a certain delta and also a certain temperature  $T_{\text{rel}}$ .

The regulation does not necessarily prescribe values for these limit temperatures, leaving this task to the competent Central Unit in relation to the characteristics of the RTB installed.

A vehicle must be discarded if presents even one axle box with temperature:

- over 70 ° C (absolute alarm);
- higher than 15 ° C compared to the average of the remaining axle boxes (relative alarm).

If on the one hand it is assumed that the discontinuity of such monitoring is in any case adequate to intercept possible failure and to prevent possible accidents, on the other hand a large number of vehicle cases after passing an RTB device without any alarm have derailed due to damage to the bearing [34] .

Thanks to the development of the wireless monitoring system, it was possible to monitor non-invasively the outside temperature of an axle box of the central bogie.

Figure 40 shows the measurements data collected on line 2. As it is possible to observe from the graph the measured temperature oscillates between 25 and 50 °C under normal operating conditions. These temperatures allow the grease to work in optimal conditions.

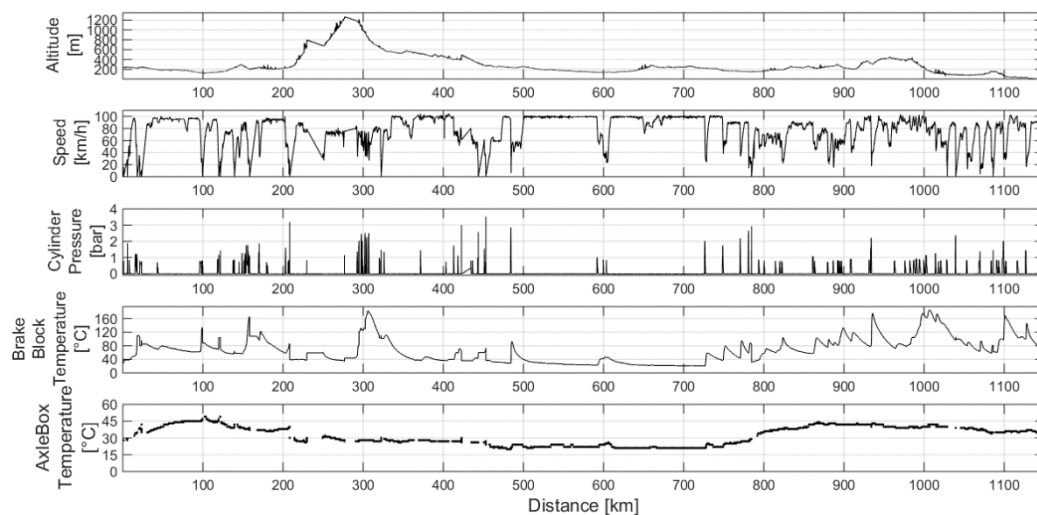


**Figure 40. Axle box wireless monitoring.**

The installed monitoring system therefore offers the possibility to monitor this parameter continuously. In the event of a sudden malfunction, the temperature of this component reaches very high levels in time of the order of seconds / minutes.

In these cases it is therefore very important to intervene in a very short time to limit the possibility of accidents.

Unfortunately, during this project it was not possible to develop a monitoring system that can also monitor the temperature of the wheel tread in order to obtain more information on the thermal loads to which the wheel is subjected during normal operation.

The rotation of the axle increases the bearing temperature, but this is not the way to generate a dangerous situation. During the normal operation the axle box and the bearings will heat up until a thermal equilibrium situation is reached where the heat generated by friction between the bodies, moving relatively to one other, is equal to the heat dispersed to the outside.

As can be seen from Figure 40, during the normal operation of the wagon the bearing reaches a temperature equilibrium that remains constant for tens of kilometers. The factors that may lead to a temperature variation, such as the one that can be observed in the figure, may be due to the type of track or the external temperature during the train run or the exposure to the solar radiation. It is therefore extremely important to operate with the same logic of the RTB system in order to get a complete picture of the temperatures of all the bearings of the wagon, thus comparing the temperature values measured on the different axle box.

The causes that may lead to overheating and failure of a bearing are many and can be excessive load, normal fatigue load, contamination, lubricant failure and low maintenance.

The information of bearing overheating must be immediately communicated to the train driver and to the company owner of the wagon in order to be able to take action as soon as possible to secure the wagon and to restore the proper functioning.

An intelligent monitoring system must be able to recognize, as well as the exceeding of a maximum threshold temperature, also the rapid rise of this, in order to guarantee the quickest possible intervention.

As can be seen from the figure, in some sections of the route, the wireless signal is not detected. This is due to the railway environment very hostile to wireless communications due to the iron present. Therefore, during the development of a wireless monitoring system it is essential to develop a wireless network and communication algorithms able to guarantee the constant wireless communication between the axle box nodes and the central node that process the data.

The measurements made also confirm the absence of a significant influence on the axle box temperature by the temperature reached by the wheel tread during the braking phases.

The experience gained in wireless communication is applicable to any other sensor. There are devices on the market for detecting wireless the pressure inside the tank cars or for monitoring the food temperature to guarantee the cold chain.

## **6.7. Braking force and longitudinal deceleration**

During the activation of the brake it is possible to synchronize the measurement of the brake cylinder pressure variation with the longitudinal deceleration.

Knowing the geometric dimensions of the braking cylinder that acts on the central bogie and monitoring the pressure values during the braking phases was possible to define the total braking force ( $H$ ) that act on the central bogie monitored. The formula used is the following:

$$H = p A \beta \quad (34)$$

Where  $p$  is the pressure inside the brake cylinder,  $A$  is the brake cylinder area and  $\beta$  is the multiply coefficient obtained by the brake lever. In this braking system  $\beta$  is equal to 2.

In order to characterize the intensity of each individual braking it was calculated the integral mean of the force  $H$ , for all the braking of the different journey, with the following formula:

$$H_{mean} = \frac{1}{t_f - t_s} \int_{t_s}^{t_f} H(t) dt \quad (35)$$

The information related to the position of the train, collected using GPS, is extremely important because it allows to know the position and speed of the train and to correlate the parameters measured. We used it to obtain the braking distance ( $d$ ) and to calculate the mean deceleration  $a_b$  during braking:

$$a_b = \frac{s_s^2 - s_f^2}{2 d} \quad (36)$$

Where  $s_s$  represent the speed of the wagon when the braking start,  $s_f$  the speed at the end of the braking and  $d$  is the braking distance. In this analysis, we take into account only braking in plain, avoiding data influenced by gravity.

The results obtained are shown in Figure 41.

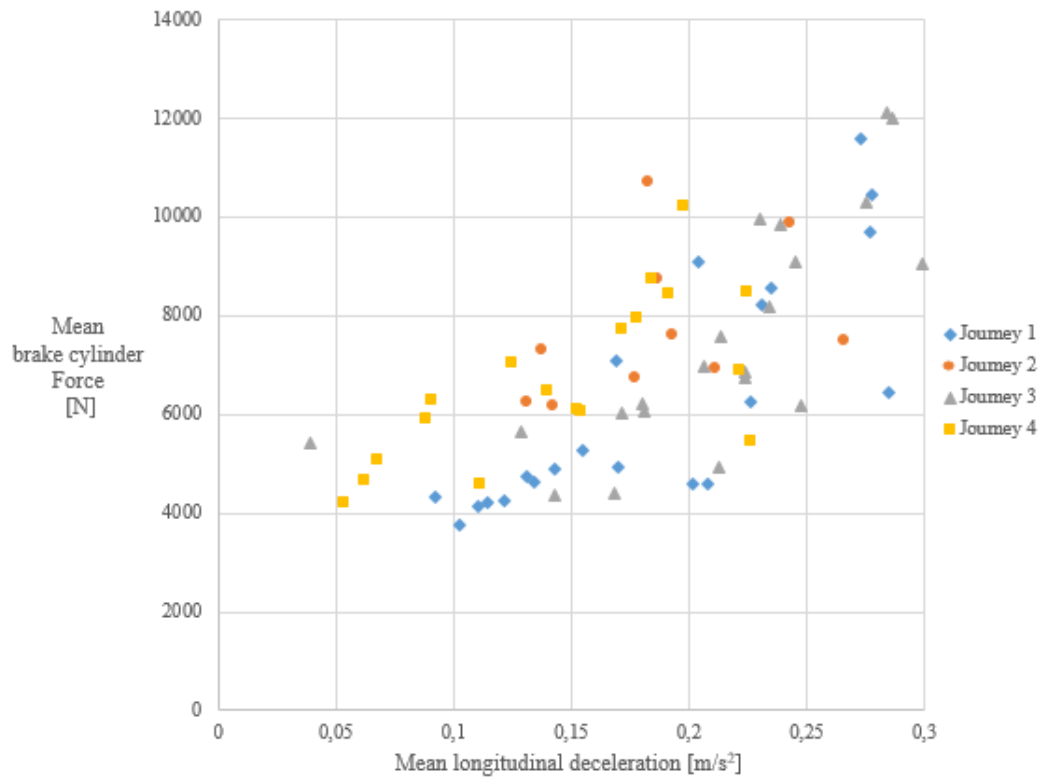


**Figure 41. Mean deceleration due to the braking.**

The previous figure summarise the results of four different journeys. It is possible to notice, as planned, the linearity relationship between the two physical quantities. The value monitored and presented are in line with those reported in literature [36] The correct operation of the braking system has allowed to obtain extremely repeatable measurements. The deceleration calculated is relative to the entire wagon but the calculated force is referred to a single brake cylinder, while for each individual car there are a total of three brake cylinders, one for each bogie.

## 6.8. The RMS longitudinal acceleration

The previously calculated deceleration does not correspond to the deceleration detected on the carriage by the tri-axial accelerometer of the central node installed on the body frame. During the braking of a train there is a strong interaction between the wagons, this is due to the braking delay and the possible non-uniform braking of all the cars. The Figure 42, as reported in [37] , shows the maximum level of

acceleration that can be reached by the container, and therefore also from the wagon frame during the transport phases.

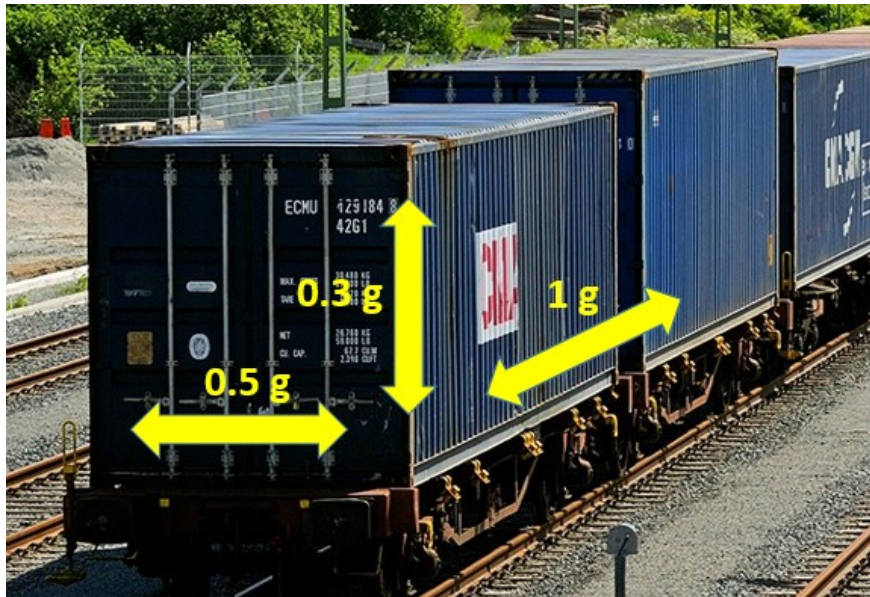


**Figure 42. Maximum acceleration values in intermodal transport.**

These values are extremely high when compared to the maximum deceleration levels due to the braking of the entire train, which are around  $0.3 \text{ m/s}^2$ . Such high acceleration values can lead to moving the goods inside the container if it is not well fixed.

The figures below (Figure 43- Figure 53) show some monitored braking cases. For each braking are reported the information of altitude, speed, brake cylinder pressure and acceleration measured on board. For each of them there is also a map on which the GPS points in which the braking took place are shown with red markers. As it is possible to observe the braking in the rail freight field they cover extreme high distances, even higher than 300 meters.

From the figures it can be seen that the on board acceleration and pressure profile of the brake cylinder are synchronized and follow the same trend. Bigger is the pressure inside the brake cylinder, greater will be the acceleration.

Furthermore, the monitoring of longitudinal acceleration allows to detect potential shock during the composition of the train. Too high longitudinal acceleration levels can lead to damage of the wagon and to displacement and damage of the goods transported.

The acceleration monitoring allowed to determine which are the lower and upper limits of the longitudinal acceleration.

In the development of a product intended for the installation on freight wagons it is appropriate that this should be able to distinguish a braking from an impact, thereby triggering an alarm. The device must be able to recognize if the recorded peak and RMS values exceed certain limit values.

During the tests conducted the position of the wagon in the composition of the wagon was not recorded, furthermore it was not possible to establish if this had been kept fixed until reaching the terminal. The absence of this data did not allow us to determine experimentally if the accelerations occurring by the wagons at the top of the train are higher than those that occur at the end of the train.

Furthermore, the monitored wagon was always loaded. Therefore, the longitudinal acceleration values reached during braking under these conditions are unknown. Being able to know these values experimentally represents very important data, in fact, as is known, most of the derailments following heavy braking occur on unloaded wagons.

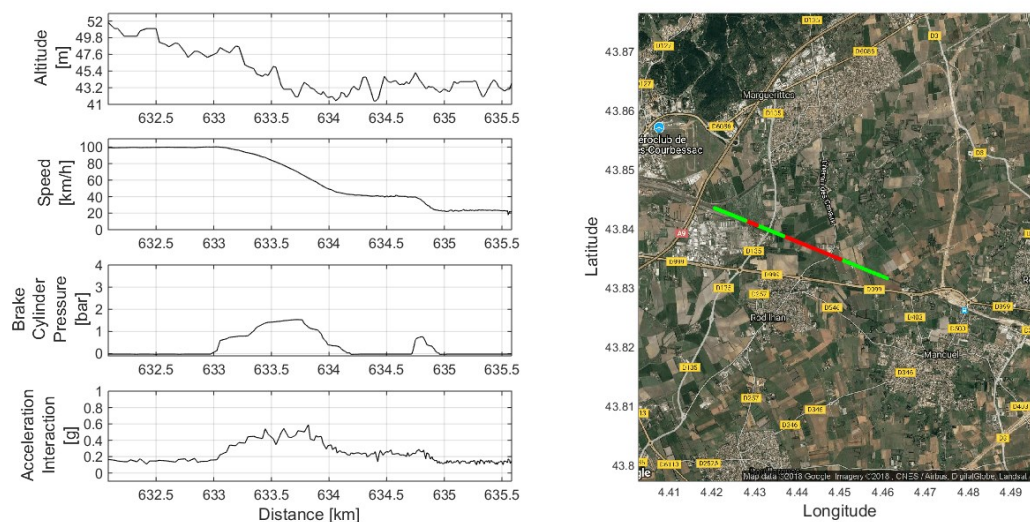


**Figure 43. RMS acceleration during braking 1.**



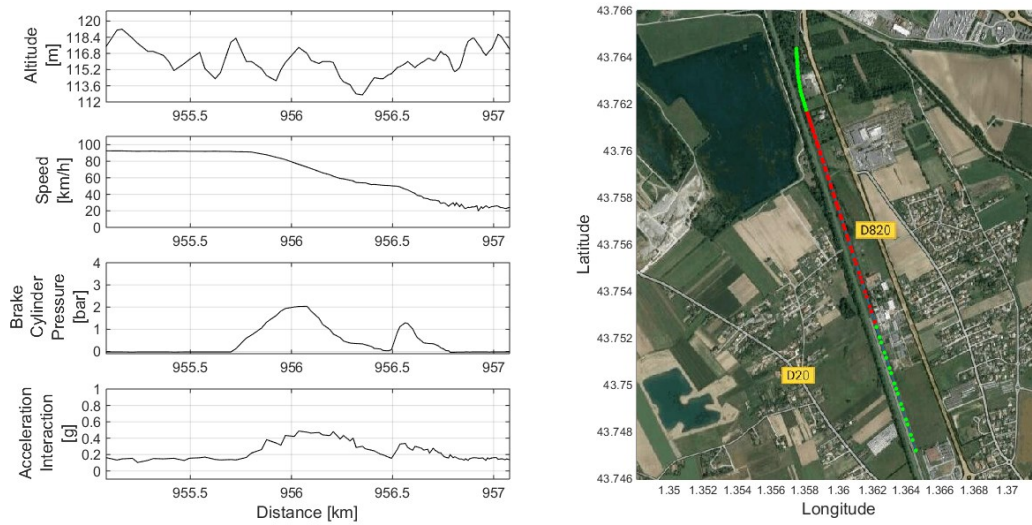


**Figure 44. RMS acceleration during braking 2.**

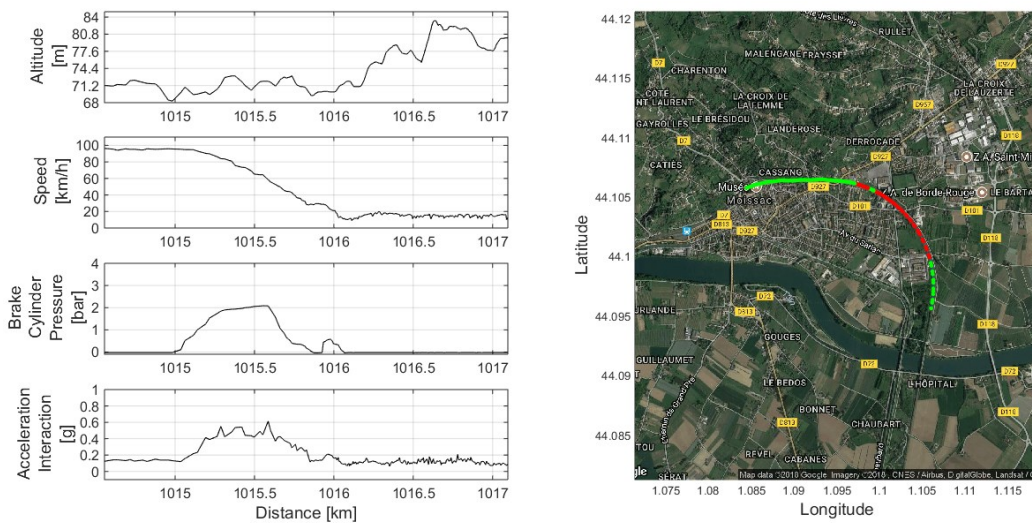


**Figure 45. RMS acceleration during braking 3.**

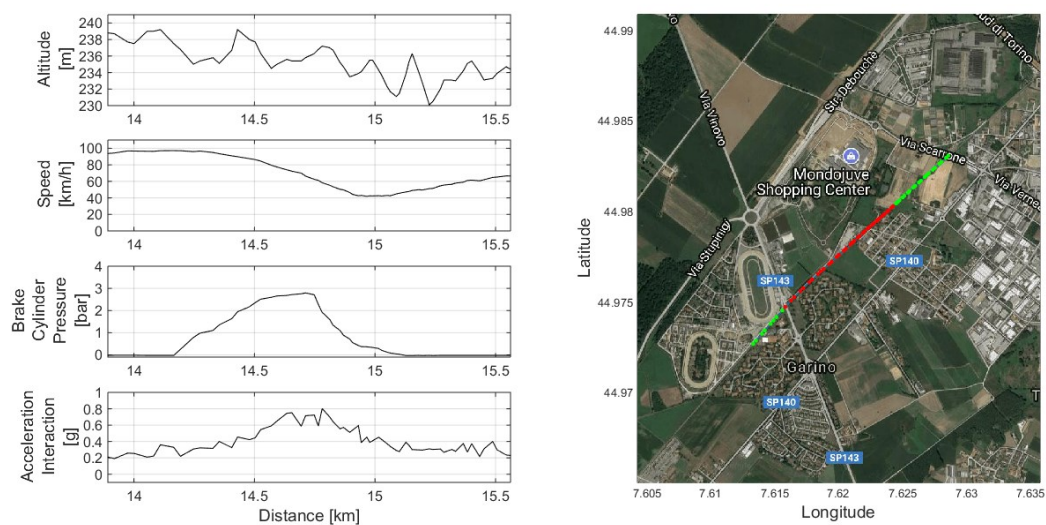


**Figure 46. RMS acceleration during braking 4.**

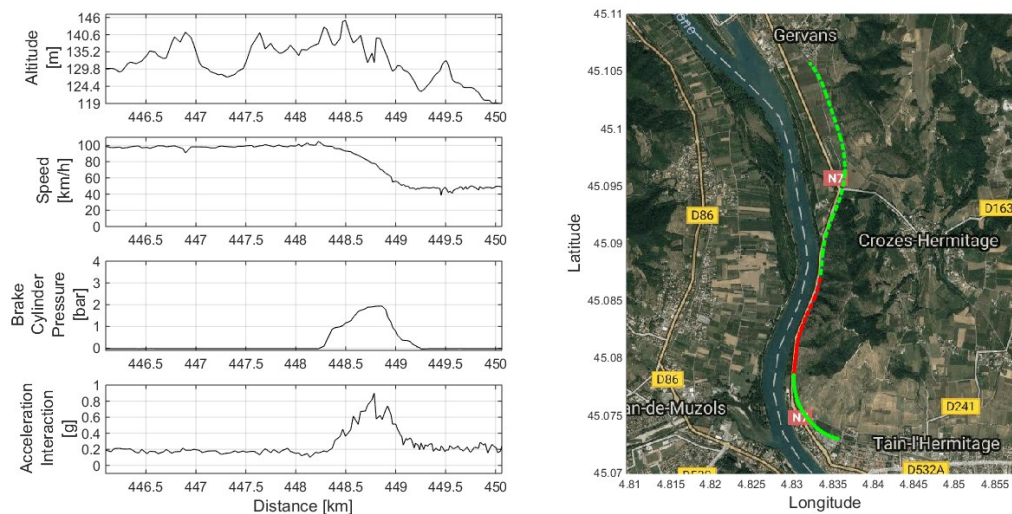


**Figure 47. RMS acceleration during braking 5.**

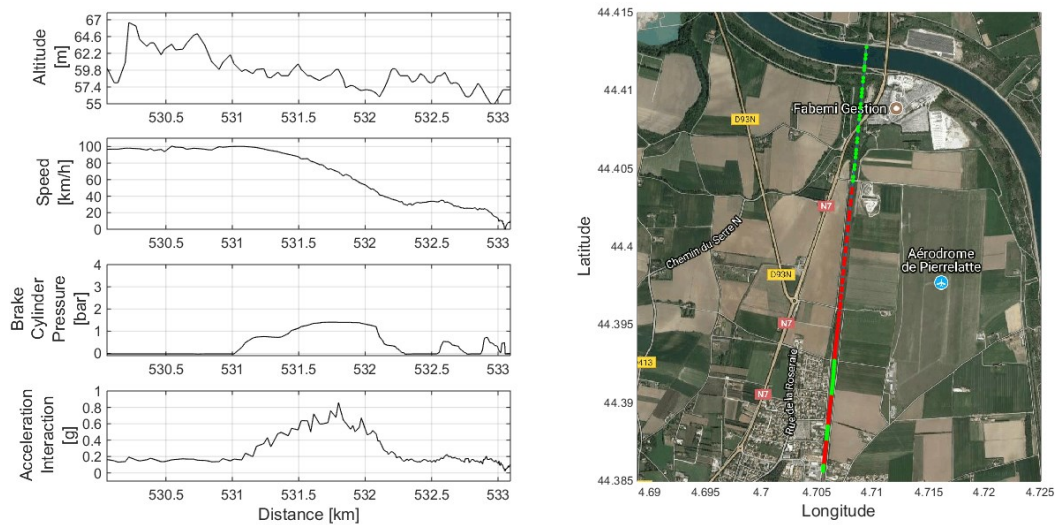


**Figure 48. RMS acceleration during braking 6.**

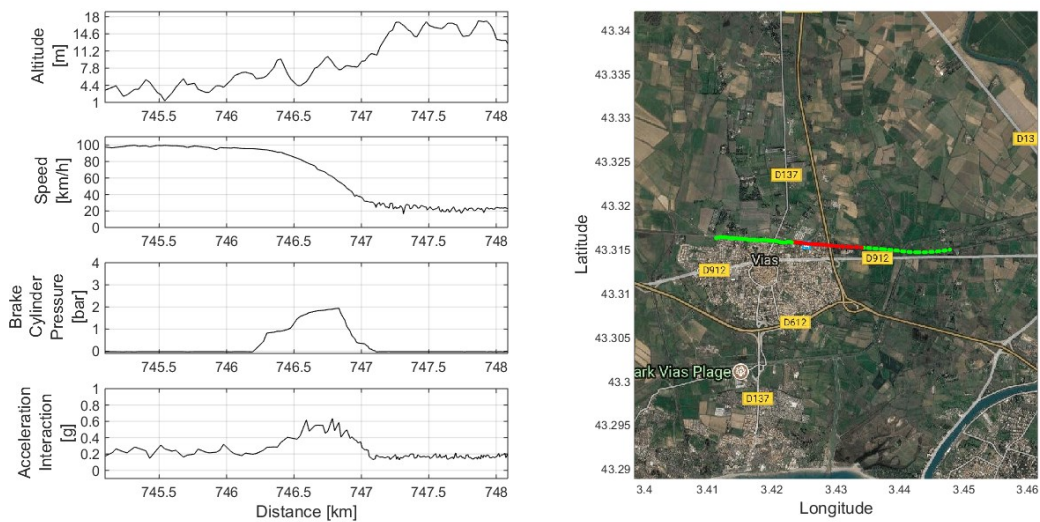


**Figure 49. RMS acceleration during braking 7.**



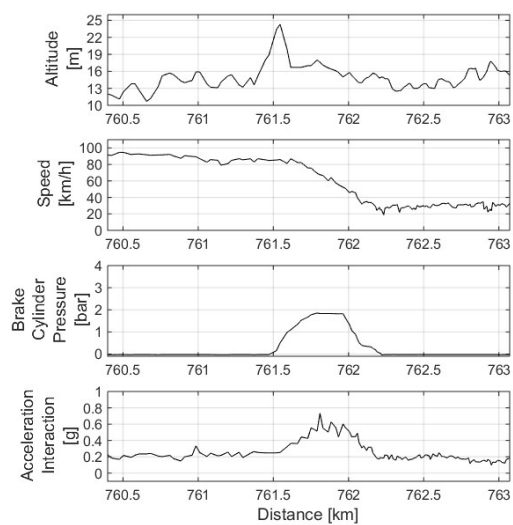


**Figure 50. RMS acceleration during braking 8.**

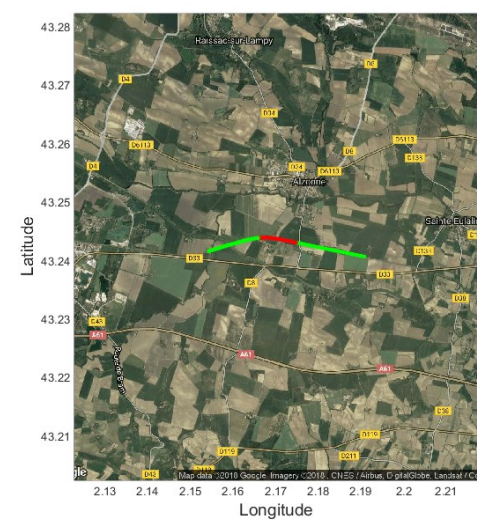
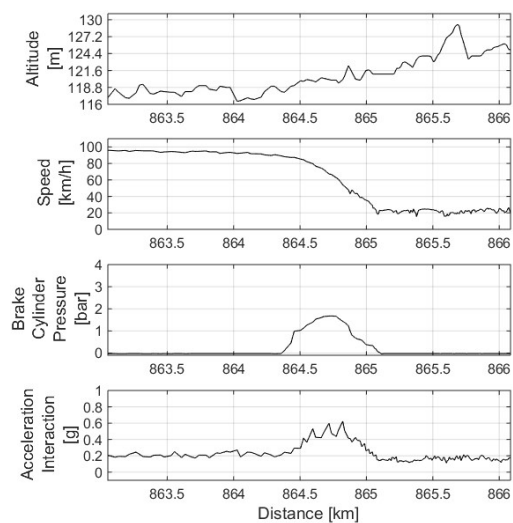


**Figure 51. RMS acceleration during braking 9.**

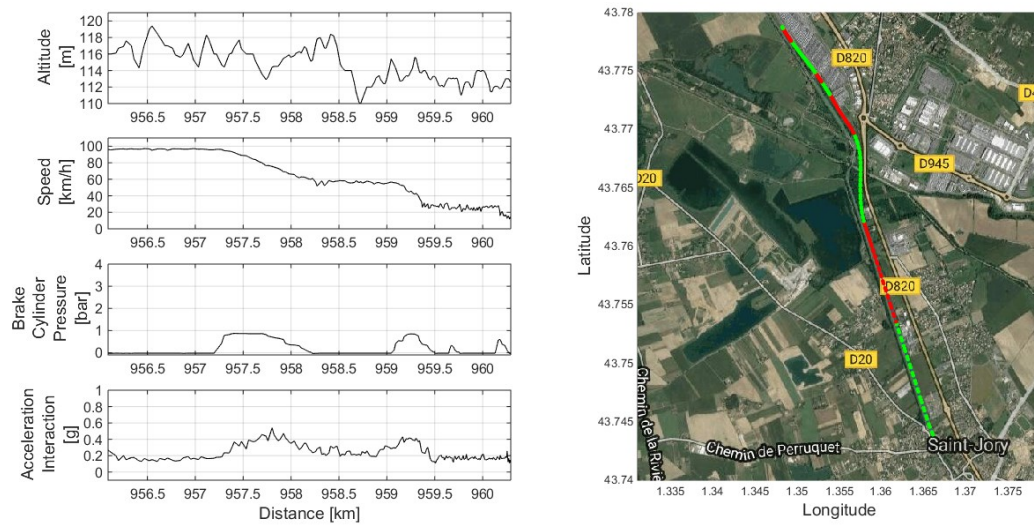


**Figure 52. RMS acceleration during braking 10.**

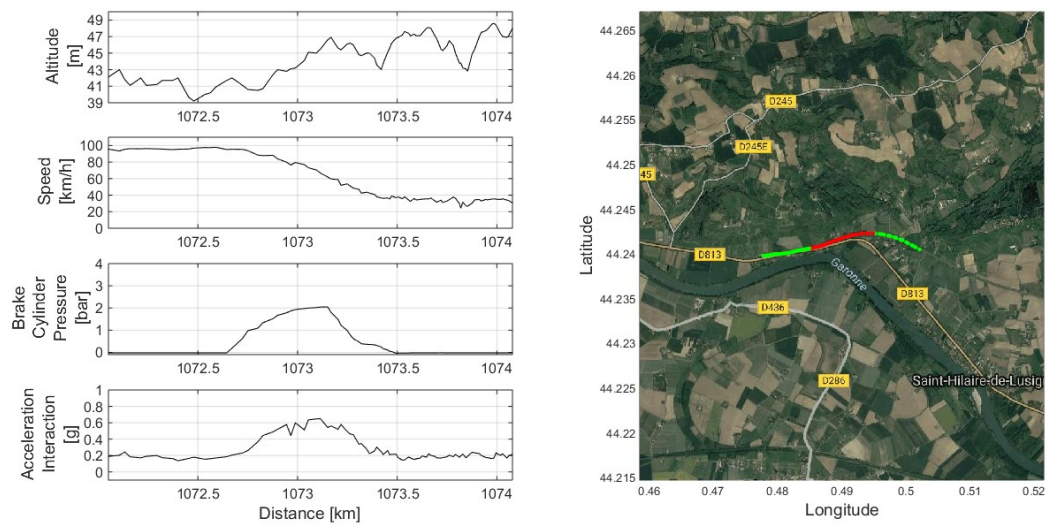


**Figure 53. RMS acceleration during braking 11.**

## 6.9. The RMS vertical acceleration

The vertical acceleration is an essential parameter in the monitoring of a railway freight car. From it can be extrapolated useful information for activities related to the safety, to study the status of the line and for the correct design of electromagnetic energy harvester to power the monitoring system install on-board wagon.

In the development of this demonstrator, wanting to develop a low energy consumption device, was decided to use one parameter for the monitoring of accelerations. This parameter, as explained above, is the RMS. In order to perform real-time vibrational analyses on the dynamics of the wagon and on the vibrations of the subsystems (e.g. bearings), it is necessary to have devices with a high computing power. This solution is adopted on vehicles for passenger transport equipped with electrical wiring and on which the cost of a monitoring system represents only a small portion of the cost of the entire wagon, this statement is particularly true for high-speed passenger transport.

The developed demonstrator calculates the RMS value of the vertical acceleration on 200 values sampled with a frequency of 200 Hz. The lower natural frequencies of the wagon chassis are generally 3 – 4 Hz, so the selected sampling frequency is enough to monitor the accelerations.

The Figure 54 shows the typical acceleration profile monitored during our tests. As can be seen, during the train run the RMS of the vertical acceleration stands at 0.2 g. The monitored values are in accordance with the literature and represent an excellent result considering the use of a very low-cost accelerometer sensor. During the two braking present in the section shown in the figure, the vertical acceleration is not affected by the longitudinal dynamics of the carriage. This demonstrates the goodness of the accelerometer and its installation.

Starting from the analysis of Figure 54 and from the data collected during the tests it is possible to develop algorithms and logics that allow to identify derailment conditions. During the project I developed the certainty that it is impossible with a low-cost device and with the information available to predict a derailment. Furthermore, once a possible derailment condition has been identified, it is necessary to inform the train driver of dangerous situation. Few seconds are required to inform the driver and start the braking operations. Therefore, an on-

board device has the real task of limiting the damage to the infrastructure and the wagon, informing the driver as quickly as possible.

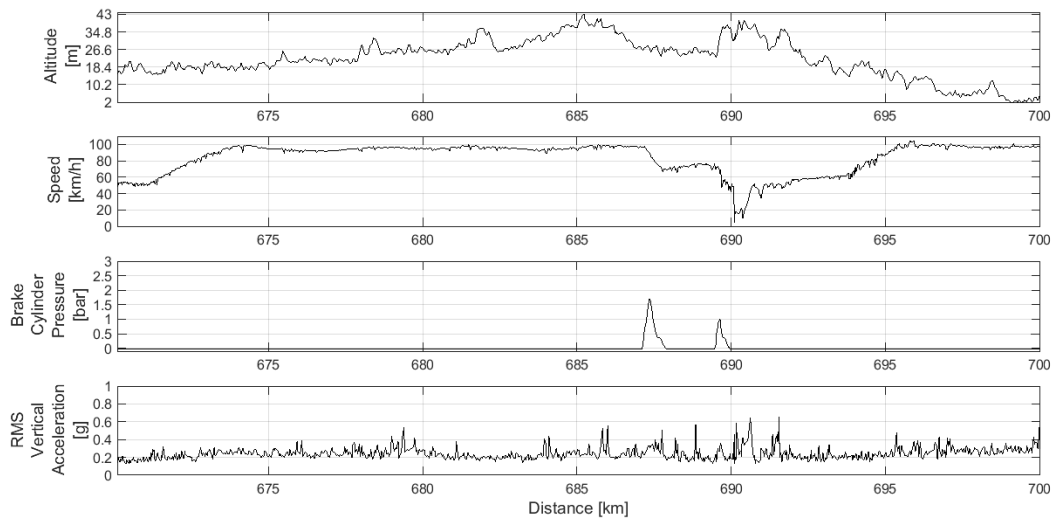


**Figure 54. Example of the RMS vertical acceleration.**

In case of derailment the recorded RMS value would be much higher than 0.2 g and the RMS values following the first peak continue to have high values. If the rotational speed of the axle was available, this could be compared with the GPS speed (referred to the axle knowing its geometry) and with the presence or absence of repeated vertical acceleration values above 0.2 g. In the event that the two speeds are not congruent and anomalous accelerations are present it would be advisable to warn the driver to stop the train.

Acceleration values can exceed the threshold value of 0.2g in some occasions and for brief instants, this is the case of the railroad switch or level crossings. This can also be caused by the presence of irregularities along the line due to the absence of maintenance.

A monitoring system installed on board a freight wagon therefore also has the possibility of monitoring the maintenance status of the line and signal to the authorities the presence of anomalous values. During the tests, always on the same railway line, was performed an analysis comparing acceleration levels with the same GPS position in order to detect possible irregularity along the line. Were analysed railroad sections in which there were no braking and the speed was as constant as possible. Two installations were taken into account and for each of them

were extrapolated the points in which the vertical accelerometric levels exceeded a certain threshold. The extrapolated points were compared each other comparing GPS position in order to find common anomalous points.

From Figure 55 to Figure 62 some example of level crossing and railroad switch can be observed. These are just few points selected from hundreds points found. The slight difference in position between the two points shown in figures is due to the accuracy of the GPS adopted and to the exact time in which the data was sampled.



**Figure 55. Level crossing 1**





**Figure 56. Level crossing 2.**

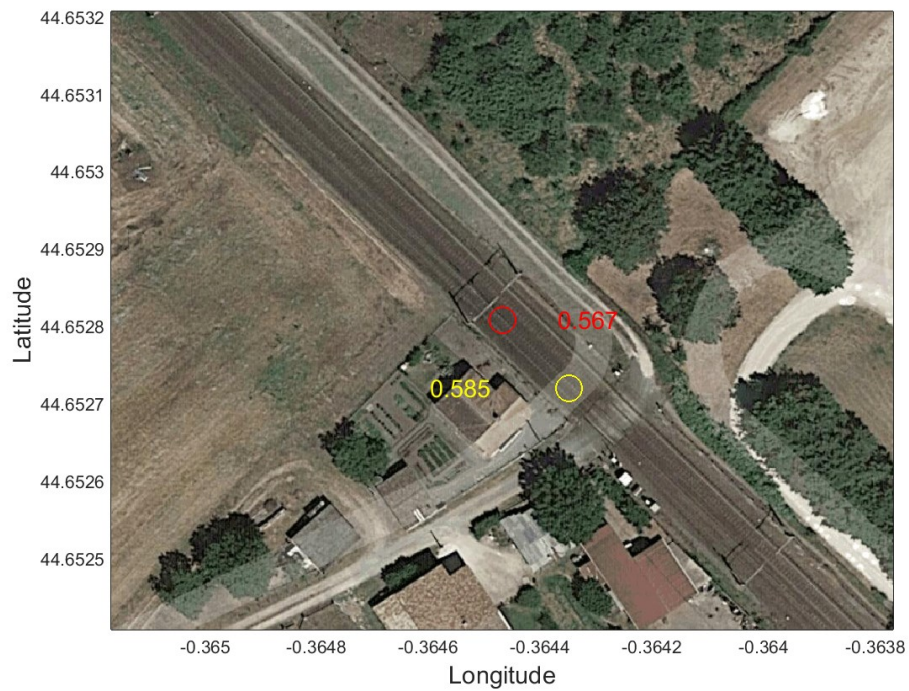


**Figure 57. Level crossing 3.**



**Figure 58. Level crossing 4.**

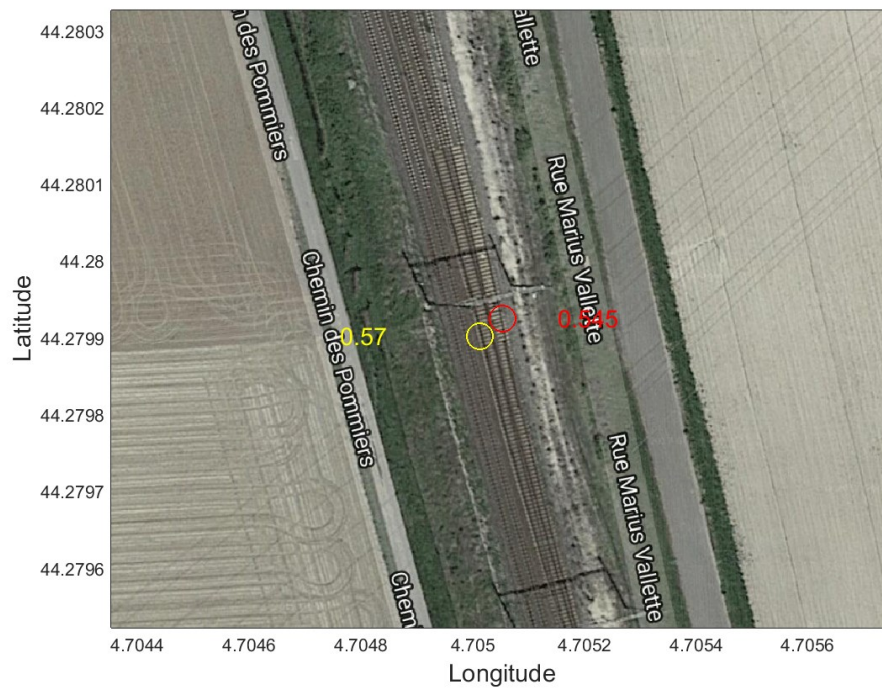


**Figure 59. Railroad switch 1.**



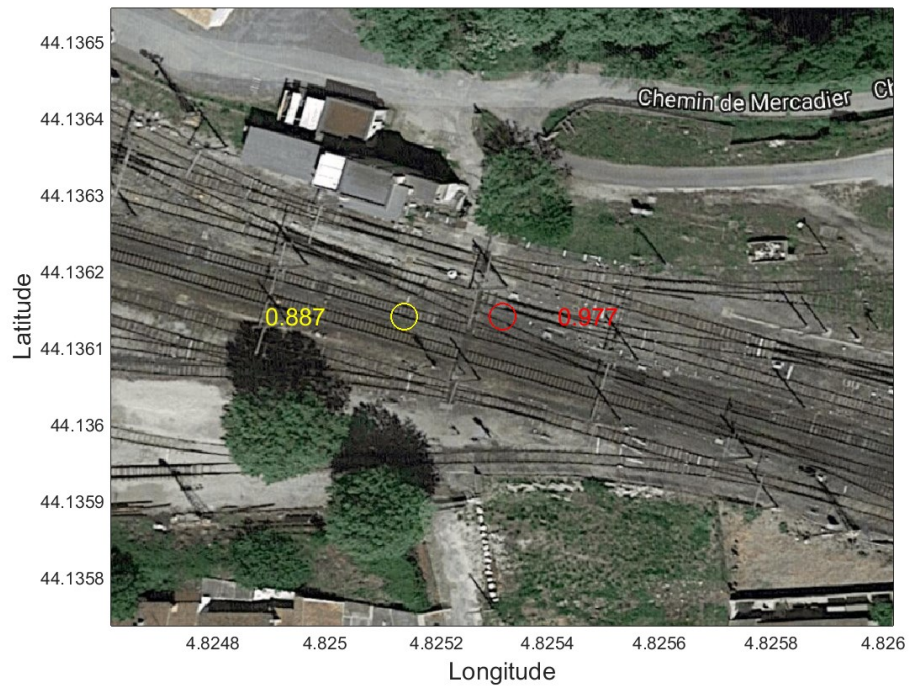


**Figure 60. Railroad switch 2.**



**Figure 61. Railroad switch 3.**

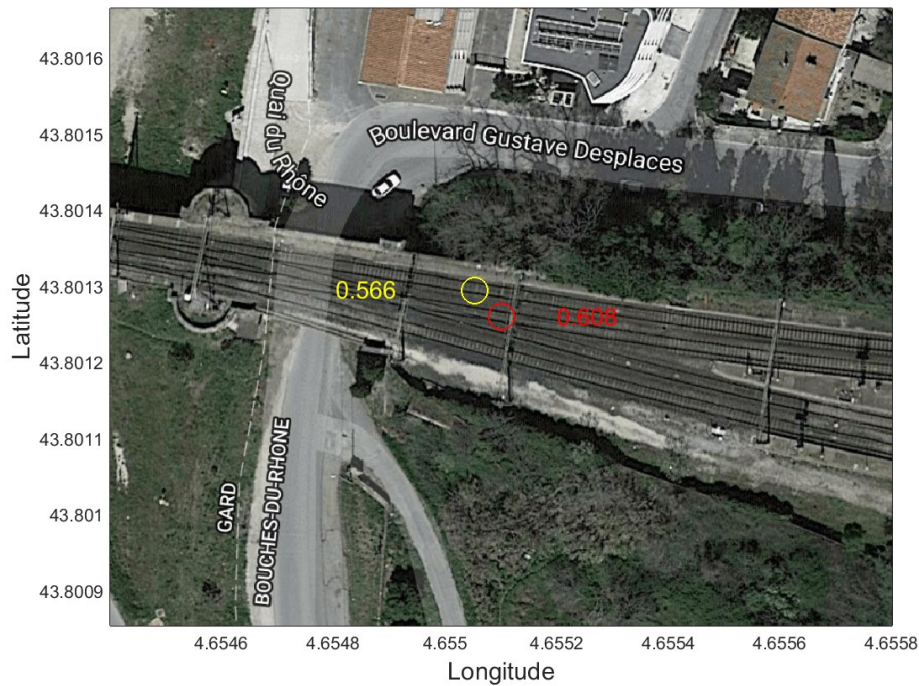


**Figure 62. Railroad switch 4.**

In Figure 63 and Figure 64 are reported two possible line defect point. This hypothesis is due to the level of acceleration detected in absence of railroad switches or level crossings near the detected points. A monitoring device installed on several wagons of a train would allow to identify any anomalies of the line even with a single pass if the anomalous accelerometric level was detected by all the monitored cars. This information would be even easier to obtain if the axle boxes of the various wagons were all monitored.

Monitoring devices, equipped with these functionalities, installed on wagons owned by private companies could provide useful information to the Infrastructure managers of the European railway lines in order to keep the railways line of the various countries in the best operating conditions.



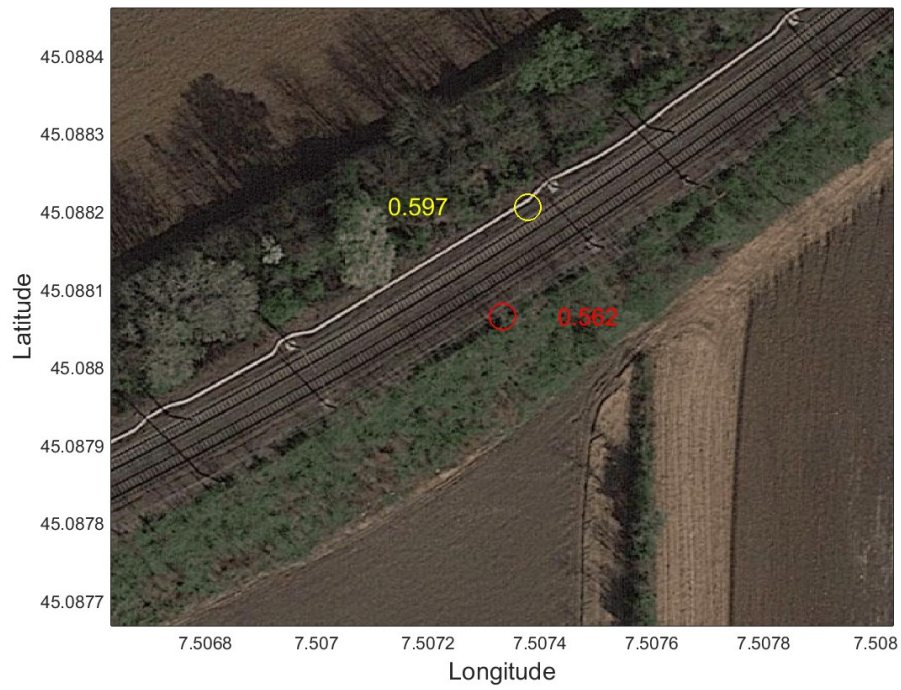


**Figure 63. Possible line defect 1.**

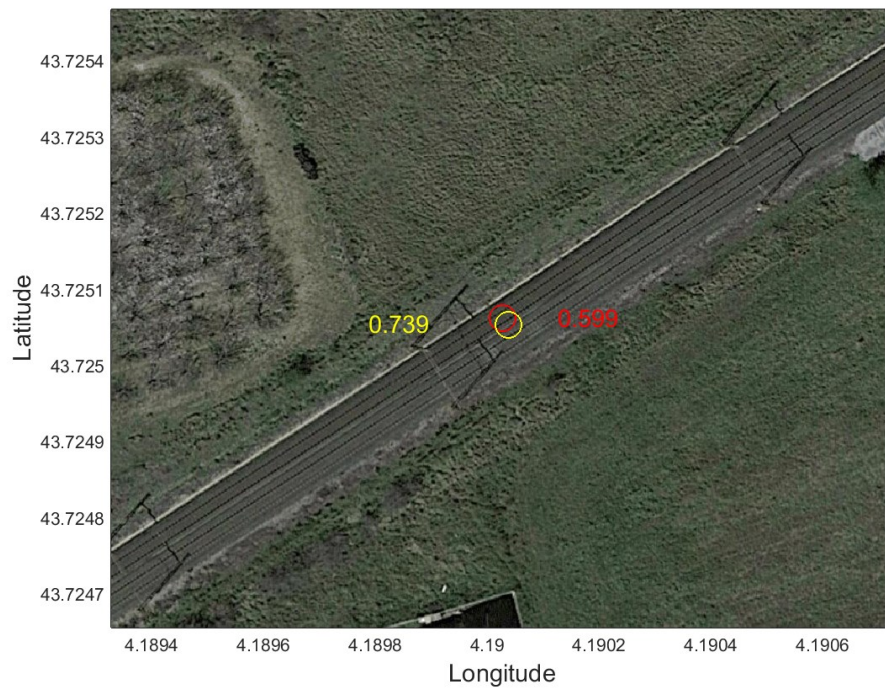


**Figure 64. Possible line defect 2.**

# Chapter 7

## 7. Thermal model results

### 7.1. Energy model results

From the simplified model previously described and using the vehicle data and the measured data, the energy evaluations that allow us to estimate the temperatures of brake blocks as a function of the running conditions of the vehicle can be performed. For this model, it was important to know the mass of the wagon because this parameter strongly influences the results. Table 15 reports the physical properties used for the calculation.

Physical quantity	Wheel	Cast iron brake block
Thermal conductivity k (W/m K)	49	48
Density (kg/m <sup>3</sup> )	7850	7100
Thermal capacity (J/kg K)	460	520
Mass (kg)	—	7.5

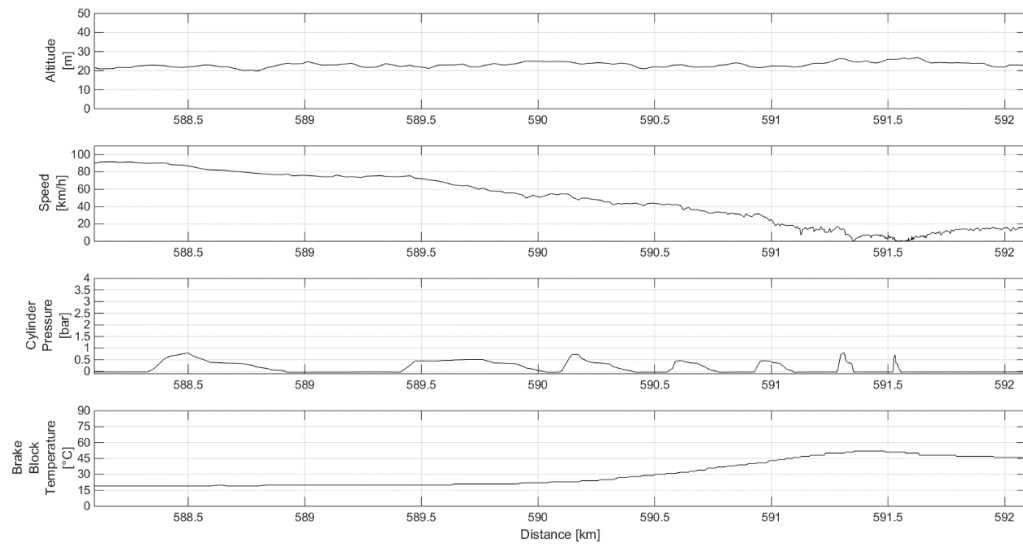
Table 15. Physical properties.

Table 16 reports the results obtained with the thermal model relating to some sections of the track in different installations.

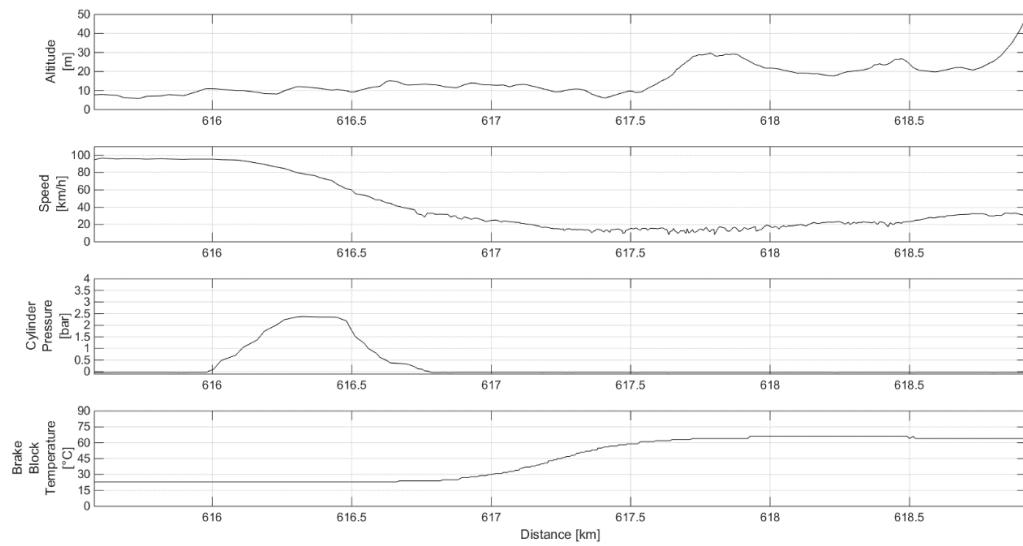
Track sector	$\Delta$ Kinetic Energy [MJ]	$\Delta$ Potential Energy [MJ]	Energy Losses [MJ]	$\Delta$ Monitored Temperature [°C]	$\Delta$ Calculated Temperature [°C]	Absolute Temperature Error [°C]
I	29.4	-3.1	2.7	33	31	2
II	29	-0.9	1.2	38	36	2
III	29.2	0.7	1.1	38	38	0
IV	21.2	-1.5	0.9	24	25	1
V	21.6	6.2	2.5	35	33	1

Table 16. Thermal energy model results.

In the following figures (Figure 65 - Figure 69) is possible to observe the different track sector analysed with the thermal model.



**Figure 65. Track sector I.**



**Figure 66. Track sector II.**

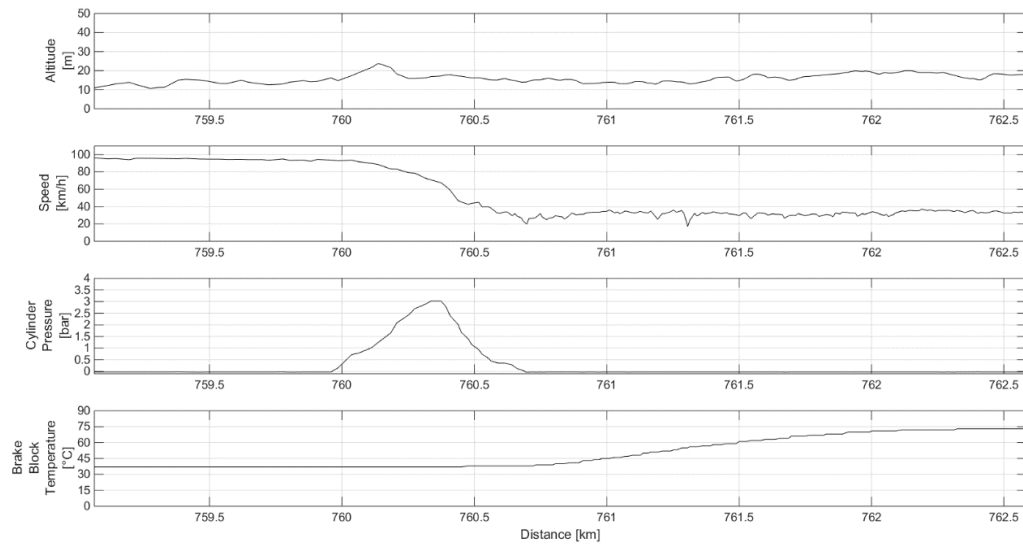


**Figure 67. Track sector III.**

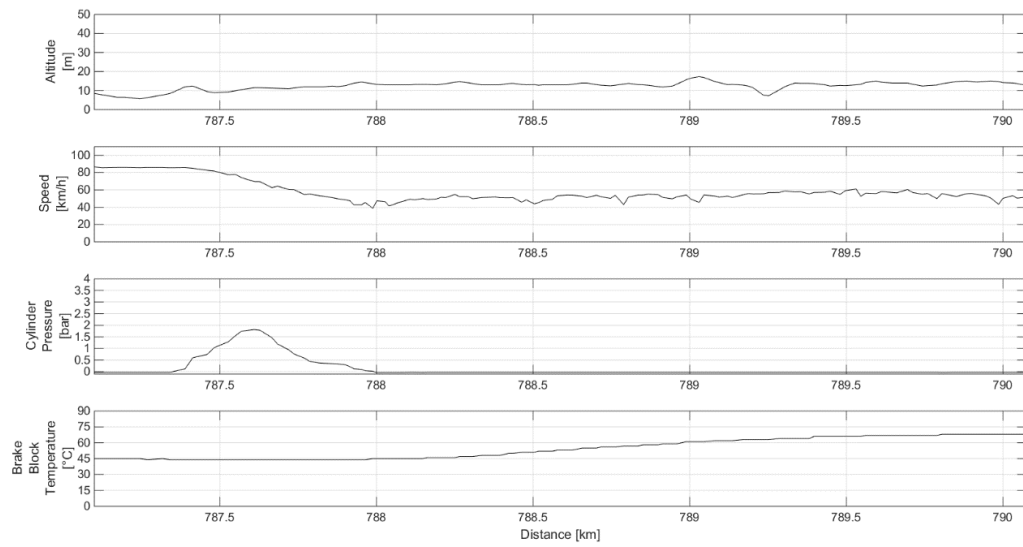


**Figure 68. Track sector IV.**



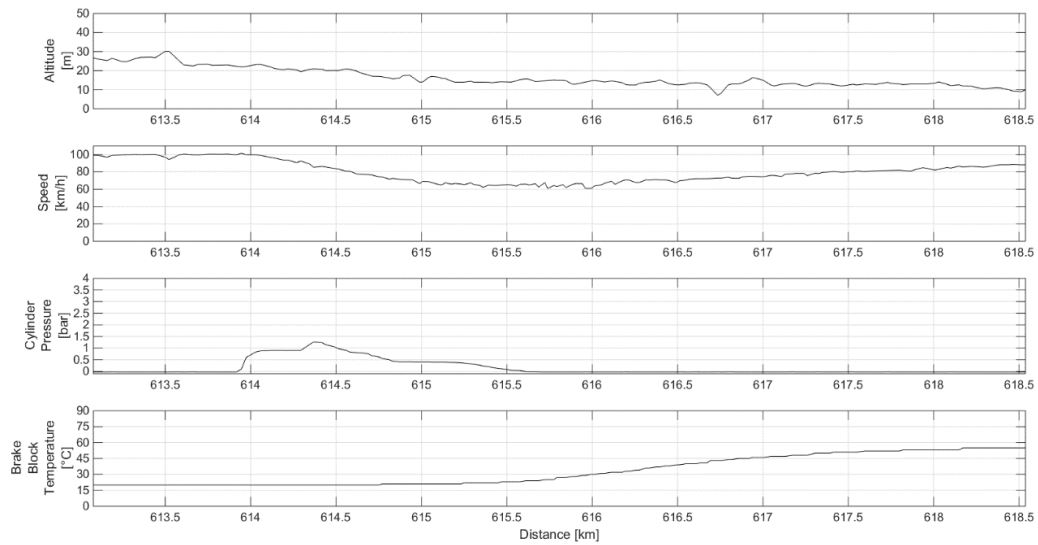


**Figure 69. Track sector V.**

The railway line covered by the monitored wagon in the different journeys was always the same. So it was possible to compare different braking carried out in the same position along the track. In Table 17 two different cases are shown.

Track sector	$\Delta$ Kinetic Energy [MJ]	$\Delta$ Potential Energy [MJ]	Energy Losses [MJ]	$\Delta$ Monitored Temperature [°C]	$\Delta$ Calculated Temperature [°C]	Absolute Temperature Error [°C]
VI	28,1	7,4	1,9	46	44	2
VI'	25,3	7,8	2,6	42	40	2
VII	28,7	2,3	2,1	39	38	1
VII'	27,6	5,1	1,8	42	41	1

**Table 17. Braking comparison.**

The following figures (Figure 70 - Figure 73) show these different cases.

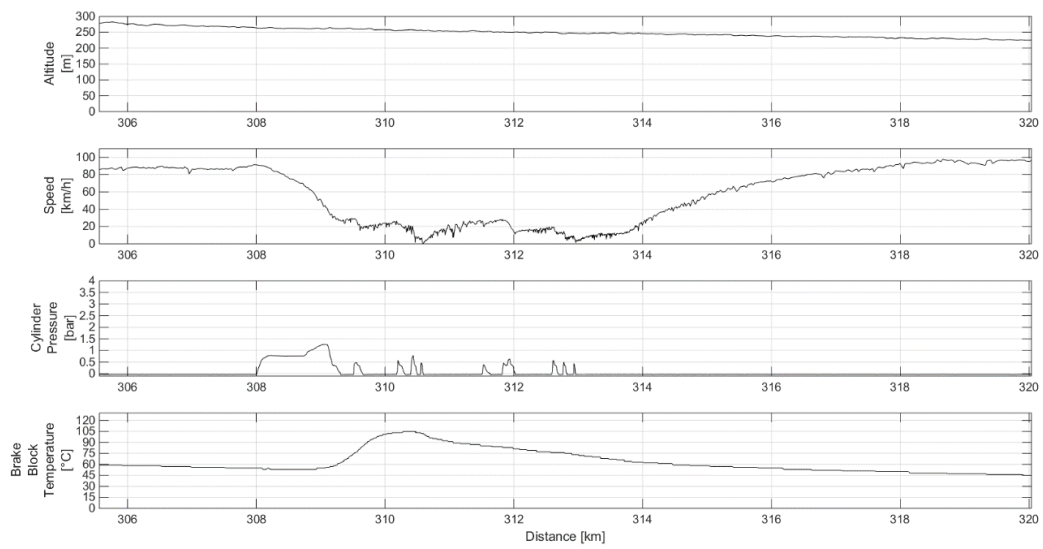


**Figure 70. Track sector VI.**

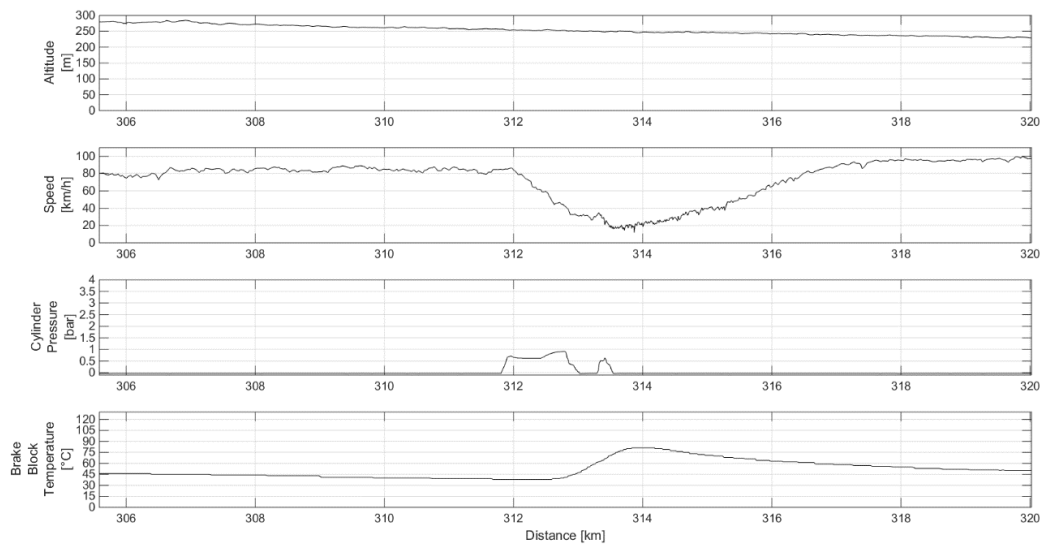


**Figure 71. Track sector VI'.**

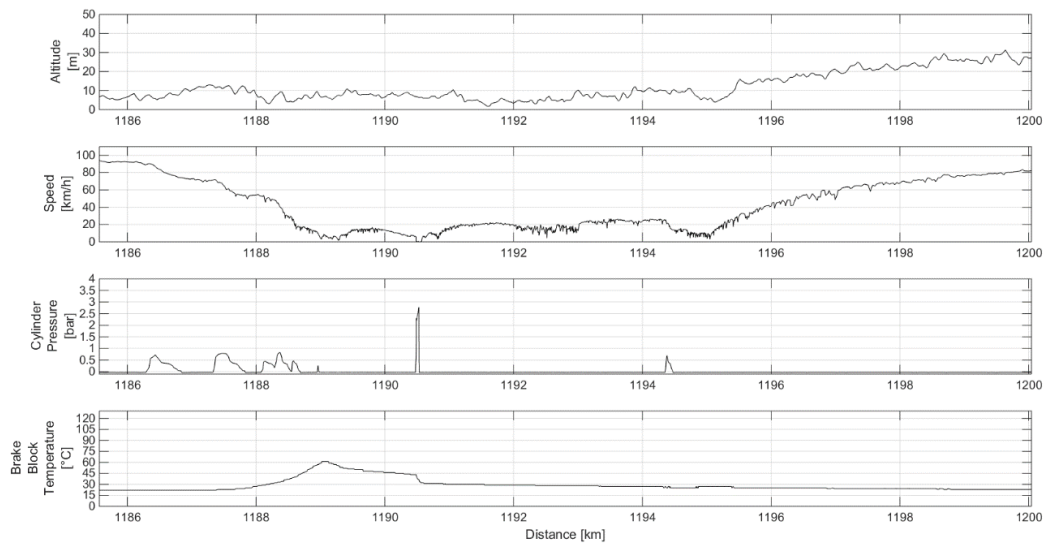


**Figure 72. Track sector VII.**

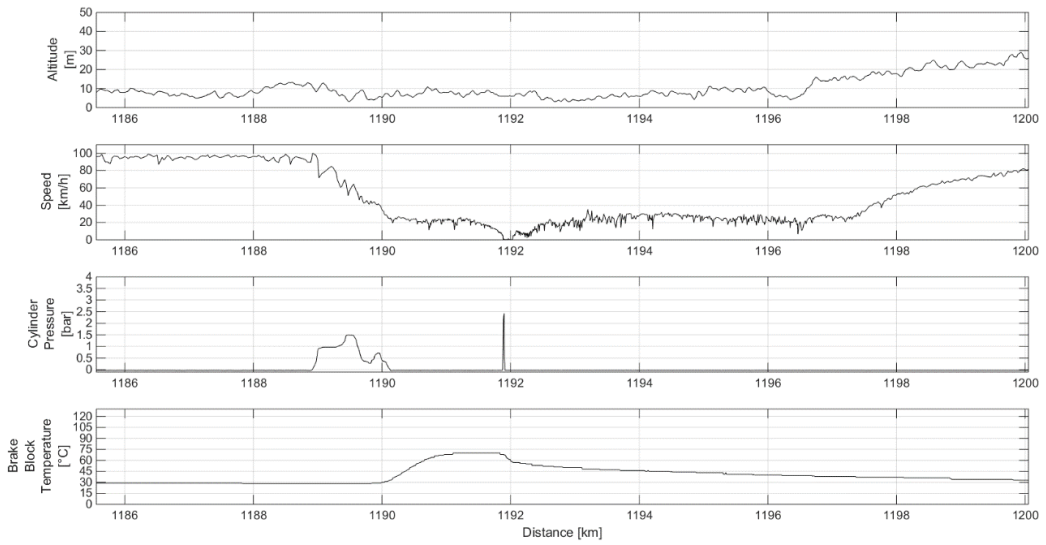


**Figure 73. Track sector VII'.**

The difference between the  $\Delta$  monitored and calculated temperature was consistent with the accuracy of the temperature monitoring system. In this work we did not consider the effects of the braking of the locomotive and the forces generated by

the other wagons. This choice was supported by the results obtained with the thermal model.

However, this type of analysis does not allow to study the temperature evolution in the point of application of the sensor. In order to conduct this type of analysis was necessary to use the FEM analysis.

## 7.2. FEM results

The FEM model illustrated in the section 4.2 allowed to analyse real braking conditions, monitored during the tests conducted. The data shown in Table 18 refer to two braking operations analyzed with the FEM model developed. The last right column in Table 18 shows the time elapsed since the brake activation and the moment in which was reached the maximum temperature monitored at the point of application of the sensor. This value is essential for the correct execution of the simulation. The two events analyzed refer to individual braking on flat.

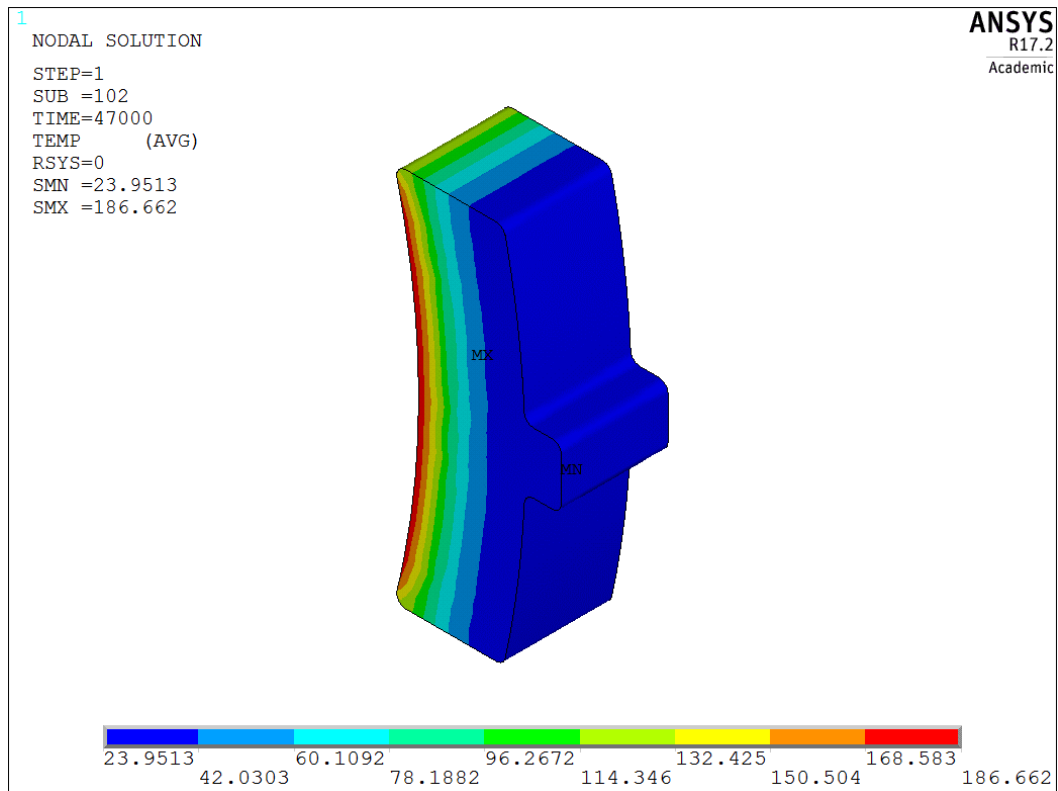
<b>Braking</b>	<b>Distance with brake activated</b>	<b>Initial speed</b>	<b>Final speed</b>	<b>Initial brake temperature</b>	<b>Mean brake cylinder pressure</b>	<b>Braking duration</b>	<b>Time simulation</b>
	[m]	[km/h]	[km/h]	[°C]	[MPa]	[s]	[s]
A	786	95	33	23	0,112	47	271
B	713	93	23	37	0,1202	46	220

**Table 18. FEM model input**

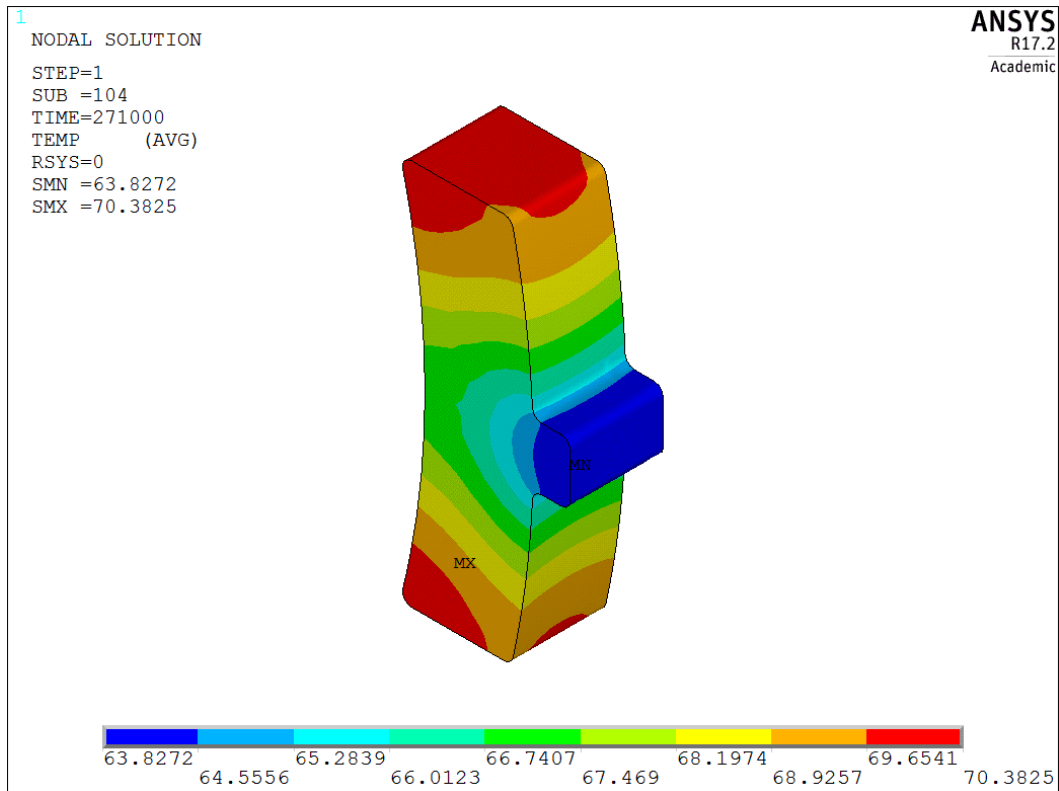
The two brakes here analyzed were performed roughly a hundred kilometers far from each other. It was decided to analyse two braking of the same installation in such a way that the parameters that could influence the simulation were limited. Among these factor, in particular, the sensor for data sampling. In fact, to be sure, the sensor was replaced every new test together with the relative brake block in order to maximize the probability of covering the entire journey.

Figure 74 shows the temperature distribution inside the brake block at the end of the braking A. As can be seen from the thermal distribution, at the end of the

braking phase, Figure 75, the maximum temperature reached in the contact area is about 187 ° C for this simulation characterized by an averaged thermal load. The heat spreads over time within the cast iron brake block after the braking phase. The peak temperature is then reached during the braking phase. As shown in the Figure 75 at the end of the simulation there are no high temperature gradients inside the brake block.

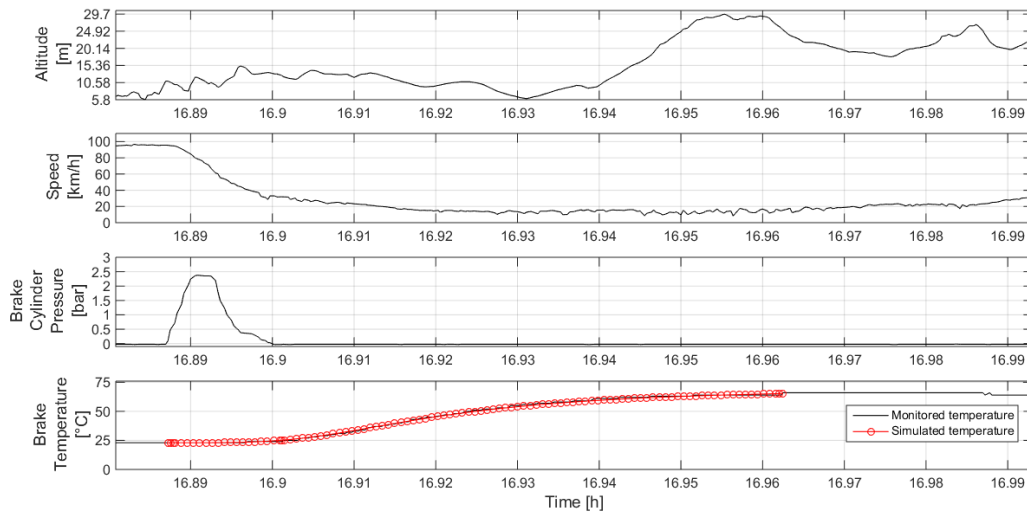


**Figure 74. End of braking A**



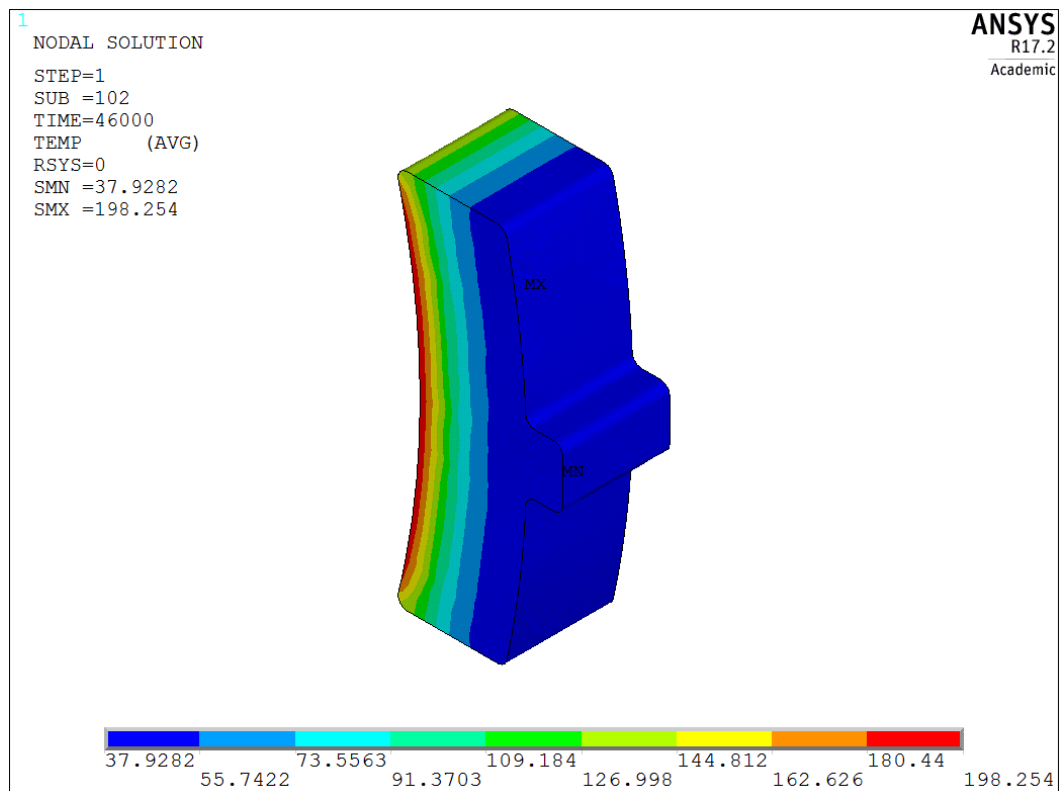
**Figure 75. End of the simulation for braking A**

Figure 76 shows the time evolution of temperature both during the simulation and for the monitored values. It is possible to observe the good fitting of the simulated data, this result is the proof that the input parameters and the expected convective losses were corrected. During the braking phase, the analyzed point does not suffer any thermal variation during the braking phase, but has a gradual temperature increase only after the brake release. Were also performed other simulations to numerically quantify the weight of the convective heat exchange, verifying that is marginal if compared with the thermal flow due to friction entering in the brake block.



**Figure 76. Comparison of monitored and simulated temperature for braking A**

The simulations performed for braking A have been repeated for braking B which has an initial temperature of 14 ° C higher. As can be seen in the figures below (Figure 77 - Figure 79), even in this case the results of the simulation correctly fit the experimentally monitored values. This braking has approximately the same time duration of the previous one but in this case the pressure reached in the brake cylinder is about 0.65 bar higher, a not negligible value in railway.



**Figure 77. End of braking B**

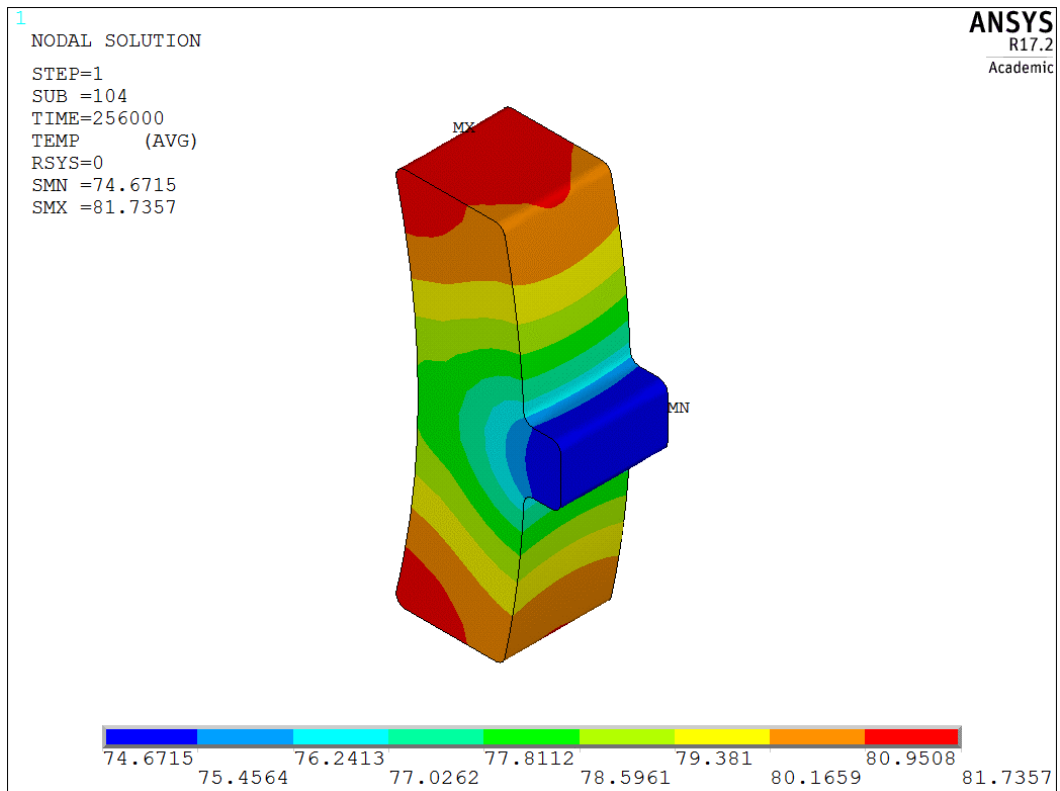


**Figure 78. End of the simulation for braking B**

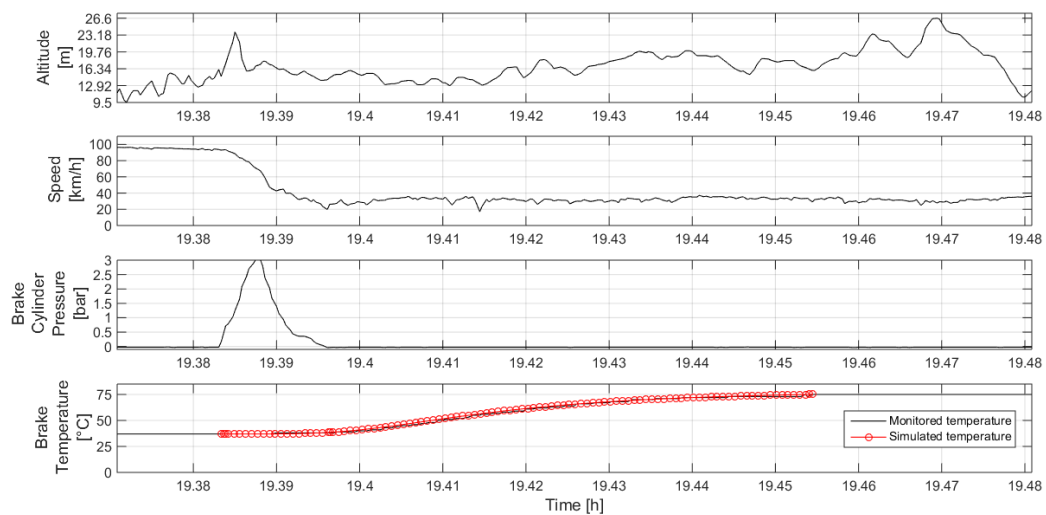


**Figure 79. Comparison of monitored and simulated temperature for braking B**

As anticipated in the paragraph concerning the explanation of the FEM model, two types of simulation have been performed regarding braking A. These



simulations had the task of verifying the goodness of the analysis and hypotheses carried out. The images presented earlier in this section show the results of the simulations that had as input the averaged thermal load calculated starting from the pressure values contained in the brake cylinder. Being an average parameter applied throughout the braking duration there are no variations and peaks of incoming thermal flux. The second analysis that was carried out therefore had as its objective the simulation of braking by applying a thermal load which, as a profile, was closer to the pressure inside the brake cylinder. The thermal load was therefore applied as realistically as possible.

The results of such simulation are visible in Figure 80 which shows a different temperature trend on the contact surface between the braked stock and the wheel. The maximum value reached by this second simulation was higher than the previous one by about 20 ° C, a non-negligible value. It can also be noted that the temperature profile is more realistic and in line with the phenomenon analyzed. Once the braking phase is over, however, the temperature reached by the surface after a certain period of time is absolutely comparable to the results of the first simulation. Which means that the amount of heat entering into the brake block is the same for the two simulations.

The temperature peak value and its trend are consistent with the experimental results reported in the literature [15] .

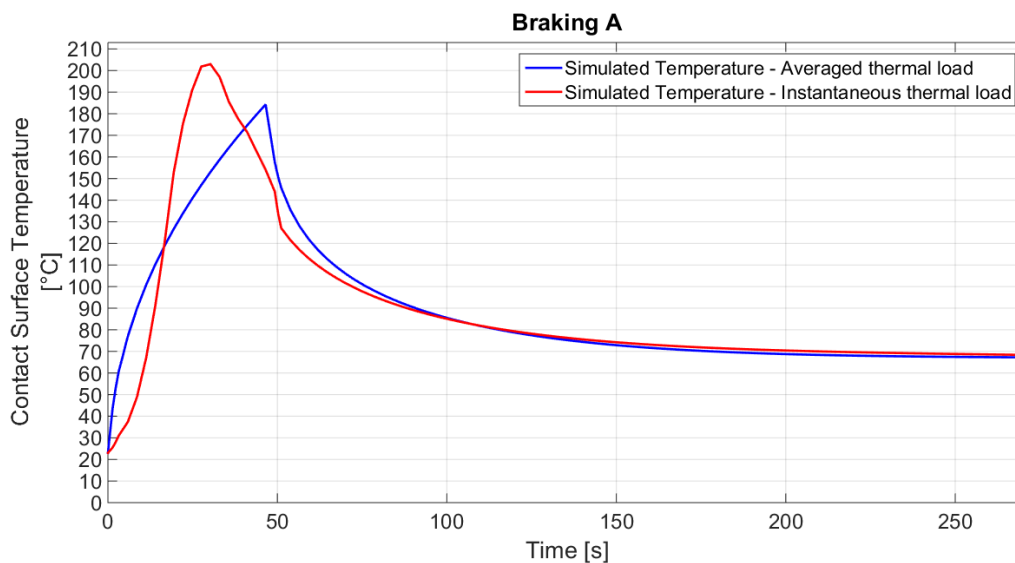


**Figure 80. Brake block contact surface temperature**

Applying the thermal load, in the instantaneous way, it was then verified that the results obtained at the point of application of the sensor were consistent with the results obtained experimentally and with the simulation with averaged load. Figure 81 shows the results of these analyses. As can be seen, there is no significant difference between the two simulations. Also this result is due to the fact that the overall amount of heat introduced into the brake block is the same in the two cases.

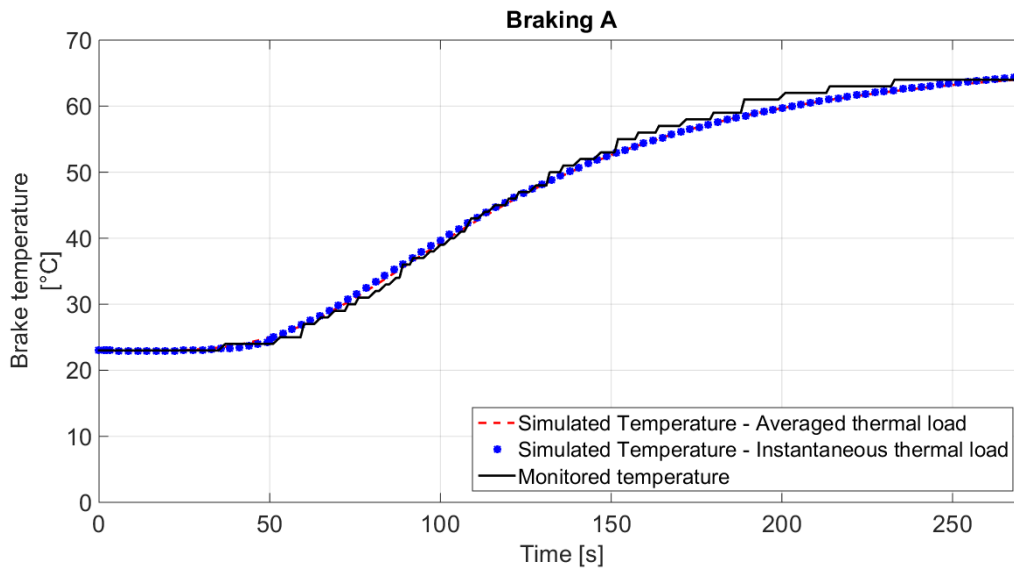


**Figure 81. Simulated temperature comparison**

In the design of a monitoring system, permanently installed on a freight wagon, it is unthinkable the sensorization of the brake blocks. The costs associated with this system would be too high and the information obtainable would need analysis with a too high computational cost.

Instead the brake block temperature monitoring is a very important activity for the development of new friction materials for the design of brake block in synthetic or composite material. The introduction of these brake blocks, called LL (Low friction) and K (high friction), is due to the need to take down the noise pollution generated during the braking phases of the freight wagons. In fact, railway stations generally rise in the heart of the cities and the noise generated creates inconvenience, especially at night during the time slot in which the goods traffic generally travels. However, the cost of these brakes is 3 to 4 times higher than that of traditional cast iron soles, but their durability is much higher. The longer life of synthetic soles and therefore their lower consumption translates into an increase in maintenance to be performed on wheelsets. The physical characteristics of LL brakes are very similar to the cast iron but the K have completely different physical

characteristics. For the adoption of the latter, the entire braking system must be updated due to these different characteristics. The traditional cast iron or the LL brakes absorb roughly the 25% of the heat generated in the braking process, while the K brakes reduce this fraction to 1.5% -2%, thus generating a greater thermal stress on wheelsets.

# Chapter 8

## 8. S.W.A.M. rail project

The experience that I gained during the PhD program, the skills of the Research Group of Railway Engineering of the Politecnico di Torino in creating prototypes and analysing data and the collaboration with rail transport companies such as Ambrogio Trasporti have allowed the creation of a new research project called SWAM Rail (acronym of Sistema Wireless Autoalimentato di Monitoraggio per la sicurezza dei veicoli Ferroviari merci). In this project three other companies have been involved, each one specialized in a specific field. These companies are the L.C.A. Ballauri, Capetti Elettronica and Movimatica.

LCA Ballauri is specialized in mechatronics with specific reference to railway sensors, for the measurement of speed, temperature and vibration parameters on board railway bogie. Its core business is represented by the design, production and sale of sensors to customers in the railway market.

Capetti Elettronica operates since 1973 as a design and production company for industrial electronic equipment for third parties. This activity has led, over the years, to a constant growth of the company in terms of technological know-how, size and quality of services. Since 2005 the company has independently undertaken an important research and development activity on the wireless sensor network technologies that has led it to make available on the market its own brand WINECAP.

Movimatica is a small company that work in diagnostic, remote monitoring and fleet management for construction and agriculture machine through advanced systems that integrate GPS and GPRS technologies together with the most advanced sensors based on MEMS / Wireless technology, which are the base of the Internet of Things. Conscious of the need to continue to introduce innovation, not only in the field of working machinery, in recent years, Movimatica has undertaken research into devices to automate the management of freight rail wagons fleets.

The union of the skills of the three partner companies and the Politecnico has led in recent months to the design of a monitoring system for European freight wagons. The designed system, Figure 82, can be divided into two macro-groups.

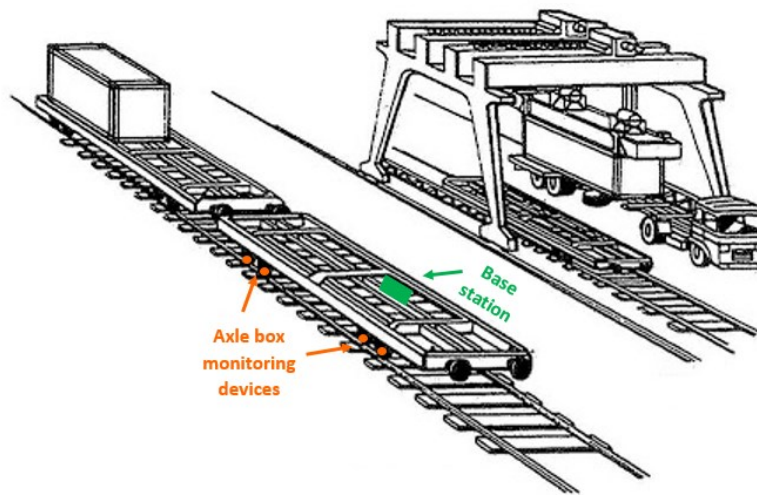


**Figure 82. S.W.A.M. Rail monitoring system diagram.**

The first group consists of all the devices installed on the axle boxes while the second is formed by the so-called base station installed on the body frame. Essential feature of this project is the complete energy autonomy of all monitoring devices. In fact, both the monitoring systems for the axle boxes and the base station are equipped with electromagnetic energy harvester systems. In the case of the axle box the greatest amount of energy can be taken from the rotary motion of the axes, while in the case of the base station, given its installation, the only energy source is represented by the vertical motion of the wagon. The two harvester therefore adopt different technical and constructive solutions in order to produce the most amount of energy possible. The amount of energy produced must be to ensure the operation of the system and, at the same time, allow the recharging of the batteries. The consumptions of the demonstrator realized in this PhD program allow therefore to have a valid reference point on the amount of energy that must be produced. The improved hardware and software design can however allow to obtain much lower energy consumption, like those of consumer electronics.

The base station must have the following features:

- the communication of the sampled data from the axle boxes (wireless local network) to the Cloud through the GSM / GPRS network;

- monitoring of vehicle dynamics;
- geolocation of the wagon;

The technical specifications for this type of activity are:

- GPS module with GSM/GPRS communication
- Accelerometer mems 3 axes  $\pm 16g$
- Solid State memory (black box function)
- Microcontroller or microprocessor with analogue and digital input
- Sensor temperature for monitoring the battery temperature.
- Energy harvester for autonomous power supply
- Wireless module for the communication with the axle box master.

Instead, the axle box must have the following feature:

- Monitoring of operating quantities
- Data processing and transmission of it in the form of index
- Communication with the base station and with the train driver form emergency

The technical specification for activities linked to the axle boxes are:

- Accelerometer mems 3 axes  $\pm 16g$
- Accelerometer mems 3 axes  $\pm 200g$  (crash detection)
- GPS module with limited size
- Temperature sensor
- Solid State memory (black box function)
- Odometer
- Wireless module for the communication with the base station.
- Energy harvester for autonomous power supply
- Battery pack resistant to the high temperatures
- Dimensions suitable for the retrofit of the standard axle box cover

To achieve these objectives without an increase in costs, it is necessary to select low cost sensors, to develop a system for collecting and processing continuous data on-site and to determine a method of real-time transmission of information. The cost of the condition monitoring system has to be less than the maintenance cost

supported by the wagon owner [35] the cost of the sensors must be compatible with the overall cost of the system.

The wireless communication is the most important technology challenge for the success of the project. The railway environment, having regard to the massive presence of iron, is particularly hostile to this type of communication as can be seen from the data collected during the PhD. The choice to adopt a wireless technology turns out to be the only way forward in the installation of monitoring devices on existing wagons on which a retrofit operation is necessary. The choice of adopting wired solutions turned to be successful, provided that the monitoring system is installed during the production phases of the wagon in such a way as to spread the costs of installing with those for assembling the wagon.

The wireless device should not be a ZigBee or Xbee module, but it must be a radio module operating on free frequencies and with its frequency it must guarantee the coverage of the entire wagon. It will then be up to appropriate communication protocols developed at hoc to make sure that the wireless signals of two adjacent cars do not conflict with each other. The radio modules must also guarantee a very low power consumption, less than 20 mA both for the writing part and for the reading part. Their management through appropriate algorithms must allow them to be switched on and off.

Once the most appropriate module has been identified, it is necessary to choose accurately the data to be transmitted, in fact the radio modules have a maximum number of transmissible bytes for each communication. Depending on the data transmission speed, and therefore the time necessary to terminate the communication of all eight axle boxes monitoring system, it is possible to develop communication logic to manage different situation that can occurs.

Each axle box node computes the following information:

- For the accelerometer  $\pm 16g$ 
  - For each axis the minimum, the maximum and the RMS, for a total of nine data.
- For the accelerometer  $\pm 200g$ 
  - For each axis the minimum, the maximum and the RMS, for a total of nine data.
- Speed
- Axle box temperature

- Battery Voltage

In order to have wireless communications lasting less than one second the following index must be used:

- Crest factor for each axis of the two accelerometer
- Speed
- Axle box temperature
- Battery Voltage

and also a byte to indicate to the base station the presence or absence of anomalous values beyond threshold levels. It will then be up to base station to identify the anomalous value and sound the alarm.

In Figure 83 can be seen the prototype of the axle box cover within which the monitoring system described in this chapter will be installed. The characteristic cross shape was chosen to allow operators to screw and unscrew the cover bolts with the traditional keys used in maintenance operations. The greater dimension in axial direction, compared to a traditional cover, is necessary to allow the installation of the energy harvester and the electronics necessary for the operation of the monitoring system. The electronics housing is separated from that of the energy harvester in order not allow to the PCB to come into contact with the grease into the axle box. It is possible to observe how the upper part of the cover has an open towards the outside. This will be covered with an ultra-resistant polycarbonate cap and has the task to allow the wireless communication, otherwise the cover would be a Faraday cage.

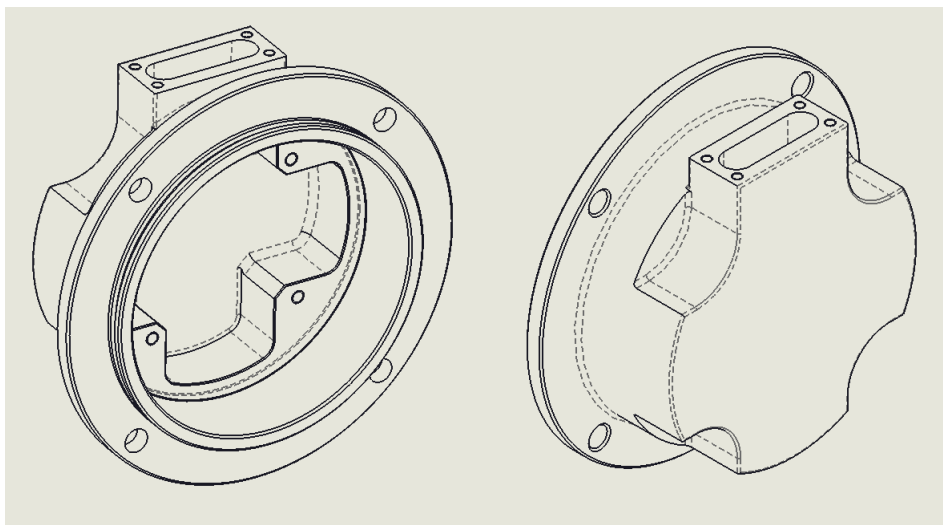


**Figure 83. S.W.A.M. Rail possible axle box cover.**



# Conclusions

The PhD thesis presented here is the result of three years of work that led to the design, implementation and tests of a wireless health monitoring system demonstrator for freight wagons.

This demonstrator is part of the results of the project Cluster ITS Italy 2020, a project within which was born the collaboration with the international transport company Ambrogio Trasporti S.p.a.

From the analysis of the temperature data two fundamental aspects emerge. The first is the need and importance of maintaining the braking system always in good conditions, doing maintenance in line with the regulations. In case of anomalous reports from the RTB devices or the thermal portals, intervene in order to verify or restore the brake system. Inefficient brake systems can lead to the absence of braking, resulting in a collision with the wagon who comes before and forcing the braking system of the latter to greater stresses. On the other hand, the block of the brake system may cause the overheating of the wheels or in the most serious cases the wheels flat. The maintenance operations on the wheelset are those that represent the highest costs of maintenance. The second is related to the adoption of new brake blocks, in particular the K type in synthetic material. In fact, in addition to the complete review of the brake system as prescribed by the regulation, also the material of the wheelsets must be suitable for the use of the new type of brake blocks. If this aspect is not complied could occur overheating phenomena that could lead to the formation of martensite on the rolling surface with the consequent formation of cracks.

However, it's unthinkable to sensorize the braking system of a freight train with temperature sensors that can inform the driver of possible overheating of the brake blocks. If the goods wagons will adopt disc brakes, the sensors could be installed on the brake caliper to monitor the temperature. On the other hand, the pneumatic part of the brake system can not be sensorized because any possible leakage of air would cause a pressure drop in the general pipe which would lead to the automatic braking of the train. Furthermore, the wireless signal would be totally shielded, if the sensors were placed inside the pipe.

The accelerations analysis is the most important aspect in the freight wagons monitoring. As mentioned, the installed device has a limited computing power but

more than enough to perform the calculation of the RMS along the three axes. In the case of a freight wagon, the acceleration parameter of greater interest is the vertical acceleration, it is a specific indicator of the stability of the vehicle.

High and consecutive RMS peaks are a clear indicator to identify the derailment of bogies or wagons, as under normal operating conditions the trend of the vertical RMS value is almost constant. In correspondence with railroad exchanges, level crossings or any other known track discontinuity, its trend presents some very short peaks.

In the first part of the PhD was paid great attention to the literature in order to identify the solutions already developed by other universities and research institutes in order to identify the best system architecture. The next step was to analyze the history of failures and anomalies recorded by the company over the years in order to identify which were the most critical issues on the wagons. The results of these two preliminary analyzes served as the base for the realization of a first wired demonstrator. All the subsystems of this first demonstrator have been long tested in laboratory in order to guarantee the maximum reliability of the device and maximum repeatability of the recorded data.

In November 2015, the first prototype was installed on a wagon made available by the company. This first installation required some calibration activity in order to obtain the desired data. In the final configuration, the monitoring system covered more than 25,000 km on the railway line connecting Candiolo (IT) to Modane (FR). This distance allowed to collect a considerable amount of data related to the operating conditions of the wagon. The parameters monitored were: the pressures of the pneumatic braking system, temperature of the outermost part of the cast-iron brake blocks, the dynamics of the body frame.

The technological limits of the developed wired system were clear from the beginning. These limitations are essentially summarized by two points, the first is the low energy autonomy due to the absence of on board power generation and joined with the adoption of low energy density batteries, the second is the extremely long installation times due to the wiring of temperature sensors and pipes connected to the braking system. The first prototype, however, has allowed us to collect a considerable amount of data and lay the foundations for the development of a second optimized demonstrator. The activity of data analysis went hand in hand

with the development of the second demonstrator in order to validate the data collected and their usefulness.

The second demonstrator developed was significantly more complex, in fact it consists of two units: a base station that represents the development of the first demonstrator and a completely new axle box node monitoring system. The first prototype developed was therefore completely revised from the software point of view, introducing a power energy management algorithm and a communication algorithm for the wireless part. The software improvements in order to be implemented and maximized have made necessary a complete re-examination of the hardware part. The algorithms developed have been implemented identically in both devices.

This second prototype was tested for a distance significantly lower than the first, equal to 2000 km on the Gallarate (IT) - Mechellen (B) railway line. Also the tests on this second device have given positive results allowing us to acquire data and knowledge.

The monitoring systems developed have not taken into account the realization costs which however are very limited in relation to the benefits that can be obtained in terms of maintenance and safety.

The activity of these three years has found natural continuation in the S.W.A.M. Rail project that aims to create and a self-powered wireless monitoring device based on eight devices for monitoring the axle boxes and a base station for the data collection.

# References

- [1] Special Report "Rail freight transport in the EU: still not on the right track", European Court Of AUDITORS, Luxembourg, 2016.
- [2] Tagliaferri A., Matricardi A., Nozioni sul freno ferroviario, CIFI collana per la formazione professionale, 2001.
- [3] Edwards M.C. et al., Improving freight rail safety with on board monitoring and control systems, in *Joint Rail Conference*, 2005
- [4] Ngigi R.W., Pislaru C., Ball A., and Gu F., Modern techniques for condition monitoring of railway vehicle dynamics, *Journal of Physics: Conference Series* **364**, 2012
- [5] Mahasukhon P., Sharif H, Hempel M., Zhou T., Ma T., Shrestha P. L. : A study on energy efficient multi-tier multi-hop wireless sensor networks for freight-train monitoring, *Wireless Communications and Mobile Computing Conference (IWCMC)*, 2011
- [6] Wascosa Infoletter, CargoCBM – Condition-based maintenance in rail-freight traffic, 22 Novembre 2014
- [7] Gericke C., Hecht M., CargoCBM – Feature generation and classification for a condition monitoring system for freight wagons, *Journal of Physics: Conference Series* 364(2012) 012003
- [8] Hecht M., Innovative rail freight wagons – A precondition to increase the market-share of rail freight, *Archives of Transport* 29(1):17-26, January 2015
- [9] Smith K., Wagon tracking opens up new avenues for VTG, *International Railway Journals*, 2017
- [10] Hempel M., Sharif H, Rakshit S. M.: Study Of A Dual Radio Sensor Platform For Effective On-Board Real-Time Monitoring Of Freight Trains, *Wireless Communications and Mobile Computing Conference (IWCMC)*, 2016
- [11] Technical Innovation Circle for Rail Freight Transport, White Paper innovative Rail Freight Wagon 2030 - The "5L" future initiative as a basis for growth in rail freight transportation, Dresden September 2012.
- [12] N. Bosso, A. Gugliotta, N. Zampieri, Design and testing of an innovative monitoring system for railway vehicles, *Proceedings of the Institution of Mechanical Engineers Part F Journal of Rail and Rapid Transit* • October 2016
- [13] Bosso, N., Gugliotta, A. Zampieri, N., 2015. Strategies to simulate wheel-rail adhesion in degraded conditions using a roller-rig. In *Vehicle System Dynamics*, 53 (5), pp. 619-634. DOI: 10.1080/00423114.2014.981194, 2015.
- [14] Vernersson T., Temperatures at railway tread braking. Part 2: calibration and numerical examples, *Proceedings of the Institution of Mechanical Engineers Part F: Journal of Rail and Rapid Transit* **221**
- [15] Vernersson T. and Lundén R., Temperatures at railway tread braking. Part 3: wheel and block temperatures and the influence of rail chill, *Proceedings of the Institution of Mechanical Engineers Part F: Journal of Rail and Rapid Transit* **221**
- [16] K. D. Cole, C. M. Tarawneh, A. A. Fuentes, B. M. Wilson, L. Navarro, Thermal models of railroad wheels and bearings, *International Journal of Heat and Mass Transfer* 53:9-10, pp. 1636–1645, (2010).

- [17] Talati F. and Jalalifar S., Analysis of heat conduction in a disk brake system, *Heat Mass Transfer* **45**, 1047–1059, 2009
- [18] Vakkalagadda M.R.K., Srivastava D.K., Mishra A., and Racherla V., Performance analyses of brake blocks used by Indian Railways, *Wear* **328–329**, 64–76, 2015
- [19] Carprignano A., *Meccanica dei Trasporti ferroviari e tecnica delle locomotive*, 1985
- [20] Bruno F.; Coviello N.; Dalla Chiara B.; Di Paola A.; Pagliero P.; Viktorov V. (2015). The energy consumption of trains in operation: simulation, a methodology for the analysis and influence of the driving style. *INGEGNERIA FERROVIARIA*, vol. LXX n. 4, pp. 327-357. -ISSN 0020-0956
- [21] Somà, A. & De Pasquale, G. 2013. Electro-mechanical coupled design of self-powered sensing systems and performances comparison through experiments. In *Frattura ed Integrità Strutturale* **23**, 94-102, 2013.
- [22] De Pasquale G., Somà A., and Zampieri N., Design, simulation, and testing of energy harvesters with magnetic suspensions for the generation of electricity from freight trains vibrations, *Journal of Computational and Linear Dynamics* **7**, 2012
- [23] Grudén, M., Hinnemo, M., Dancila, D., Zherdev, F., Edvinsson, N., Brunberg, K., Andersson, L., Bystrom, R., Rydberg, A. 2013. Field operational testing for safety improvement of freight trains using wireless monitoring by sensor network. In *IET Wireless Sensor Systems Volume: 4, Issue: 2*, pp. 54-60, June 2014.
- [24] Franceschinis, M., Rossi, M., Spirito M.A., Pastrone, C., Mauro, F. 2013. Predictive monitoring of train wagon conditions using wireless network technologies. In *23rd International Conference on Artificial Reality and Telexistence (ICAT)*, pp: 1-8, 2013. Tokyo, Japan.
- [25] Chiochio, S., Persia, A., Santucci, F., Di Claudio, V., Di Grande, D., Giugliano, P., Guidotti, G. 2016. A cloud-based heterogeneous wireless platform for monitoring and management of freight trains. In *8<sup>th</sup> International Congress on Ultra Modern Telecommunications and Control Systems and Workshops (ICUMT)*, 2016. Lisbon, Portugal.
- [26] Hodge, V.J., O'Keefe, S., Weeks, M., Moulds, A. 2015. Wireless Sensor Networks for Condition Monitoring in the Railway Industry: A Survey. In *IEEE Transactions on Intelligent Transportation Systems*, VOL. 16, No. 3, June 2015.
- [27] Lo Schiavo, A. 2016. Fully autonomous wireless sensor network for freight wagon monitoring. In *IEEE Sensors Journal*, VOL. 16, No. 24, December 2015.
- [28] Mahasukhon, P., Sharif, H., Hempel, M., Zhou, T., Ma, T., Shrestha, P.L. 2011. A study on energy efficient multi-tier multi-hop wireless sensor networks for freight-train monitoring. In *Wireless Communications and Mobile Computing Conference (IWCMC) 7th International*, 2011. Istanbul, Turkey
- [29] Aimar, M., Somà, A., Study and results of an on-board system for braking monitoring of freight wagons. *Part F Journal of Rail and Rapid Transit*, 2017.
- [30] A. Somà, M. Aimar, Study and design of a wireless monitoring device for intermodal freight wagons, *Proceeding of 25<sup>th</sup> International Symposium of Dynamics of Vehicle on roads and tracks*, 2017

- [31] Aimar M., Somà A., and Fraccarollo F., An on-board braking monitoring system for intermodal freight trains, in *Third International Conference on Railway Technology: Research, Development and Maintenance*, 2016
- [32] Mathias Grudén et al., Field operational testing for safety improvement of freight trains using wireless monitoring by sensor network, *IET Wirel. Sens. Syst.*, 2014, Vol. 4, Iss. 2, pp. 54–60.
- [33] M. Koch, M. Kurch, D. Mayer, "On a Methodical Design Approach for Train Self-Powered Hot Box Detectors", in J. Pombo, (Editor), "Proceedings of the First International Conference on Railway Technology: Research, Development and Maintenance", Civil-Comp Press, Stirlingshire, UK, Paper 90, 2012. doi:10.4203/ccp.98.90
- [34] R.R. Newman, J. Tabacchi, G.G. Maderer, R.C. Leedham, D. Purta, R. Galli, Hot bearing detection with the "Smart Bolt".
- [35] Baumgartner J.P., Prices and costs in the railway sector, École Polytechnique Fédérale de Lausanne – LITEP, 2001
- [36] V. A. Profillidis, "Railway Management and Engineering", Fourth Edition, ISBN 978109464631, 2014.
- [37] Container Handbook, "Cargo loss prevention information from German marine insures", Paragraph 2.3.5 Mechanical stresses in rail transport.

# List of Tables

Table 1. PJM models characteristics.....	21
Table 2. Nomenclature used in the model. ....	26
Table 3. Physical properties.....	28
Table 4. Thermophysical quantities of cast iron brake blocks .....	30
Table 5. ATmega2560 characteristics. ....	35
Table 6. Temperature sensor characteristics.....	38
Table 7. Average sensitivity. ....	40
Table 8. GPS characteristics. ....	45
Table 9. ATmega328P characteristics .....	51
Table 10. Energy consumption in different phases.....	59
Table 11. Logistical information: Line 1 - Case A. ....	66
Table 12. Logistical information: Line 1 - Case B. ....	66
Table 13. Frejus Tunnel Line 1 - Case A.....	67
Table 14. Frejus Tunnel Line 1 - Case B.....	67
Table 15. Physical properties.....	92
Table 16. Thermal energy model results. ....	92
Table 17. Braking comparison.....	95
Table 18. FEM model input.....	98

# List of Figures

Figure 1. Goods Transported by Railway in EU – Total Transport Traffic Volume .....	2
Figure 2. Goods Transported by Railway in EU – National Transport Traffic Volume.....	2
Figure 3. Good Transported by Railway in EU – International Transport Traffic Volume.....	3
Figure 4. Accidents involving transport of dangerous goods in UE.....	4
Figure 5. Accidents in which dangerous goods are released in UE.....	5
Figure 6. Vehicle subsystems: diagram and possible failures. ....	9
Figure 7. Freight wagon braking system diagram. ....	11
Figure 8. CargoCBM, on the left the OBU installed on a Wascosa wagon, on the right an axle box bearing sensorized.....	15
Figure 9. Intelligent freight wagon 5L - On the left the wagon presented and on the right the monitoring system. ....	17
Figure 10. On the left a Bosch AMRA installed on a wagon, on the right the operating principle of the device. ....	18
Figure 11. Nexiot AG Crossmodal. ....	18
Figure 12. SAVVY CargoTrac-Ex. ....	19
Figure 13. On the left different axle box cover for monitoring different axle box, on the right the monitoring system installed.....	21
Figure 14. The WaggonTracker ADV, the most complete monitoring system produced by the PJM. ....	22
Figure 15. Exploded view of the Schaeffler energy harvester.....	23
Figure 16. Brake block mesh. ....	32
Figure 17. Wired prototype scheme.....	35
Figure 18. Voltage divider scheme. ....	38
Figure 19. Voltage range with different fix resistance value in the voltage divider circuit. ....	39
Figure 20. Multi-meter accuracy. ....	42
Figure 21. Differential pressure sensor characteristics. ....	44
Figure 22. Base station diagram. ....	47
Figure 23. Base station with battery pack.....	49



Figure 24. Axle box node diagram. ....	50
Figure 25. Axle box node. ....	52
Figure 26. Interrupt used for the power save algorithms. ....	56
Figure 27. Diagram of the power save algorithm. ....	57
Figure 28. Intermodal freight wagon Sggmrs 90. ....	60
Figure 29. Central monitoring systems installed on steel plate. ....	61
Figure 30. Axle box node monitoring system. ....	61
Figure 31. Brake block sensorization. ....	62
Figure 32. The railway line Candiolo (IT) - Mouguerre (FR). ....	64
Figure 33. The railway line Gallarate (IT) - Mechelen (B). ....	64
Figure 34. Line 1 - Case A: Outward journey. ....	68
Figure 35. Line 1 - Case A: Return journey. ....	69
Figure 36. Line 1 - Case B: Outward journey. ....	69
Figure 37. Line 1 - Case B: Return journey. ....	70
Figure 38. Line 2 - Case A: Outward journey. ....	71
Figure 39. Line 2 - Case A: Return journey. ....	71
Figure 40. Axle box wireless monitoring. ....	73
Figure 41. Mean deceleration due to the braking. ....	76
Figure 42. Maximum acceleration values in intermodal transport. ....	77
Figure 43. RMS acceleration during braking 1. ....	78
Figure 44. RMS acceleration during braking 2. ....	79
Figure 45. RMS acceleration during braking 3. ....	79
Figure 46. RMS acceleration during braking 4. ....	80
Figure 47. RMS acceleration during braking 5. ....	80
Figure 48. RMS acceleration during braking 6. ....	81
Figure 49. RMS acceleration during braking 7. ....	81
Figure 50. RMS acceleration during braking 8. ....	82
Figure 51. RMS acceleration during braking 9. ....	82
Figure 52. RMS acceleration during braking 10. ....	83
Figure 53. RMS acceleration during braking 11. ....	83
Figure 54. Example of the RMS vertical acceleration. ....	85
Figure 55. Level crossing 1. ....	86
Figure 56. Level crossing 2. ....	87
Figure 57. Level crossing 3. ....	87

Figure 58. Level crossing 4.....	88
Figure 59. Railroad switch 1.....	88
Figure 60. Railroad switch 2.....	89
Figure 61. Railroad switch 3.....	89
Figure 62. Railroad switch 4.....	90
Figure 63. Possible line defect 1.....	91
Figure 64. Possible line defect 2.....	91
Figure 65. Track sector I.....	93
Figure 66. Track sector II. ....	93
Figure 67. Track sector III. ....	94
Figure 68. Track sector IV.....	94
Figure 69. Track sector V. ....	95
Figure 70. Track sector VI.....	96
Figure 71. Track sector VI'. ....	96
Figure 72. Track sector VII.....	97
Figure 73. Track sector VII'. ....	97
Figure 74. End of braking A .....	99
Figure 75. End of the simulation for braking A.....	100
Figure 76. Comparison of monitored and simulated temperature for braking A	101
Figure 77. End of braking B .....	101
Figure 78. End of the simulation for braking B.....	102
Figure 79. Comparison of monitored and simulated temperature for braking B.	102
Figure 80. Brake block contact surface temperature .....	103
Figure 81. Simulated temperature comparison .....	104
Figure 82. S.W.A.M. Rail monitoring system diagram. ....	107
Figure 83. S.W.A.M. Rail possible axle box cover. ....	110